The origin and development of novelty: eyespots and immunity

Maria Adelina Jerónimo

Dissertation presented to obtain the Ph. D. degree in Evolutionary Biology

Instituto de Tecnologia Química e Biológica António Xavier | Universidade Nova de Lisboa

Oeiras,
November, 2016

UNIVERSIDADE NOVA DE LISBOA

The origin and development of novelty: eyespots and immunity

Maria Adelina Jerónimo

Dissertation presented to obtain the Ph.D. degree in Evolutionary Biology

Instituto de Tecnologia Química e Biológica António Xavier | Universidade Nova de Lisboa

Research work coordinated by:

FUNDAÇÃO CALOUSTE GULBENKIAN
Instituto Gulbenkian de Ciência

Oeiras, November, 2016

Declaração/Declaration

Esta dissertação é o resultado do meu próprio trabalho desenvolvido entre Maio de 2011 e Maio de 2015 no laboratório da Dra. Patrícia Beldade, Instituto Gulbenkian de Ciência em Oeiras, Portugal, no âmbito do Programa da FCT de Doutoramento (2010). Com base no trabalho desenvolvido, a minha orientadora e eu esperamos submeter dois artigos científicos para publicação.

This dissertation is the result of my own research, carried out between May 2011 and May 2015 in the laboratory of Dr. Patrícia Beldade, Instituto Gulbenkian de Ciência in Oeiras, Portugal, under the FCT Doctoral Programme (2010). From this work, my supervisor and I expect to submit two papers for publication.

Apoio Financeiro/Financial Support

Apoio financeiro da FCT e do FSE no âmbito do Quadro Comunitário de Apoio, bolsa de doutoramento # SFRH/BD/73658/2010, dos projectos atribuidos a P. Beldade (PTDC/BIA-BEC/ 099808/2008 e PTDC/BIA-EVF/2170/2012) e da Fundação Calouste Gulbenkian.

Financial support for this thesis was provided by the FCT and FSE thourgh the Quadro Comunitário de Apoio, doctoral fellowship # SFRH/BD/73658/2010, research grants to P. Beldade (PTDC/BIA-BEC/ 099808/2008 and PTDC/BIA-EVF/2170/2012) and Fundação Calouste Gulbenkian.

Acknowledgements

I would like to thank the IGC for giving me the opportunity to do my Ph.D..

To all elements of my thesis committee: in the very beginning Victor Barbosa, António Jacinto, and more recently Élio Sucena and Jorge Carneiro.

To all the present and past members of Variation: Development & Selection Lab, Evolution and Development Lab and Development, Evolution and the Environment lab. Thank you for all your help, patience and fruitful discussions that contributed a lot for this work.

For all my friends and family outside IGC that encouraged me throughout this journey. Thank you for your patience and your curiosity about my work.

Finally, I would like to thank to Patrícia Beldade, the supervisor that gave me the opportunity, the guidance and the freedom to dive into the wonderful word of evolution and development.

Summary

The infinitude of forms across living beings always fascinated scientists and laymen alike. Phenotypic variation is the raw material for natural selection and is transversal in biological systems. Evolutionary novelties are lineage specific traits with adaptive value. How such traits arise in organisms is still an open question. To understand this process we used the butterfly eyespots as a model, which are evolutionary novelty. Our testing hypothesis was that butterflies had rewired ancient genetic mechanisms used for the wound-response to develop eyespots, co-option. The major fact supporting this hypothesis is that wounding an early pupal wing can develop an eyespot-like pattern around wound site. This pinpoints the existence of genetic and cellular commonalities between eyespot development and wound response.

First, we characterized the genetic wound response on the wings of our model system, *Bicyclus anynana*, comparing the genetic profiles of wounded and non-wounded wing pairs (Chapter 2). Wounded wings were enriched for immunity-related genes. These genes are expressed in circular patterns around wound sites. Additionally, we observed faint expression patterns at the presumptive eyespot center, especially for the antimicrobial peptide gene *Gloverin 2*. Antennapedia, a transcription factor involved in eyespot development was also observed at wound sites. At presumptive eyespot centers and wound sites there are higher cell density due to migration of hemocyte-like cells.

Secondly, we explored the role of immunity into the development of wound-induced patterns (Chapter 3). We manipulated the immune system activation during pupal development and quantified the dorsal

adult wing patterns. Wounds with high immunity activation developed larger wound-induced eyespots. This enlargement is mediated through local immunity. With this experiments we noticed that not only dorsal wound-induced patterns had changed, but also the ventral wing patterns were different.

Thirdly, we characterized the immunity-mediated developmental plasticity, one genotype producing different phenotypes according to the environmental conditions, on ventral wing patterns (Chapter 4). As in low developmental temperature individuals, high immunity activation induced long developmental time, smaller eyespots, lower wing color contrast, and lower ecdyson hormone levels. This effect was independent of the organ where the immunity treatment was applied. To our knowledge, this is the first time that immunity is mediating developmental plasticity in butterfly wing patterns.

Lastly, we explored the immunity effects on wing size and shape (Chapter 5). Contrary to low developmental temperature, wings of high immunity individuals were smaller. However, this effect only occurred when immune treatment was applied in one of the developing wings, which reduced the proliferation rate. High immunity and low developmental temperature induce similar shape changes, pulling the wing shape in the same direction. This indicates that different stresses activate a common developmental program determining wing shape.

In summary, this work reinforces the hypothesis of wound genetic circuitry co-option for the evolutionary origin of butterfly eyespots. Moreover, it uncovered the crucial role of immunity in the butterfly wing patterns development. It also open up new perspectives to understand the origin and diversification of novelties, developmental plasticity and the ecological meaning of phenotypic variation on butterfly wing patterns.

Sumário

A infinitude de formas dos seres vivos sempre fascinou os cientistas e demais pessoas. A variação fenotípica é a base da seleção natural e é transversal aos sistemas biológicos. Novidades evolutivas são características exclusivas de uma linhagem e têm valor adaptativo. Como surgem num organismo ainda é uma questão em aberto. Para compreender este processo utilizámos os ocelos da borboleta que são uma novidade evolutiva. A hipótese que testámos foi que as borboletas reutilizaram mecanismos genéticos preexistentes necessários para a resposta às feridas, para formarem ocelos, co-opção. O facto mais relevante que suporta esta hipótese é que uma ferida na asa da pupa pode desenvolver um padrão de cores semelhante a um ocelo à volta da ferida. Isto indica que existem semelhanças genéticas e celulares entre o desenvolvimento dos ocelos e a resposta às feridas.

Primeiro, nós caracterizámos geneticamente a resposta à ferida nas asas do nosso modelo biológico, *Bicyclus anynana*, comparando os perfis genéticos de pares de asas feridas e não feridas (Capítulo 2). As asas feridas expressam níveis mais elevados de genes relacionados com a imunidade. Estes genes são expressos em padrões circulares à volta das feridas. Também observámos ténues padrões de expressão no presumível centro dos ocelos, especialmente para o péptido antimicrobiano *Gloverin 2*. Antennapedia, um factor de transcrição envolvido no desenvolvimento dos ocelos também foi detectado nas feridas. Nos presumíveis centros dos ocelos e nas feridas há maior densidade cellular devido à migração de células semelhantes a hemócitos.

Em segundo lugar, nós investigámos o papel da imunidade no desenvolvimento de padrões induzidos pela ferida (Capítulo 3). Nós manipulámos a ativação do sistema imune durante o desenvolvimento da pupa e quantificámos os padrões das asas dorsais. Nas feridas com

maior activação da imunidade os ocelos induzidos pela ferida foram maiores. Este efeito é mediado pela imunidade local. Observámos também que não só os padrões dorsais induzidos pela ferida foram alterados, como também os padrões ventrais das asas eram diferentes.

Em terceiro lugar, caracterizámos a plasticidade no desenvolvimento (quando um genótipo produz diferentes fenótipos de acordo com as condições ambientais) mediada pela imunidade nos padrões das asas ventrais (Capítulo 4). Tal como a baixa temperatura, a elevada ativação da imunidade induziu um desenvolvimento mais longo, ocelos menores, menor contraste de cor nas asas, e níveis mais baixos da hormona ecdisona. Este efeito foi independente do órgão afectado. Do que pesquisámos, esta é a primeira vez que a imunidade está a mediar plasticidade no desenvolvimento dos padrões das asas das borboletas.

Por fim, nós explorámos os efeitos de imunidade no tamanho e forma das asas (Capítulo 5). Contrariamente ao efeitos da baixa temperatura, as asas dos indivíduos com maior activação da imunidade foram menores. No entanto, este efeito só ocorreu quando o tratamento imunológico foi aplicado em uma das asas, o qual induz a redução da taxa de proliferação cellular. Uma activação elevada da imunidade e baixas temperaturas induziram diferenças de forma similares, na mesma direção. Isto indica que diferentes stresses activam o mesmo programa de desenvolvimento determinando a forma da asa adulta.

Em resumo, este trabalho reforça a hipótese de co-opção do circuito genético usado para responder às feridas na origem evolutiva dos ocelos das borboletas. Além disso, demonstrámos que a imunidade tem um papel crucial no desenvolvimento dos padrões das asas das borboletas. O trabalho aqui apresentado abre também novas perspectivas para entender a origem e diversificação das novidades evolutivas, a plasticidade no desenvolvimento e o significado ecológico das variações fenotípicas dos padrões das asas das borboletas.

Table of contents

Chapter 1 – General Introduction

The endless diversity of morphological forms across living beings, the ecological niches colonized and the good match between the two has always fascinated scientists and laymen alike. Phenotypic variation is a universal property of biological systems and the raw material for natural selection. The molecular and genetic mechanisms and the environmental factors underlying the production of phenotypic variation are a key subject in ecological evolutionary developmental biology (eco-evo-devo). One of the most studied traits in this field is body pigmentation. There is great intra-specific variation and inter-species diversity in body pigmentation, and this trait is ecologically relevant and experimentally tractable. Here, we focused on a model for studies of the origin and modification of novel traits (i.e. traits for which there are no clear homologs in other lineages) and of developmentally plasticity (i.e. the environmental regulation of development that can result in the production of distinct phenotypes without genetic differences): wing pigmentation patterns in butterfly wings.

1.1. Evolutionary novelties

Among the diversity of morphological traits, novel traits such as flowers, bird feathers, mammalian placenta, insect wings, beetle horns and butterfly eyespots (e.g. Figure 1.1) are especially fascinating and their origin is especially challenging to explain. There is no single universally accepted definition of what constitutes an evolutionary novelty and of how that can be ascertained. Different authors consider different levels of biological organization and focus on different criteria (Ravosa 1991), including 1) lack of clear homology in the ancestral

species (Muller & Wagner 1991), 2) new ecological function within the lineage (Massimo Pigliucci 2008), or 3) new ecological function that permit new functions and open up new adaptive zones. Here, we consider as novel traits those that are restricted to a lineage and have a specific adaptive value.

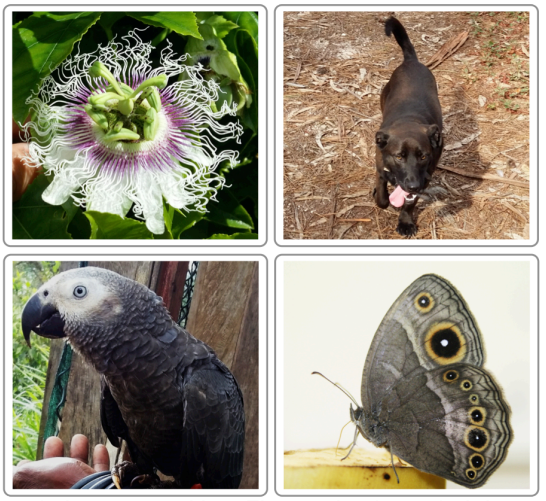

Figure 1.1- Examples of evolutionary novelties. Flowers in plants, hair in mammals, feathers in birds and scale-based wing patterns in butterflies.

1.1.1. Novel traits on butterfly wing patterns

The beauty and astonishing diversity of butterfly wing patterns have been inspiring scientists for centuries, and have been used to address questions in disciplines as different as systematics and evolution, development and genetics, biochemistry, and immunity. During last decades several evo-devo (Brakefield et al. 1996; Saenko et al. 2011; Hines et al. 2012) and eco-devo (Prudic et al. 2011; Prudic et al. 2015) studies have increased our understanding about development, genetics and ecological relevance of butterfly wing patterns. However, many questions remain. For example, the evolutionary origin, the genetic regulation and the role of the environment during development of the butterfly wing patterns.

Butterfly color patterns are formed by the two-dimensional arrangement of single color scales. Those patterns are evolutionary novelties and have allowed wing surfaces to perform new ecological functions in thermoregulation and visual communication (Beldade & Brakefield 2002). The diversity between species is dramatic, but there is also variation even within a population considering different wing surfaces, different sex and different seasonal forms (Nijhout 1991). Homology relationships between pattern elements are represented in the "nymphalid groundplan" (Schwanwitsch 1929; Nijhout 1991). In this model, different wing pattern elements, such as eyespots, chevrons and bands, are organized in parallel series; individual elements are repeated along the anterior-posterior wing axis within so-called wing cells that correspond to wing compartments bordered by veins. The extent to which wing pattern elements can evolve in an independent way will impact how easily they can respond to different selection pressures and it will also impact the diversification of butterfly wing patterns (Nijhout 1991; Nijhout 2001).

Several studies focusing on the genetic mechanisms underlying wing patterns development and evolution have provided important insight into homology of different wing pattern elements (Monteiro et al. 2006; Shirai et al. 2012; Saenko et al. 2011). Among the different types of wing pattern elements, eyespots that are composed of rings of contrasting colors are arguably those most studied at several levels, such as molecular, genetic, developmental, ecological and evolutionary.

1.1.2. Developmental plasticity on butterfly wing patterns

Phenotypic plasticity is the ability of an organism to react to environmental input with a change in phenotype (West-Eberhard

2003). It is also defined as the ability of a single genotype to produce more than one alternative form in different environmental conditions, whether the alternative phenotypes are continuous or discontinuous (Stearns 1989). Developmental plasticity is a particular case of phenotypic plasticity where environmental input during pre-adult development induces alternative phenotypes in the adult stage (Beldade et al. 2011). Temperature-dependent sex differentiation in turtles (Pieau et al. 1999), predator-induced change in head morphology of Daphnia (Boersma et al. 1998), and nutritional regulation of horns size in scarab beetle (Moczek & Emlen 2000) are examples of developmental plasticity.

Developmentally plastic traits typically have a particular period in which organisms sensing a different environment shift their developmental programs, and environmental changes outside this sensitive period do not induce phenotypic changes (Beldade et al. 2011). The sensitive period precedes the development of the final adult phenotype by a period of time that may be as brief as a few days or as long as several months (Nijhout 1999). For example, the sensitive period for the seasonal adult wing pattern polyphenism in butterflies is during later larval instars and early pupal stage (Nijhout 1999; Kooi & Brakefield 1999).

This study focuses on the eyespots of *Bicyclus anynana*, which are novel and developmentally plastic traits. *B. anynana* is an African butterfly living in tropical environments with two main seasons: the wet and the dry seasons which are very distinct in terms of temperature, humidity and food availability (Windig et al. 1994). This butterfly exhibits clear seasonal polyphenism in wing pattern and other traits (Brakefield & French 1999; Brakefield et al. 2009; Oostra et al. 2011). Wet season larvae produce adults with conspicuous ventral wing

patterns with large marginal eyespots, while dry season larvae produce adults with dull brown colors and very small eyespots (Figure 1.2A). These two alternative wing patterns are believed to correspond to seasonally different strategies to avoid predation. While the marginal large eyespots of the wet-season butterflies are thought to attract the predator's attention to the wing margin and away from the vulnerable body, the all-brown dry-season butterflies are cryptic against a background of dry leaves (Lyytinen et al. 2003; Prudic et al. 2015; Beldade et al. 2011). Thus, this seasonal polyphenism provides an adaptive response to the alternating seasonal environments increasing the individual's fitness.

Studies have shown that the temperature during late larval development, which predicts the season of adults, is an important environmental cue determining the development of the adult wing pattern phenotypes through changes in hormonal dynamics (Kooi & Brakefield 1999; Koch et al. 1996; Mateus et al. 2014) (Figure 2.2C and D). The eyespots on the ventral surface of *B. anynana* wings, the one exposed to predators when the butterfly is resting, are the ones most thermally plastic (Brakefield et al. 2009; Mateus et al. 2014) (Figure 2.2A). The dorsal eyespots, which are implicated in mate choice, are much less plastic, at least in relation to temperature (Breuker & Brakefield 2002; Westerman et al. 2014; Mateus et al. 2014) (Figure 2.2B).

1.1.3. Eyespot development

During the past decades, a number of eco-evo-devo studies focused on butterfly eyespots and provided insight into their evolutionary origin, ecology and developmental plasticity (e.g. Saenko et al. 2011; Prudic et al. 2015; Mateus et al. 2014). The experimental

tractability of developing eyespots is an advantage in evo-devo studies. For example, easy detection and access to the position of veins and developing eyespot centers on the dorsal forewing of developing pupae allows for very precise surgical manipulations under a simple stereoscope.

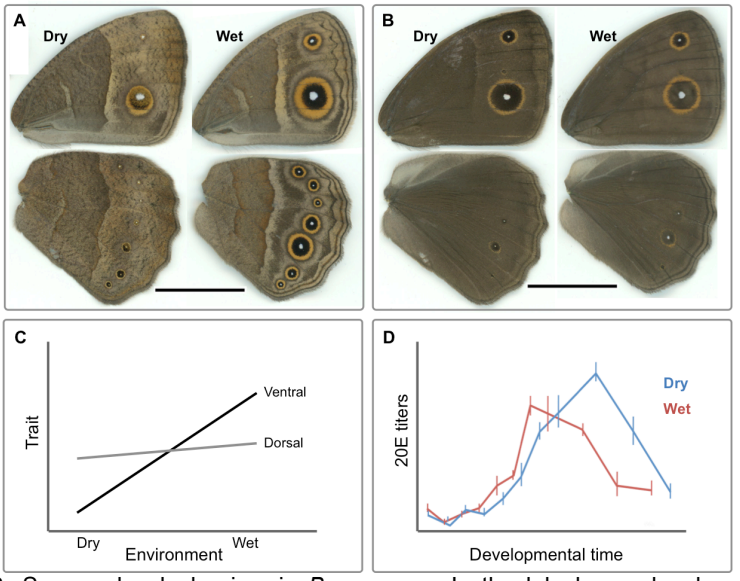

Figure 1.2- Seasonal polyphenism in *B. anynana*. In the lab, lower developmental temperatures (e.g. 19°C) lead to the production of adults with wing patterns resembling those of the dry season, while warmer developmental temperatures (27°C) lead to the production of adult wing patterns resembling those of the wet season. Temperature during development mediates phenotypic plasticity for ventral wing patterns (A) and has a much smaller effect on dorsal patterns (B). Ventral patterns are more plastic than dorsal patterns in response to environmental temperatures (Mateus et al. 2014) D) Different 20E dynamics in the hemolymph of pupae from the different seasonal forms (cf. Oostra et al. 2011).

Wing development starts during the first larval instar when the wings greatly increase in size and the venation system increases in complexity. During this stage, the eyespot development starts with determination of eyespot centers or foci (Figure 1.3) (Brakefield et al. 1996; Saenko et al. 2011). A series of genes have been associated

with this phase of eyespot development, including *Antennapedia* (*Antp*), *Distal-less* (*Dll*), *Notch* (*N*), *engrailed* (*en*), *hedgehog* (*hh*), *cubitus interruptus* (*ci*), *patched* (*patch*) and *spalt* (*sal*) (Saenko et al. 2011; Monteiro et al. 2006; David N Keys et al. 1999). Later, in early pupal wings there is the positioning of the eyespot rings around the focus (Brakefield et al. 1996; Wittkopp & Beldade 2009). Surgical manipulations of pupal wings have led to the suggestion that focal cells produce (or degrade) a diffusible morphogen-like signal that determines the fate of surrounding cells (Nijhout 1980; Monteiro et al. 1994; French & Brakefield 1995). Depending on the concentration of the morphogen-like signal they are exposed to, surrounding cells express different (combinations of) transcription factors (during early pupal stage), which correspond to the production of different color pigments (in late pupae). In *B. anynana*, Dll and Sal map the black ring and en the golden ring (Brunetti et al. 2001; Beldade et al. 2002). The identity of the morphogen-like signal triggering the expression of these transcription factors is still unknown. The synthesis of pigments and their deposition is the last stage of eyespot development and takes place only during the last days of the pupal life (Figure 1.3).

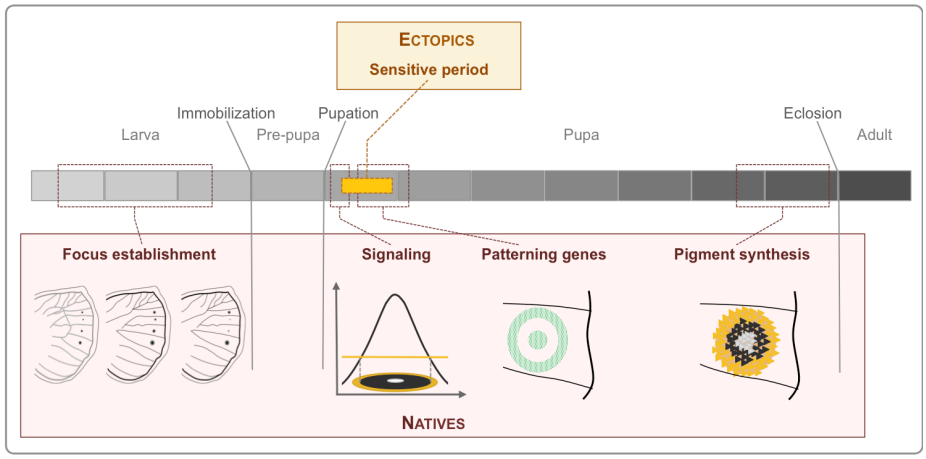

Figure 1.3- *B. anynana* eyespot development during larval and pupal stages. Focal determination occurs during the last larval stage (Brakefield et al. 1996). In early

pupae, the eyespot center presumably produces (or degrades) a morphogen-like signal inducing the transcription of "positioning" genes in rings around the focus (Brunetti et al. 2001). In the last days of the pupal stage, pigment synthesis takes place (Iwata & Otaki 2016). The sensitive period to induce an ectopic eyespot in this butterfly is from 6 to 18 hours post-pupation for 27°C rearing temperature individuals (Brakefield & French 1995).

1.1.4. The evolutionary origin of butterfly eyespots

The origin of evolutionary novelties is one a key question in evo-devo (Muller & Wagner 1991; Müller 2007; Moczek 2008). The factors promoting the diversification of novel traits have been studied for a long time (Stebbins 1970), but the genetic and developmental mechanisms underlying their origin have become the focus of research only in the last decades (Wagner & Lynch 2010; Saenko et al. 2008). "Co-option" has been proposed as the main mechanisms explaining the origin of evolutionary novelties (True & Carroll 2002). This mechanism refers to an evolutionary process by which evolution recycles ancestral genetic circuitries shared across lineages to produce novel traits (True & Carroll 2002; Ganfornina & Sánchez 1999). There are several studies showing that the origin of novel traits largely relies on existing genes and gene networks that are re-deployed and subsequently modified to give rise to novel morphological structures (Moczek & Nagy 2005; Saenko et al. 2011; Prum 2005). Gene recycling highlights the pleiotropy of genetic networks, which are involved in various processes during development and in different body organs. Recent whole genomic studies have raised the possibility that lineage-specific genes can also play a role (Khalturin et al. 2009; Donoghue et al. 2011; Zhou et al. 2015).

Scientists have highlighted the co-option of different genetic circuitries for the evolutionary origin of butterfly eyespots, such as leg-development, wing margin determination, anterior-posterior wing compartmentalization, embryonic development and wound response (Held 2013; Monteiro 2015; Saenko et al. 2011). In this thesis I have focused on the commonalities between eyespot development and response to epidermal wounds. The fact that some butterflies develop organized color patterns around wound sites resembling the adult eyespot patterns (Brakefield & French 1995; Monteiro et al. 2006; Otaki 2011) reveals commonalities between eyespot development and the response to wounding. While it is common to have dark pigmentation spots at wounded sites (Tang 2009; Levesque et al. 2012; Binggeli et al. 2014), the production of organized color patterns centered on wound sites is less common, but not restricted to butterflies (Ohno & Otaki 2012). In *B. anynana*, ectopic eyespots can be induced by wound on pupal wings from six to 18 hours post pupation, with 12 hours post-pupation corresponding to the highest probability of induction for butterflies reared at 27°C(Brakefield & French 1995).

These observation of wound-induction of ectopic eyespots led to the hypothesis of co-option of the wound response genetic circuitry for the evolutionary origin of eyespots (Monteiro et al. 2006). The genes involved in the differentiation of ectopic eyespots have not been extensively investigated and, thus, it is unclear whether native eyespots and ectopic eyespots are using the same genetic circuitry. Monteiro and co-workers investigated the gene expression of some known eyespot-related genes and saw that en, Sal and Dll were expressed in cells around wound sites several hours after wounding (Monteiro et al. 2006). In this case, eyespots are like “painted scars” on wings. This work presented here started off to investigate the

genetic and cellular basis of wound-induced eyespot formation. For this reason, the next section provides a brief overview of the mechanisms of wound response in insects.

1.2. Wound response and immunity

Multicellular organisms can repair their epithelia after an injury. This process is essential to maintain homeostasis (Davis & Engström 2012) and restore the integrity of the outer barrier. Wound response integrates evolutionarily conserved cellular and genetic mechanisms to form a protective scab, fight pathogens, and restore epidermis integrity (Moussian & Uv 2005; Wood et al. 2002). During the last decades, insects, and in particular *Drosophila melanogaster*, have become key model systems to explore the cellular and molecular mechanisms of wound healing, epithelial repair and regeneration (Wood et al. 2002; Bosch et al. 2005; Jiang et al. 2011). In insects, the wound response can be divided into five main steps: 1) early wound signaling, 2) plug formation through hemolymph coagulation and attraction of hemocytes, 3) melanin accumulation, degranulation of hemocytes and wound site stabilization, 4) phagocytosis and, 5) reepithelization (Lai et al. 2002; Galko & Krasnow 2004; Yoo et al. 2012) (Figure 1.4). Failure in any of these processes can seriously compromise survival. For example, the activation of melanogenesis is crucial and Drosophila mutants lacking hemocyte-phenoloxidases cannot properly heal compromising development and survival (Galko & Krasnow 2004; Binggeli et al. 2014).

The few existing studies of wound healing in Lepidopterans have focused on the larval stage (Madhavan & Schneiderman 1969; Rowley & Ratcliffe 1978). Wound response in Lepidopterans shared the main aspects of wound response in Drosophila and also in

mammals (Moussian & Uv 2005; Krautz et al. 2014). Despite much evolutionary conservation in wound healing mechanisms, there are also particularities to some taxa (e.g. regeneration of entire organs in adult starfish (Fan et al. 2011; Gurtner et al. 2008)) and also differences between developmental stages of the same species (e.g. embryonic wounds, unlike those of adults, usually regenerate without scar (Wood et al. 2002; Galko & Krasnow 2004)). In this thesis, I focused in a particularity of butterfly wound response, which is restricted to a very specific time window during early pupal development: induction of ectopic rings of colors.

1.2.1. Wound response includes tissue repair and immune mechanisms

After a wound, homeostasis needs to be restored rapidly and efficiently. Towards that, wounded cells send some kind of alarm signals (such as Ca^{2+} and H_2O_2) to their neighboring cells to activate wound response (Yoo et al. 2012; Razzell et al. 2013) (Figure 1.4). In this way wounded cells behave like organizers, releasing signals to surrounding cells and to immune cells that readjust their transcriptional programs to induce melanization, coagulation, cell shape changes, the formation of functional actomyosin structures, the recruitment of immune cells, the production of AMPs and reepithelization (Niethammer et al. 2009; Cordeiro & Jacinto 2013; van der Vliet & Janssen-Heininger 2014) (Figure 1.4). During wound response, there is activation of tissue repair and immune processes. Grossly, we can distinguish various immune mechanisms: the inflammation process in which hemocytes migrate towards the wound site, melaninzation and the massive production of anti-microbial peptides (AMPs) in the fat body (the insect equivalent to the

mammalian liver). On the other hand, the formation of the plug, stabilization of the wound site, and reepithelization can be grouped as tissue repair mechanisms. Although it could be argued that wound healing is not part of the immune response, apart from in highly controlled laboratory experiments, it is nearly impossible to achieve wounding without exposure to potentially infectious organisms. Moreover, both tissue repair and immunity processes are intrinsically linked and even in sterile wounds, where in theory the immunity should not play a role, immune mechanisms are present as well as the expression of immune related genes such as AMPs (Márkus et al. 2005).

1.2.2. Regulation of insect immunity

Upon infection, insects orchestrate a humoral and a cellular immune response to control pathogens. This response integrates the production of a battery of AMPs in the fat body, which are then released into circulation (Bulet & Stocklin 2005; Aggarwal & Silverman 2008), adjustment of blood cell behavior (Williams 2007; Lavine & Strand 2002) and melanization (Nappi & Christensen 2005; Eleftherianos & Revenis 2011). These processes are tightly regulated through hormones immune signaling pathways such as Toll and immune deficiency (IMD).

The molecular events initiating the transcriptional induction of AMP genes are well characterized (De Gregorio et al. 2002; Lemaitre & Hoffmann 2007; Valanne et al. 2011; Myllymäki et al. 2014). Upon infection, pathogens are recognized through microbial patterns recognition receptors (PRRs), such as peptidoglycan recognition proteins (PGRPs) and Gram-negative binding proteins (GNBPs). Binding of pathogen-derived molecules to these receptors activates

Toll and IMD signaling cascades. Toll pathway is activated by fungal and many Gram-positive bacteria, whereas the IMD pathway responds to Gram-negative bacteria (De Gregorio et al. 2002; Tsakas & Marmaras 2010). Among insects, these pathways are more studied in Drosophila (Lemaitre & Hoffmann 2007; Valanne et al. 2011), but the conservation of the main aspects of these pathways in other insects is remarkable (Casanova-Torres & Goodrich-Blair 2013; Wang et al. 2007).

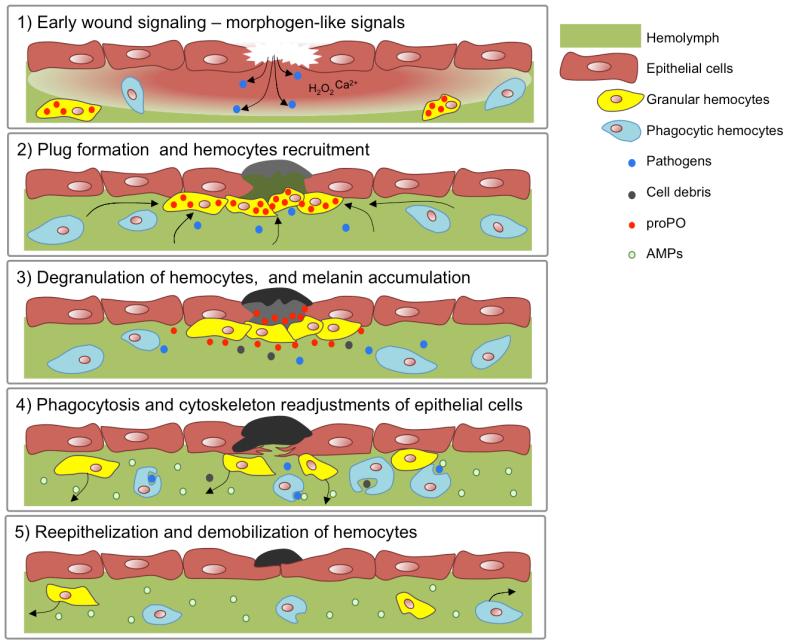

Figure 1.4- Five different stages of wound response in insects. Adapted from (Krautz et al. 2014).

Juvenile hormone (JH) and 20-hydroxy-ecdysone (20E) are highly versatile hormones, coordinating development, growth, reproduction, and aging in insects. Changes in 20E levels during development provide key signals for initiating developmental and physiological transitions, while JH promotes or inhibits these signals in a stage-specific manner (Beckstead et al. 2005; Nijhout et al. 2007; Andersen

et al. 2013). These two hormones also control immune response in Drosophila (Flatt et al. 2008; Rus et al. 2013; Regan et al. 2013), and in other insects (Tian et al. 2010; Wang et al. 2014).

To better respond to environmental conditions, insects can adjust hormone levels and/or the sensitivity of target organs to the hormone (West-Eberhard 2003). Hormonal levels can directly affect gene expression (Herboso et al. 2015). For example, in Drosophila, higher levels of 20E increase the expression of AMPs while JH has the opposite effect (Flatt et al. 2008). In *B. anynana,* 20E affects eyespot development (Koch et al. 1996; Mateus et al. 2014; Monteiro et al. 2015). Target organs can change their sensitivity to hormonal levels. For example, to decrease plasticity in genitalia, Drosophila males reduce the expression of FOXO, so this organ is less sensitive to insulin (that reflect nutrition levels) (Tang et al. 2011). To increase thermal plasticity in some eyespots, *B. anynana* express more ecdysone receptors in those eyespots' centers (Monteiro et al. 2015).

3. Aims and thesis scope

The origin of evolutionary novelties remains one of the most challenging topics in evo-devo. Here we investigated the involvement of an ancient genetic circuitry in the development of a novel trait through a series of different approaches, including analysis of candidate genes and less biased genetic analysis; manipulations and analysis of developing wings; characterization of various aspects of the adult wing pattern phenotype in treated and control groups.

We started investigating the 1) genetic and cellular mechanisms underlying the evolutionary origin of eyespots (Chapter 2), 2) the effects of wound-associated immune activation on wound-induced eyespots (Chapter 3), 3) the immunity-mediated developmental

plasticity in wing patterns and its hormonal regulation (Chapter 4) and 4)) the molecular basis of immune-induced regulation of organ size and shape.

Previous studies support the co-option of wound response genetic circuitry hypothesis for the evolutionary origin of butterfly eyespots. Namely 1)the fact that wounds on early pupal wings can lead to the development of an eyespot-like pattern (e.g. Brakefield & French 1995) and 2)that some "eyespot" genes are expressed around wound sites (Monteiro et al. 2006). However, if this hypothesis is correct we also expect to have expression of some typically "wound" genes in developing eyespots. In Chapter 2 we addressed this hypothesis by investigating genetic and cellular commonalities between wound response and eyespot development. We started by comparing gene expression profiles of wounded *vs.* non-wounded pairs of pupal wings to identify wound-induced changes in gene expression putatively associated with the formation of ectopic eyespots in *B. anynana.* We picked some of the genes differentially expressed after wounding to validated and extended the microarray-based analysis with a targeted study of gene expression spatial patterns and level dynamics. In this chapter, we also compare the cellular organization at the wound site and at the center of the presumptive eyespots. This study allowed us to ascertain which aspect of the wound response process (tissue repair or/and immunity) contributed to wound-induced eyespot formation and might have been involved in the evolutionary origin of eyespots.

In Chapter 3 we explored the possible involvement of immune-related mechanisms/processes in specification of cell color fate around wound sites inflicted on pupal wings. The development of a wound-induced ectopic eyespot means that wounds somehow can

change the cell fate of surrounding cells, acting much like an eyespot organizing center. Previous studies revealed that severe wounds could change the likelihood of production of an ectopic eyespot around a wound site, but not its size (Brakefield & French 1995). Our results suggest a new role of immune-related pathways into the eyespot size regulation, which does not interfere in the likelihood of production of an ectopic eyespot.

In Chapter 4, we describe the effect of an immune challenge in pupae on *B. anynana* adult wing patterns. This effect phenocopies the well-known effect of cooler developmental temperatures on wing pattern, as well as on ecdysone dynamics. We explored the effect of immune activation with different bacterial types and upon wounding of different body parts on developmental time, ecdysone dynamics, and adult wing patterns. These experiments open new perspectives for a role of immune challenge as a mediator of plasticity in wing color patterns.

In Chapter 5 we explored the effects of immune challenge on organ size and shape and discuss its impact on interorgan communication and readjustment of growth during development. Typically, the investment in immune defense is associated with depletion of energetic resources and, consequently, with trade-offs with various life history traits. We compared the effects of immune challenge from wound on different body parts on size and shape of adult wings. We further investigated the mechanisms behind the reduction of wing size by analyzing the effect of the immune challenge on the number of mitotic cells. We also compared differences in wing size and shape resulting from immune challenge with differences in wing size and shape between individuals reared at different temperatures. These experiments allowed us to understand how the

two factors affecting wing development (temperature and level of immune challenge) affect different axes of wing growth.

Finally, in Chapter 6, we discuss the main contributions of this work and present possible future directions of research that could further help us understanding the genetic basis of evolutionary novelties and how immune challenge can act as a cue inducing phenotypic change in butterfly wing patterns.

1.4. Acknowledgements

We would like to thank the 'evo-devo' community at Instituto Gulbenkian de Ciência, including the labs headed by Patrícia Beldade, Christen Mirth, and Élio Sucena, as well as Magda Atilano for fruitful discussions throughout my PhD.

Chapter 2 – Molecular and cellular commonalities between wound response and pigmentation patterning

2.1. Summary

The response to epidermal wounding is an evolutionarily conserved process and is typically tightly connected to pigmentation. An interesting example occurs in some Lepidopterans that can develop organized pigmentation patterns around wound sites that resemble native pattern elements called eyespots. This suggested the existence of molecular and cellular commonalities during development of both wound-induced and native eyespots. To reveal these commonalities, we studied the wound responseon pupal developing wings of the butterfly *Bicyclus anynana.* Microarray analysis comparing gene expression in wounded *vs.* non-wounded pairs of wings reveled enrichment for antimicrobial peptides (AMPs) and melanin pathway enzymes, both related with innate immunity in insects. We validated and extended the microarray analysis through quantitative RT PCR (qPCR), and *in situ* hybridization (ISH). We also found that the cell organization of the epidermis was similar at wound sites and at the center of presumptive eyespots: more cells between dorsal and ventral epithelia, expressing more Actin, Antennapedia (Antp) and *Gloverin 2* (*Glov2*) (an AMP). Higher cell density is not a consequence of higher cell proliferation around wound sites suggesting cell migration towards wound sites. The cell shape and

gene expression of those cells suggests that they are hemocytes. Our experiments brought new insight onto a specific wound response (post-growth and pre-adult stage) and also reinforce the hypothesis of the evolutionary origin of eyespots through co-option of the ancient wound response genetic mechanisms.

2.2. Introduction

Multicellular organisms can repair their epithelia after an injury. This process is essential to maintain homeostasis (Davis & Engström 2012) and restore the integrity of the outer barrier. Wound response integrates evolutionarily conserved cellular and genetic mechanisms of tissue repair and immunity (Moussian & Uv 2005; Wood et al. 2002). During the last decades, insects and in particular *Drosophila melanogaster*, have become a key model system to explore the mechanisms of wound healing, epithelial repair and regeneration (Wood et al. 2002; Bosch et al. 2005; Jiang et al. 2011; Moussian & Uv 2005). There are extensive similarities between insect species (Krautz et al. 2014; Eleftherianos & Revenis 2011; Kanost et al. 2004) and even between insects and mammals wound response (Moussian & Uv 2005).

After wounding, insects form a melanin clot to seal wounds and trap microorganisms, blocking their entry into the insect open body cavity (Lavine & Strand 2002; Eleftherianos & Revenis 2011). The microorganisms are subsequently agglutinated, immobilized, and killed by various lectins and antimicrobial peptides (AMPs) (Eleftherianos & Revenis 2011). To restore epithelium integrity, epidermal cells spread along and through the clot until they meet and reestablish a continuous epithelial sheet (Galko & Krasnow 2004). During this process, there is reorganization of epithelial structure and

cell's cytoskeleton adjustments (Moussian & Uv 2005; Jacinto et al. 2001). Insect immunity consists of a panel of humoral and cellular defense mechanisms, acting local and systemically, which together provide efficient protection against pathogens. The humoral component of the immune system include the transcriptional activation of genes that lead to the production of effector molecules that recognize (Pattern Recognition Patterns, PRPs) and kill pathogens (AMPs, reactive intermediates of oxygen and nitrogen, and melanization of hemolymph) (Lavine & Strand 2002). AMPs are produced in the insect fat body and released into the hemolymph, but also in epithelial cells and in the insect´s blood cells, hemocytes (Lemaitre & Hoffmann 2007). Hemocytes, are involved in processes such as phagocytosis, formation of multicellular hemocyte aggregates, nodulation and encapsulation of invading pathogens, and production of oxygen and nitrogen reactive species (Strand 2008; Eleftherianos & Revenis 2011; Yi et al. 2014). Hemocytes are recruited to the wound site and engulf damaged epithelial cells and pathogens (Wood et al. 2006; Lavine & Strand 2002; Losick et al. 2013). These wound response processes are highly conserved, but there are also particularities of wound response in different species and in different developmental stages and/or tissues (Bosch et al. 2005; Gurtner et al. 2008).

An interesting particularity of wound response occurs in some Lepidopterans, the insect order of butterflies and moths. Wounds in developing pupal wings can lead to the formation of organized pigmentation patterns centered at wound sites (Nijhout 1985; Brakefield and French 1995; Otaki 2011). The wound response process is typically and broadly tightly connected to pigmentation, and presence of different pigmentation patches and spots at wound sites is very common (Levesque et al. 2012; Binggeli et al. 2014). In this

particular wound response in a pre-adult and post-growing developmental stage, there is the formation of well-organized pigmentation patterns that resemble native wing eyespots, pattern elements composed of concentric rings of different colors (Figure 2.1A).

Butterfly eyespots have been prime models for evo-devo studies (Beldade & Brakefield 2002) including studies of the origin and diversification of evolutionary novelties, lineage specific traits (Beldade & Brakefield 2002; Saenko et al. 2008). Eyespots develop around organizing centers that, early in pupal wings are though to produce diffusible signals that induce surrounding epidermal cells to form rings of different colors (French & Brakefield 1995). Wound sites also behave like organizers, releasing signal to the surrounding and promoting recruitment of immune cells and reepithelization (Niethammer et al. 2009; Bidla et al. 2009; Galko & Krasnow 2004). The fact that wound sites can induce the production of eyespot-like patterns lead to the suggestion that the evolutionary origin of butterfly eyespots might be related to the co-option of wound response genetic circuitry conserved across insects (Monteiro et al. 2006). Co-option is a process by which evolution recycles ancestral genetic circuitries shared across lineages to produce novel traits (True & Carroll 2002; Ganfornina & Sánchez 1999). Melanogenesis is a good example of this pleiotropy; being involved in body pigmentation, but also in other important physiological functions such as immunity (Kim et al. 2013; Wittkopp & Beldade 2009). Since immunity is activated after wounding, the melanin pathway genes are good candidates to bridge the wound response and the developmental mechanisms to form eyespot-like patterns. However, until now the expression of these genes or other immune related genes was not reported in early stages of eyespot development. Early studies revealed that the ability to induce

eyespots around wound sites is restricted in time (6-18h post-pupation, for *B. anynana* individuals developing at 27°C) and space (on the distal half of the dorsal surface of forewings) (Brakefield and French 1995).

In this study we aimed at characterizing the molecular and cellular commonalities between wound response and eyespot development, which underlie the hypothesis of co-option of wound response genetic circuitry into the evolutionary origin of eyespots. We wounded *B. anynana* pupal wings to compare gene expression profiles of wounded and non-wounded wings, and we investigated the spatial patterns of gene expression of “wound genes” and “eyespot genes” at eyespot centers and wound sites respectively. We also analysed the cellular organization at wound sites and presumptive eyespot centers. Our results shown that, genes (AMPs and melanogenesis enzymes) and cells of innate immune system (hemocyte-like cells) are present at wound sites and also at presumptive eyespot centers. Antp, which is known to be involved in eyespot development, is also expressed at wound sites. This suggests that innate immunity mechanisms might have been co-opted during evolution for eyespot development.

2.3. Materials and Methods

2.3.1 Animals

B. anynana wild-type laboratory stock was reared as described in (Brakefield et al. 2009). Briefly, the butterflies were maintained at 27°C (+/- 0.5ºC) with 65% (+/-1%) humidity on a 12h light/dark cycle. Eggs were collected in young maize plants from adult cages (45x45x45cm; BugDorm-44545) with approximately 400 individuals fed with fresh banana on top of wet cotton. Larvae were fed with fresh maize plants and maintained at densities of 150 to 200 individuals per

cage (same size as adult cages). During the fifth larval instar we sexed larvae keeping only females for this study. Pre-pupae were collected onto 25 well plates and pupation time was recorded during the night via time-lapse photography (one photo every 10 min; Canon 1000D digital camera, Hahnel Giga T Pro 2.4GHz wireless timer remote control).

2.3.2 Wing wounding and dissections

The experiments had two groups: non-wounded individuals (NW) with no manipulation, and wounded (W) individuals, which were wounded twice for gene expression microarray analysis and qPCR. Wounds were inflicted with a tungsten needle (cat. no. 501317; World Precision Instruments) on the dorsal surface of the right forewing; in the two vein-bound wing compartments below the anterior eyespot, approximately halfway between the wing margin and the normal location of the eyespots (Figure 2.1B). In experiments of spatial patterns, in situ hybridization (ISH), fluorescent in situ hybridization (FISH)) and immunohistochemistry (IHC) we wounded as before, but only did one wound on the first wing compartment below the anterior eyespot. All wounds were inflicted at 12 hours post-pupation, according to Brakefield and French this is the best time point to induce an ectopic eyespot (Brakefield & French 1995). After wounding, all pupae were returned to 27°C until further manipulations.

For gene expression microarrays analysis and qPCR we dissected the wings removing the attached external cuticle. We dissected wings at two different time points for gene expression microarray analysis (four and eight hours post-wounding (Figure 2.1B) and five different time points for qPCR analysis (two, four, six, eight and 10h post-wounding). For the gene expression spatial patterns

(ISH) and cellular structure analysis (IHC) we dissected the wings keeping the attached external cuticle, which helps to maintain the wing integrity.

2.3.3 RNA isolation and cDNA preparation for microarray

The distal half of each dissected forewing (without the cuticle) was used for RNA isolation. We had two replicate pairs of samples (wounded and non-wounded wings) for each of two time points (16hr and 20hr post-pupation, corresponding to 4hr and 8hr post-wounding, respectively). Total RNA was extracted with TRIzol (Invitrogen) following manufacturer's instructions. RNA in RNAse-free water was checked for concentration and purity (A260/A280 ratio of > 1.8) by spectophotometry (NanoDrop), and for integrity by running in a 1.1 % agarose gel. We used total RNA to synthesized and amplify cDNA using the Ovation System (NuGEN) with oligo-dT primer and following manufacturer's instructions. We then purified the cDNA using Quiaquick cleanup kit (Qiagen) with a final elution volume of 30 µl in 1x TE buffer. Purity and concentration of cDNA samples was assessed in NanoDrop and agarose gel. All cDNA samples met the requirements for NimbleGen-Roche hybridization (A260/A280>1.7, A260/A230>1.5, >1µg cDNA/sample) and were stored at -20°C prior to shipment to NimbleGen-Roche (Madison, WI, USA) on dry ice. Cy3 labeling of cDNA was done at NimbleGen-Roche starting with 1 µg of quality-controlled cDNA (Agilent Bioanalyzer) and using Cy3 random primers and Klenow enzyme. Each sample of cDNA with added Cy3 random primers was heated to 98°C for 10 min and then cooled on ice for 10 min, after what Klenow and dNTPs were added before incubation at 37°C for 2hr. Reaction was stopped by adding 10 µl EDTA. Labeled cDNA was then precipitated and used in hybridization.

2.3.4 Microarrays, hybridization and slide scanning

To measure gene expression levels, we used Custom Nimblegen-Roche microarrays (Gene Expression 4x72K Arrays) with features designed to represent 15830 *B. anynana* gene objects, corresponding to contigs or singletons resulting from the assembly of >200,000 ESTs (mostly from developing wings) described elsewhere (Beldade et al. 2006; Beldade et al. 2009), as well as a number of other genes that had been previously cloned and implicated in *B. anynana* wing patterning. A gene can be represented by multiple gene objects, which are named with C[number], standing for contig; S[number], standing for singleton, a contig uniquely associated to a UniGene (c.f. (Beldade et al. 2006); and P[number] for those previously cloned by P. Beldade. The custom array contained 76,697 60mer probe features including 69,921 corresponding to the *B. anynana* genes (each gene object being represented by 1-6 probes) and a number of different types of controls (including 2,000 random probes). Microarray hybridization, scanning and image extraction was performed at Nimblegen-Roche following standard protocols (NimbleGen 2011). NimbleGen provided access to the image files as well as to the corresponding PAIR files. We used the non-normalized fluorescence values (raw intensities) for further analysis.

2.3.5 Data normalization and levels of gene expression

The raw intensities provided for each microarray feature were normalized with the software ANAIS, a web-based tool for the processing of NimbleGen expression data (Simon & Biot 2010). Briefly, raw intensities were normalized for intra-array (RMA background correction) and inter-array (quantile) variation. The same tool was also used to do the “probe to gene conversion” (using median value of all

probes for each gene) and a quality control analysis. We verified the result of the normalization through the alignment of all arrays boxplots (Quality Controls; Boxplots by array option – Figure 2.1C top), and also the reproducibility of results, by clustering analysis (Quality Controls; Hierarchical clustering of all arrays option –Figure 2.1C bottom). The latter revealed that samples clustered first by individual (wounded and non-wounded wings of each individual) and second by time point (16 and 20hrs). Details of these analyses are described in (Simon & Biot 2010). Having only two biological samples per time point precluded the typical analysis of gene expression differences using false discovery rate (Reiner et al. 2003). On the other hand, the design of comparing wounded and non-wounded (control) wings of single individuals allows a paired analysis.

Statistical analysis of normalized intensities was done in R (R Development Core Team 2015). For each gene object in each individual we first calculated the gene expression in wounded relative to control wing (log2Fold Change (FC) = log2 (intensity in wounded wing) - log2(intensity in control wing)), and after the respective fold change (FC = 2 ^ log2FC) (Quackenbush 2002). We considered as differently expressed, gene objects that were at least FC>2 (up-regulated) or FC<2 (down-regulated) in both biological replicates at each of the two time points.

2.3.6 Gene annotation and GO enrichment analysis

To determine whether the differently expressed genes represented particular functional classes we ran an enrichment analysis of Gene Ontology (GO) terms associated with those genes. Microarray gene objects were first annotated by blastx (in Blast2Go v2.2.25+ (Conesa et al. 2005)) against Arthropoda genomes,

comprised of 2,411,977 proteins (from NCBI data bases; March 2015), with 2,062,374 corresponding to insects. For each gene object, we retained the best hits (threshold e-value <= e-10). From 15,830 gene objects in the array, 3,635 were annotated in this way. Each annotated gene object was associated to single or multiple GO terms, and the list of GO terms associated to each gene object was used as a "customized genome reference" in gene enrichment analysis done in Cytoscape v2.8.3 , using the BINGO v2.4.4 plugin (Smoot et al. 2011; Maere et al. 2005). Cytoscape runs the hypergeometric test using Benjamini–Hochberg false discovery rate (Benjamini & Hochberg 1995) of 5% to assign overrepresented GO-biological processes categories in the list of differentially expressed genes.

2.3.7 RNA isolation and cDNA preparation for qPCR

Left and Right forewings were extracted, together with overlying cuticle, from NW and W pupae (see above) at five different time points: 2, 4, 6, 8, and 10h post wounding. The wings were collected directly into a 2mL epp with a 7mm glass bead and 500µL of TRIzol (Invitrogen), kept at -20°C until all the samples of that day were collected and then they were disrupt and homogenized for 5 min at maximum speed in TissueLyserII (Qiagen) and stored at -80°C until RNA isolation.

Total RNA isolation was performed following manufacturor's protocol without DNase treatment. To avoid possible genomic DNA contaminations we designed all qPCR primers spanning an intron. RNA was diluted in 25 µL of RNAse-free water, checked for integrity by running in a 1 % agarose gel and stored at -80°C until cDNA synthesis. RNA concentration was measured for 30 wings (from 15 individuals) and it ranged from 150 to 400 ηg/µL. Differences in RNA

concentration measured in nanodrop were well correlated with differences in intensity of bands in the agarose gel. We classified the band intensity in three classes: 200, 300 and 400 ± 25 ηg/μL and added 100, 200 and 300 μL of RNAse-free water respectively. The final concentration was ranging from 30 to 40 ηg/μL (nanodrop measurement after dilution in 20 wings). We optimized the cDNA synthesis for a 10μL of total reaction volume with 40U of the reverse transcriptase (M-MLV RNase H Minus, Promega) using oligo(dT) as primer and ~400ng of total RNA as template and following manufacturer's instructions. The cDNA was diluted in 40 μL of PCR graded water in a final volume of 50 μL of cDNA per sample. We synthesized cDNA twice to obtain two technical replicates for each RNA sample.

2.3.8 qPCR reference genes

To find a suitable reference gene, we defined three criteria: 1) different amplicon sizes for cDNA and gDNA, 2) primer efficiency between 90 and 110%, and 3) gene expression stability across treatments (NW and W) and wings (left/control and right/wounded) (Taylor et al. 2010). For the sequences of eight possible reference genes (*Elongation Factor1-β* (*EIF1β*); *β-Tubulin* (*β-Tub*) and six ribosomal like proteins: *RpL3*, *RpL8*, *RpL9*, *RpL10A*, *RpL15*, and *RpL19*) (Beldade et al. 2006), we first did a nucleotide blast against *Bombix mori* data base (Goldsmith et al. 2005) to know the possible intron locations and designed primers spanning an intron. This design allows us to distinguish cDNA and genomic DNA amplifications based on size of amplification product. Three genes had same size bands for cDNA and genomic DNA (*β-Tub, RpL9* and *RpL19*) and were excluded. Second, to test the efficiency of the primers of other five

genes we ran a qPCR with serial dilutions of a mix sample with left and right wings from NW and W individuals. Three genes, *RpL8, RpL10A* and *RpL15*, had efficiency between 90 and 110% (Taylor et al. 2010). Third, we ran another qPCR to test if there were differences in candidate reference genes between left and right wings and between NW and W groups. In this experiment we used two biological samples per wing and per treatment. Ct values were input in the online-available tool NormFinder (Vandesompele et al. 2002; Teng et al. 2012), which tests gene expression stability. Briefly, this method is based on the principle that the expression of control should be identical in all samples, regardless of the experimental condition or cell type, with increasing variation corresponding to decreasing expression stability (Vandesompele et al. 2002). *RpL10A* and *RpL15* genes had higher stability values and they were selected to be the endogenous reference genes. After we had run six 384 well plates (corresponding to the samples of 4hrs and 8hrs post-pupation), we verified that the two selected reference genes behaved in the same way and we selected *RpL10A* as the reference gene because the Ct values were more similar to those of our samples.

2.3.9 qPCR reaction and gene expression quantification

We used the 7500 Real-Time PCR equipment (Applied Biosystems®, Inc.) to run 10μL qPCR reactions with: 5μL iQTM SYBR® Green supermix (BioRad), 3.6μM of each primer, 1μL of cDNA template. The temperature cycling included an initial step of 95°C for 10min, followed by 40 cycles of 95°C for 20 sec, 59°C for 20 sec, and 72°C for 30 sec. We excluded samples with primer dimmers or unspecific amplifications based on the analysis of melting picks

(Ririe et al. 1997) obtained from the dissociation curve (59-95°C), using SDS software (version 1.4; Applied Biosystems®, Inc.).

Gene expression levels were determined for eight genes, eight biological replicates (each with left and right wings), five time points (2, 4, 6, 8 and 10hrs post-wounding), two treatments (NW and W) and two technical replicates (two cDNA replicates from same RNA). The eight target genes were selected from the microarray analysis: *Glov2*, *tyrosine hydroxylase* (*ple*), *primo-1* (*pri1*), *c-type lectin 10* (*c-tl10*), *lysozyme-like protein 1* (*lys-lp1*), *cecropin 6* (*cec6*), *cecropin D* (*cecD*) and *protease inhibitor 6* (*pro-in6*), and were reported having immune related functions in other organisms. The qPCR reaction efficiency for these genes, as determined using the methods described by Taylor and colleagues (Taylor et al. 2010), was 100%±10% (Taylor et al. 2010). The ΔΔ Ct method (Livak & Schmittgen 2001; Pfaffl & Pfaffl 2001) was used to calculate the relative expression levels taking the left wing, which for NS group was the non-wounded wing, as the reference. The relative expression of right relative to left wings was imported to R (R Development Core Team 2015) for graphical representation and statistical analysis.

For the statistical analysis we first tested if the residuals of a linear model (lm(relative expression ~ treatment * time point * technical replicate * qPCR plate) were normally distributed (Shapiro test) (Royston 1993).They were not normally distributed and we could not transform it to obtain a normal distribution. Thus, we used the generalized linear model (glm). The residuals increased as the relative expression increases, so we used the glm for a Gamma distribution (Crawley 2007). For each gene, we tested if the most complex model, glm(relative expression ~ treatment * time point * technical replicate * qPCR plate), was explaining significantly better the variation across

samples than simpler models without technical replicate and qPCR plate effects. There were no statistical differences for any gene relative to technical replicates, so we used the mean of technical replicates. The qPCR plate had effects only in two genes, *cecD* and *pro-in6*. After running the pairwise multiple comparison analysis for these genes (lsmeans package) (Lenth & Hervé 2015), we saw that there were no differences between qPCR plates in any time point (2, 4, 6, 8 and 10h) or in treatments (W and NW). This indicates that even for these genes the effect of qPCR plate was marginal, so we considered a simpler model, glm(relative expression ~ treatment * time), to test if there were statistical differences between treatments, time points and interactions between them, for all genes. To know if the treatments were different for each time point we used the R package lsmeans for a pairwise comparison analysis (Lenth & Hervé 2015).

2.3.10 *In situ* hybridization (ISH) and fluorescent *in situ* hybridization (FISH)

Wings were collected attached to the cuticle at 4 and 8h post-wounding, fixed and dehydrated, as described in (Reed et al. 2011), before storage in methanol at -20°C until ISH or FISH. After rehydration (Reed et al. 2011), we followed the ISH protocol for wings described in (Saenko et al. 2011). We tested five genes: *Glov2*, *pri1*, *lys-lp1*, *pro-inh6* and *ple*, which were revealed in microarray analysis. We also had *Dopa decarboxylase* (*Ddc*) a well-known melanogenesis gene that also was up regulated in microarrays. Gene-specific primers (supplementary Table S2.1) were used to amplify the gene fragments inserted in pGMT-easy plasmid vector (Promega) and to synthesize antisense RNA probes. All RNA probes were ranging from 500 to

650bp. For ISH, the probes were labeled with digoxigenin (DIG) by in vitro transcription with T7 or SP6 RNA polymerase (Promega) in a reaction containing DIG-UTP (DIG RNA labeling mix, Roche) and following manufacturor's instructions. For FISH, we labeled ple probe with DIG as before and Glov2 probe with biotin, using a BIO RNA labeling mix (Roche) following the same protocols described for ISH. We detected DIG and biotin with sheep anti-DIG (Roche) and mouse anti-biotin (Roche) primary antibodies, respectively. These primary antibodies were then detected with secondary antibodies, anti-sheep and mouse coupled with Alexa 488 and 594 (Invitrogen), respectively, following the protocol described in (Kosman et al. 2004).

ISH images were acquired in a stereoscope (Leica MZ6 Stereoscope) coupled to a digital camera (Leica DFC420 C Digital Camera SW Kit) and analyzed in Fiji-ImageJ software (Schindelin et al. 2012). FISH images were acquired in the SP5 Leica SP5 confocal, using the 40x 1.3NA Oil immersion objective and for more detail of cells we applied zoom. Z-stacks were then converted into a single image, and its brightness and contrast were adjusted in Fiji software (Schindelin et al. 2012).

2.3.11 Immunohistochemistry (IHC)

We used wounded and control forewings with overlaying cuticle that were collected at 4 and 8 h post-wounding. The wings were fixed, dehydrated (5min sequential washed with 25%, 50%, 75% and 100% ethanol) and stored at -20°C until use. Immediately before starting the immunohistochemistry protocol described in (Saenko et al. 2011), the wings were rehydrated (5min sequential washes with 100%, 75%, 50% and 25% ethanol). We used DAPI or To-Pro and rhodamine phalloidin (Invitrogen) and followed manufacturer's instructions, to

stain nuclei and actin, respectively. We used antibodies against Antp 4C3 (dilution 1:200) (Condie et al. 1991), obtained from the Developmental Studies Hybridoma Bank, Engrailed (En) 4F11 (dilution 1:50) (Patel et al. 1989) and phospho-histone H3 (Ser10) 6G3 (Cortez et al. 2001) from Cell Signaling Technology (dilution 1:500). We detected them with anti-mouse Alexa 488 (Antp, and En) and anti-mouse Alexa 647 (phospho-histone H3 (Ser10)) (dilution 1:200) (Invitrogen).

For IHC we used the Lightsheet microscope (Gualda et al. 2013) available at Instituto Gulbenkian de Ciência. Light sheet microscopy is a fluorescence microscopy technique, where the illumination is done perpendicularly to the detection. The technique shapes the illumination laser beam into a rectangle and then focuses it down only in one direction, using a cylindrical lens (SPIN). This forms a thin "sheet of light" right in the focal plane of the detection objective, illuminating the whole sample plane at the same time. After staining, wings were introduced in a glass cylinder filled with of liquid agarose (0.1%), after solidification the glass cylinder was removed and the wings were imaged with the 4x and/or the 10x objectives with 0.13 and 0.30NA, respectively. Because of the wing curvature, it was difficult to obtain images with eyespots and wound sites focused on the same plane.

Mitotic cells were detect in the Zeiss' Stereo Lumar fluorescent stereoscope (wings dissected 1h30 min after wounding) in z-stack series that were converted into a single image through z-projection maximum intensity in Fiji software (Schindelin et al. 2012). Mitotic cells were quantified in wings dissected at 4h post-wounding. Images were acquired in a SP5 Leica SP5 confocal, using 10x 0.40NA objective. Z-stacks were converted into a single image, and its brightness and

contrast were adjusted in Fiji software (Schindelin et al. 2012). The wings were imaged in the anterior distal area with anterior eyespot and wound site or corresponding wing region. We quantified the area of fluorescence for DAPI and for phospho-histone H3 (Ser10) in the total image area (1550 μm2) for five individuals. The fluorescence intensity was adjusted equally in all images for each fluorophore using the threshold intensity tool of Fiji, which selects all the pixels in the image above certain fluorescence intensity. We saw that there was interaction between the wing (wounded and control) and the total area, so we could not use the ANCOVA for the statistical analysis. Thus, we used a glm model to test if despite these interaction, there were differences in the area of mitotic cells between wounded and control wing taking the area of total cells in the image as covariant (glm(mitotic cells area ~ wing * total area)).

2.4. Results and Discussion

Co-option is a recurrent evolutionary strategy to develop lineage specific traits (True & Carroll 2002). Here, we explored the recruitment of genes related with wound response, an ancient evolutionarily conserved process (Moussian & Uv 2005; Neves et al. 2015; Vilmos & Kurucz 1998), for the development of the Lepidopterans eyespots, lineage specific traits (Beldade & Brakefield 2002; Saenko et al. 2010). We also investigate the expression of genes related with eyespot development at the wound site and the cellular structure at the wound site and presumptive eyespot center. We started comparing the gene expression profiles (microarrays, Figure 2.1 and 2.2), dynamics (qPCR Figure 2.3) and spatial patterns (ISH, Figure 2.4 and FISH 2.5) for pairs of wounded and non-wounded wings. After we compared the expression of target genes related with eyespot development (Figure

2.6) and the cellular structure at wound sites and presumptive eyespot centers (IHC, Figure 2.7).

2.4.1 Wound response induces the expression of AMPs and melanogenesis enzymes in *B. anynana* early pupal wings

The wound response in insects is well-studied in Drosophila, mainly during embryonic and larval developmental stages (Lemaitre & Hoffmann 2007; Mace et al. 2005). The genetic response during pupal stage, a post-growth and pre-adult stage, is poorly understood in insects (Regan et al. 2013). Here, we used the butterfly *B. anynana*, which develops organized pigmentation patterns around wound sites (Brakefield & French 1995) (Figure 2.1A), to understand the "generalities" and the "particularities" of pupal wound response. We compared gene expression profiles of wounded (manipulated wings, M) *vs.* control (C) wings of the same individual (paired samples) to access gene expression changes induced by wounding pupal wings in a manner that typically leads to the production of wound-induced ectopic eyespots (Brakefield & French 1995). M and C wings of two biological replicates were collected at 4 and 8h post-wounding (Figure 2.1A) and mRNA levels therein used on a custom-made microarray of *B. anynana* genes.

This experiment was a pilot test performed in 2007 and designed to test and validate the Custom Nimblegen-Roche microarrays made with *B. anynana* gene objects. For economic reasons, it was decided use only two biological samples and compare wounded and non-wounded wings in two different time points (Figure 2.1B). It was expected that paired wings clustered together as well as same time point wounded individuals. Indeed, this was the case (Figure 2.1C bottom). It was also expected that wounded wings expressed some

well-known genes related with insects wound response, which also happen (Figure 2.2B). This experiment was enough to validate the *B. anynana* Custom Nimblegen-Roche microarrays as a methodology to study gene expression in this model system. However, with only two biological replicates it was not enough to make a proper microarray statistical analysis (Pawitan et al. 2005). Nevertheless, once we were studying the wound response in this model system we decided to look at this data, considering its limitations and adopting a conservative approach that reduces false positives at the expense of increasing false negatives hits. After normalization analysis (Figure 2.1C top), we considered as differentially expressed gene objects that were expressed at least twice (fold change (FC)>2; up-regulated), or half (FC<2; down-regulated) on M *vs.* C wings in both biological replicates. With these criteria, we obtained a total of 7821 differently expressed gene objects, corresponding to 3160 at 4h and 4661 at 8h.

The comparison of gene expression in paired wings revealed that the majority of differently expressed genes were not common for the replicate individuals (93% at 4h and 92% at 8h)(Figure 2.1D). The variation in wound response gene expression might indicate other levels of variation such as 1) developmental time: the time in hours that we quantified (4 and 8h post-wounding) might not correspond to the same biologic developmental time in both biological replicates; 2) genetic: biological replicates might have considerable genetic differences since we were using an outbred stock, and 3) developmental and genetic: a conjugation of the two previous variation sources.

We only proceeded with the analysis of genes objects that were differently expressed in both biological replicates (Figure 2.1D). This conservative approach reduces false positives, which is critical

because the limitations in the experimental design. Considering only those genes, we obtained a list of 624 gene objects, 20% (126 genes) were up-regulated in M *vs.* C wings at 4h, 40% (249) at 8h, and 18% (112) and 22% (137) were down-regulated at 4 and 8h, respectively.

From the 624 gene objects differently expressed in M *vs.* C wings of both replicates only 34% were annotated (214 genes). 60% of annotated genes were up regulated (52 at 4h and 74 at 8h) and 40% down regulated (33 at 4h and 55 at 8h) (Figure 2.2A). All annotated genes were used in a gene enrichment analysis for GO biological processes. This analysis revealed that in total for both time points there were 48 genes in the enriched biological processes (hypergeometric test with Benjamini & Hochberg False Discovery Rate correction (p-value<0.005)), distributed over 52 different GO terms (one gene can be included in one or more GO terms). At 4h there were 20 genes representing 36 enriched GO terms and at 8h there were 29 genes representing 40 enriched GO terms. In total, 24 GO terms were enriched in both time points (Figure 2.3B) containing seven up-regulated genes (three antimicrobial peptides (AMPs) and four melanogenesis related genes) that were common to both time points. The only down-regulated enriched genes are from GO terms related with cuticle development at 8h.

The same gene is typically associated with several GO terms, so we grouped the GO terms list in three general categories according with their biological processes: peptides that kill cells of other organisms or modulate this response were grouped as AMPs, enzymes related or similar to melanogenesis pathway enzymes as melanogenesis, and none of these as other. At 4h there were seven enriched genes in the AMP category and six at 8h, but at 4h all genes were related with activation of immune system and at 8h there were

also negative regulation of immune response (Figure 2.2C). The enrichment for melanogenesis genes was higher for both time points relative to the other two categories with same number of genes (13), including known melanogenesis pathway enzymes such as *ple* and *Ddc*.

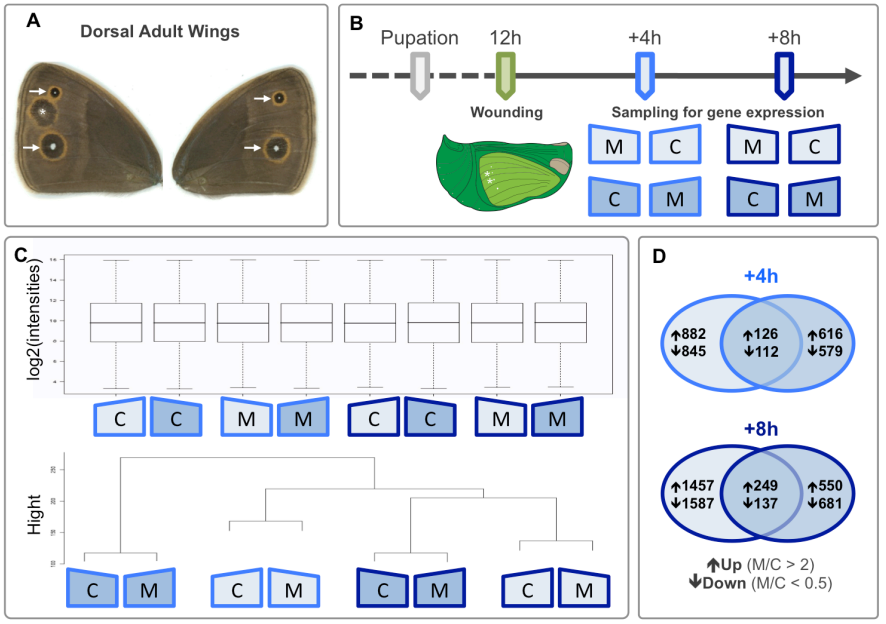

Figure 2.1- Wound response transcriptomic analysis. A) Phenotypic effects on adult wing dorsal side. Epidermal wounding on wings of 12h old pupae induces the formation of an organized pigmentation pattern around wound sites (*) similar to native eyespots (arrows). B) Experimental design: pupae were wounded twice in one of the forewings (asterisks in green drawing representing a pupa) at 12h post-pupation and both their wings (wounded/manipulated, M, and contralateral/non-wounded, C) were collected 4 or 8h post-wounding. We had two individuals per time point (represented as two shades of light (4h) or dark (8h) blue). C) Quality control graphics of the microarray data. Boxplot of intensities after data normalization (top) and hierarchical cluster of normalized intensities (bottom). D) For each collection time point, the Venn diagram represented the number of differentially expressed genes, at least two-fold difference in gene expression between C and M wings of each individual (each circle). Upwards and downwards arrows represents genes over-expressed and under-expressed, respectively, in M *vs.* C wings of each individual.

The annotated genes that were differentially expressed in M *vs.* C wings were mainly from two main categories: AMPs and melanogenesis pathway enzymes (Figure 2.2B and C). Both categories have well-known functions in insect wound response and infection (Lemaitre & Hoffmann 2007; Tanaka & Yamakawa 2011). The other differentially expressed genes without annotation can be considered candidates to "particularities" of this wound response, which might cover specific wound genes acting during pupal stage across insects, and also specific genes that promote the development of pigmentation color patterns in Lepidopterans. In this list also can be represented new "general" conserved wound response genes.

We validated and extended the microarray results through qPCR. We selected differently expressed genes and quantified the gene expression at 4 and 8h post-wounding as in microarray analysis. We added three more time points (2, 6, and 10h post-wounding) to better understand the gene expression dynamics of these genes after wounding. The criteria to select genes in this analysis were expression difference between M and C wings we considered only genes with at least one intron, which allows intron spanning primer design to differentiate the cDNA and gDNA amplification products. We selected *cec6* and *cecD*, two AMPs, from AMP category and *ple* and *pri1* from melanogenesis category. We also included non-annotated genes (see supplementary File S2.1 – available only online) with high sequence similarity with genes or protein domains described to be involved in insect defense mechanisms. Glov2 is an AMP (Kaneko et al. 2007) and lys-lp1 is a lysozyme like protein, both are effector gene in immune system playing a role in killing bacteria (Crava et al. 2015). c-tl10 is a (Ca(2+))-dependent lectin and is involved in pathogen recognition (Cambi et al. 2005). Pro-in6 is a protein with a trypsin

inhibitor-like cysteine-rich domain; proteins containing this domain play an

Figure 2.2- Wounded wings are enriched for genes encoding for AMPs and melanogenesis pathway enzymes. A) Number of annotated and non-annotated genes differentially expressed in M *vs.* C wings. B) Heatmap table representing the gene enrichment analysis for the list of annotated genes. GO terms of up-regulated genes are in red; those of down-regulated genes are in blue. White represents the non-enriched GO terms. The numbers represent the proportion of genes differently expressed relative to genes of these GO term present in the microarray. Negative values represent down-regulated GO terms. C) Percentage and number of genes that are related with AMPs, melanogenesis and other than these biological processes.

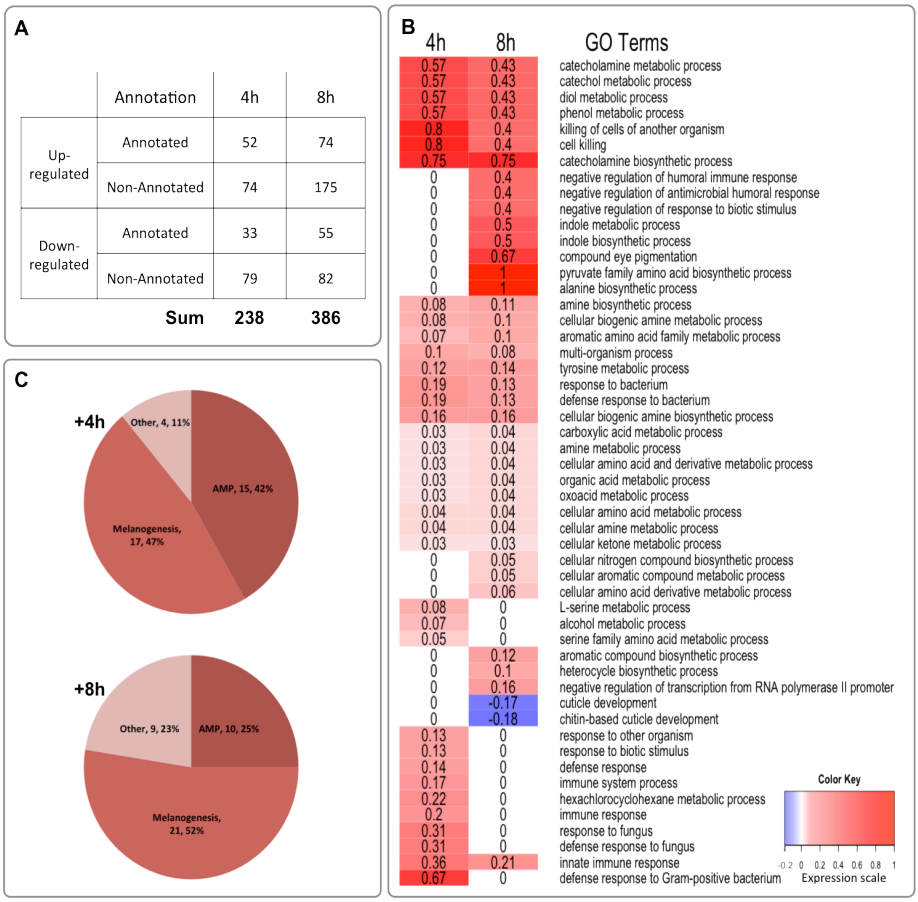

important role in immune response and anticoagulation (Zeng et al. 2014; Jin et al. 2011) . Based on these putative functions we grouped the *Glov2*, *lys-lp1* and *c-tl10* together with *cecD* and *cec6* in the AMP category. *pro-in6* was grouped in melanogenesis category because in insects this pathway is involved in coagulation processes (Márkus et al. 2005). According to microarray results, three of the eight genes were up-regulated at 4 and 8h post-wounding: *Glov2* (4h: 14.73, 5.51 and 8h: 8.04, 6.50; results of two biological replicates), *pri1* (4h: 3.83, 3.20 and 8h: 3.45, 4.05) and *ple* (4h: 9.34, 10.59 and 8h: 16.43, 23.14); four genes only at 4h: *cec6* (4h: 2.12, 2.18), *cecD* (4h: 2.32, 2.63), *c-tl10* (4h: 6.67, 5.93) and *pro-in6* (4h: 6.89, 2.65); and one

gene only at 8h *lys-lp1* (8h: 5.33, 3.71) (supplementary File S2.1 – available only online).

In this experiment we compared gene expression differences of M and C wings between wounded individuals (wounded group, W) and non-wounded individuals (non-wounded group NW) (Figure 2.3). There was substantial variation in expression levels among biological replicates, particularly in the W group. Still, it is clear that for all genes in both time points the W group had more individuals with higher fold change differences between M and C wings than the NW group. Expression fold differences within NW individuals are generally very close to 1 (dashed line), reflecting no differences between the two wings of each individual. The statistical analysis demonstrated that the treatment (W and NW) had a significant effect for all genes, that there were differences in gene expression across time points for *cec6*, *cecD* and *ple* and that there were an interaction between treatment and time point for *ple* and *pri1* (Figure 2.3).

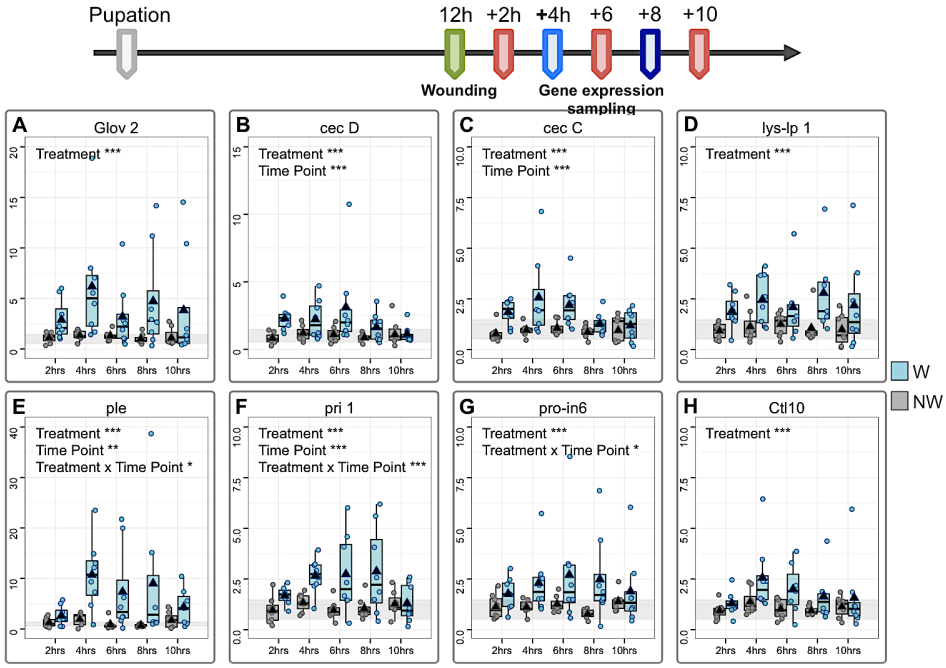

Figure 2.3- Relative to contra-lateral control wings, wounded wings express higher levels of genes involved in immunity and melanogenesis. Gene expression is represented as fold change of expression in wounded or right wings relative to control or left wings. Gene expression differences are shown for two different treatments: non-wounded group (NW; gray dots) in which left and right wings were not manipulated, and wounded group (W; blue dots) in which the right wing was wounded 12h post-pupation, We quantified genes expression at 2, 4, 6, 8, and 10h post-wounding. Each dot represents the mean of two technical replicates for each biological replicate and black triangles represent the mean for the biological replicates. The dashed line represents fold change equal to 1 (no differences in gene expression between both wings). Differences were tested for treatments, time point and interactions between both; (ns) p-value>0.05, (*)p-value<0.05, (**)p-value<0.005. (***)p-value<0.0005. Within each time point identical letters correspond to values that are not significantly different (p>0.05), while different letters indicate significant differences between groups (p<0.05). Sample sizes were between five and eight replicate wing pairs per treatment per time point. The top scheme is the experimental design.

For *Glov2* there were differences between W and NW in all time points. All the other genes had consistent but smaller differences in gene expression between groups. This result confirms that hits revealed in the microarray analysis are indeed up-regulated in wounded wings. Thus, the list of differentially expressed genes (supplementary File S2.1 – available only online) might be explored in future work to better understand the “particularities” of this wound response that induces the development of organized pigmentation patterns. Nevertheless, a study with more biological samples can improve this list including genes that might be excluded here.

The expression of *Ddc* (Figure 2.3C) and *ple* after wounding was already described for embryos in drosophila and was regulated by Grainy head transcription factor (Wang et al. 2009). These results indicate that during pupal stage the wound response also might

activate the same pathways leading to transcriptional activation of *Ddc* and *ple*, and probably also genes with similar domains as *pri1* and *pro-in6* (Figure 2.3E and F) (Meister 2004; Crava et al. 2015). We did not find clear evidence of well-known melanogenesis genes (such as *ple* and *Ddc*) expressed in native eyespot field in early pupae.

The expression of these enzymes in the eyespot field is more likely to happen at later time points, when pigments are synthesized in pupal wings. This is the case for *Ddc* gene that is expressed in the corresponding adult wing darker pigment areas in late pupal stage (Supplementary Figure S2.1) (Wittkopp & Beldade 2009; Nappi & Christensen 2005). On the same wings we observed that four genes were expressed at the presumptive eyespot center: *Glov2* (Figure 2.4A) and *pro-in6* (Figure 2.4F) at 8h, and *lys-lp1* (Figure 2.4B) and *pri1* (Figure 2.4E) at both 4 and 8h. These expression patterns at the eyespot center are very faint. While for *pro-in6*, *lys-lp1* and *pri1* this experiment was run tested once, *Glov2* was detected in 11 of 17 wounded wings and six of 12 control wings (Figure 2.4A). For *ple*, we did not observe expression at presumptive eyespot centers for either 4 or 8h (0 in 13 wings stained) (Figure 2.4D). The expression of these genes around wound sites not only confirms the microarray data but also reveals were these genes are up-regulated in specific wing areas: around wound sites. Additionally, their expression in the presumptive eyespot centers underscores the existence of genetic commonalities between wound response and eyespot formation.

To better understand the cell distribution and gene expression at wound site and eyespot center we double stained mRNA for *Glov2* (Figure 2.4A), and *ple*, only at wound sites (Figure 2.4D). We observed, as in previous experiment, that *Glov2* and *ple* were up-regulated at wound sites (Figure 2.5B) relative to other wing areas

(Figure 2.5A). *Glov2* is expressed in diffuse pattern and *ple* is expressed in a smaller area but more intensely. Scrolling through z-stacks we realized that the cells that intensely stain for *ple* were localized on the surface of ventral epithelia (Figure 2.5E2) and that cells between both epithelia were staining for *Glov2* (Figure 2.5E5). The organization of these cells is different from those in the ventral wing epithelium (compare Figure 2.5A with Figure 2.5D), which are well organized in parallel rows of larger nuclei cells, alternated with cells with smaller nuclei (Nardi 1994). Cells in between epithelia near wound sites look like spread towards the wound edge (Figure 2.5D). Looking carefully to the nuclei shape and *Glov2* expression cells appear to have different shapes (drawings in Figure 2.5E1 and E5). However, in this experiment we did not stain the cells for a membrane marker, so we could not be certain about cell shape. We found cells expressing *Glov2* between epithelia (Figure 2.5D and E5) and also in what seems to be a cell compartment that stains heavily for Glov2 (Figure 2.5E7).

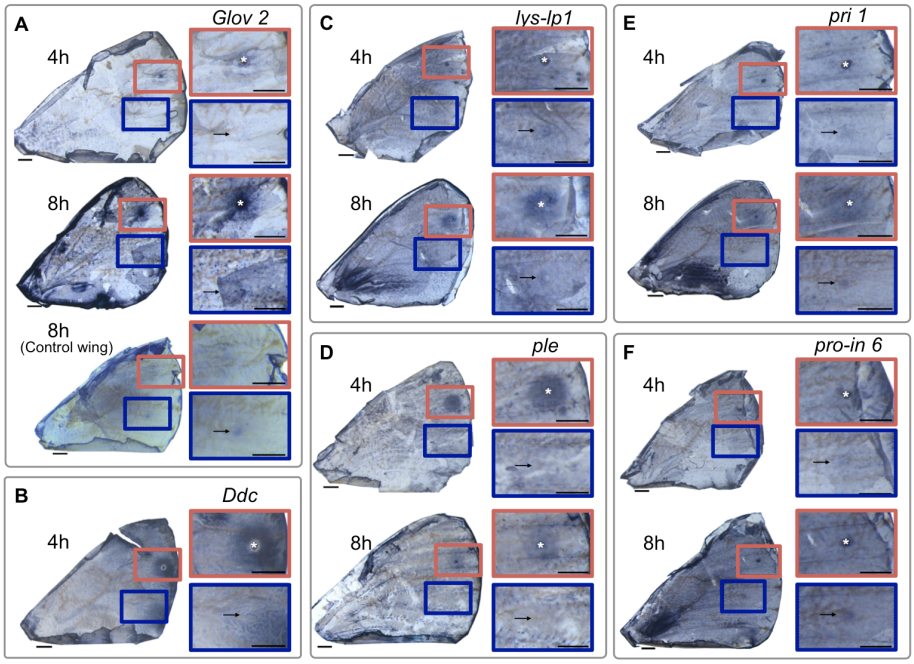

Figure 2.4- Selected genes from microarray study are expressed around wound sites and, in a few cases, at presumptive eyespot centers. Spatial patterns of *Glov2* (A), *lys-lp1* (B), *Ddc* (C), *ple* (D), *pri1* (E) and *pro-in6* (F) for wounded wings dissected at 4h and 8h post-wounding. The wings are presented and detail images of the wound site (red rectangle) and the most-posterior presumptive eyespot center (blue rectangle) are shown. The exact wounding position is represented with white asterisk and the black arrow indicating the position of eyespot center. The brownish background lines/patterns are from the cuticle, which is still attached to wings. All scale bars are 0.5mm.

The expression of AMPs after septic injury is well known (Lemaitre et al. 1997; Kaneko et al. 2007; Samakovlis et al. 1990), and it is more describe to occur in fat body and hemocytes, but it also occurs in epithelial cells, especially in the gut (Samakovlis et al. 1990; Kaneko et al. 2007; Crava et al. 2015). Cells between dorsal and ventral epithelia look like circulating hemocytes (Figure 2.5E5) (King & Hillyer 2013; Regan et al. 2013). During inflammation, which occurs after epidermal damage, there is migration of immune cell to the

injured sites (Wu et al. 2009; Williams 2007). This also might be the case in wounded pupal wings of Lepidopterans.

At the presumptive eyespot center only *Glov2* has increased staining relative to other wing areas (compare Figure 2.5B and C). As at wound site the z-projection images revealed a diffuse pattern for *Glov2*, so we looked to particular sections in the ventral (Figure 2.5E7 and E8) and in between both epithelia (Figure 2.5E9). In the ventral epithelia near the presumptive eyespot center we saw very few cells expressing *Glov2* and *ple*. We found cells expressing *Glov2* and *ple* (spread in the cytoplasm of elongated cells) (Figure 2.5E8) and cells expressing *Glov2* and in a presumptive cell compartment (Figure 2.57). Those last cells were very rare in the ventral epithelia (two posterior eyespots in seven observed). In between epithelia there were smaller clusters of cells expressing *Glov2* (Figure 2.5E9). These cells are very similar to the cells in same relative position at the wound site (Figure 2.5E5). The number of cells is reduced, but contrary to the cells in the ventral epithelium, this is not a rare event in posterior eyespot (six posterior eyespot centers in seven observed). This result raises the hypothesis that these cells might play a role in eyespot development.

To our knowledge, there are no reports of AMPs being expressed in developing butterfly eyespots. However, it is well-known that hemocytes produce AMPs and are present in young pupal wings in between dorsal and ventral epithelia (Nardi 1994; Nardi et al. 2006). In young pupal wings, hemocytes help to clean the cell debris resulting from molting (Nardi et al. 2001; Regan et al. 2013). The presence of patches of hemocyte-like cells at eyespot centers can occurs just because there are more cell debris at these sites, so there is need for more cells at this position. Epidermal wounding on eyespot centers 12h post-pupation induces an enlargement of the eyespot size

(Brakefield & French 1995), which might indicate that more hemocytes at presumptive eyespot centers produce larger eyespots. Furthermore, we only found these patches of cells in the posterior eyespot the larger one; at the anterior eyespot the presence of these cells was not different from other wing areas. Future studies in natural mutants with differences in eyespot size (P Beldade et al. 2008) might elucidate if larger eyespots are correlated with the presence of higher number of hemocyte-like cells at presumptive eyespot centers.

2.4.3 Antp, an "eyespot gene", is expressed at wound site

We tested two "eyespot genes", En and Antp, both known to be expressed during larval and pupal stage at presumptive eyespot centers (Monteiro et al. 2006; Saenko et al. 2011; Tong et al. 2014) and En also during pupal development at presumptive golden ring (Brunetti et al. 2001). Our results demonstrated that Antp is also expressed at eyespot centers during early pupa (16h post-pupation) (Figure 2.6B). In Satyrinae butterflies this Hox gene is the first known gene to be expressed at larval presumptive eyespot centers (Shirai et al. 2012; Saenko et al. 2011) and its expression might be essential through development to produce an eyespot.

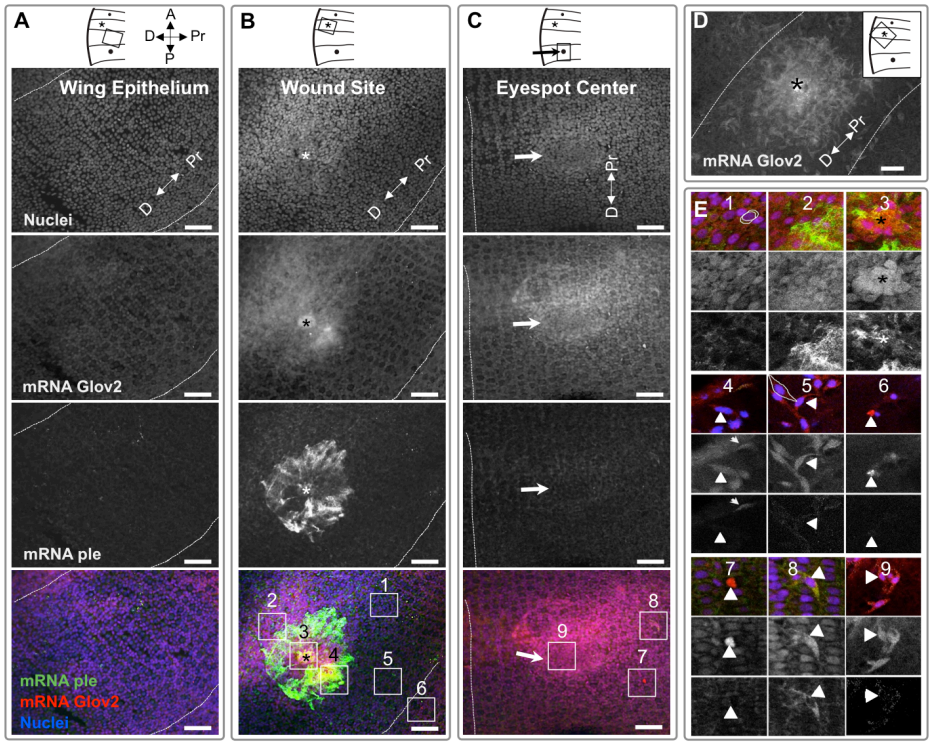

Figure 2.5- Cells of different shape and expressing *Glov2* are present between dorsal and ventral epithelia at wound site and presumptive eyespot center. A) *Glov2* and *ple* expression in epithelial cells is reduced relative to it's expression at wound sites (B). At the wound site, the expression pattern of *Glov2* is diffuse because there are cells staining for *Glov2* between dorsal and ventral epithelia (D); *ple* expression is very intense and restricted to cells near wound sites. C) *Glov2* expression is increased at presumptive eyespot center (arrow) but *ple* is not. Detailed images of the square sections (from 1 to 9) are shown in E. Gray images are Glov2 (center) and ple (bottom) expression. E1,E 2, E3, E7 and E8 are images from cells in the ventral epithelium and E4, E5, E6 and E9 from space between both epithelia. Images from A,B and C are z-projections of 19 - 23 stacks. D is a lower amplification of wing area shown in B for *Glov2* where we excluded the stacks containing ventral cells. In E1 to E9 the images are z- projections of 2 - 4 stacks. Drawings on E1 and E5 represent the approximate cellular shape. Arrowheads are pointing cells expressing *Glov2*. The drawings on the top indicate the approximate positions of the images and the crossed arrows the wing orientation; anterior (A), posterior (P), distal (D), proximal (Pr). Scale bars are 50µm and images from 1 to 9 are squares of 50x50µm. Images are from an

individual dissected 8h post-wounding, but similar results were found at 4h post-wounding.

As in previous studies, En was expressed at eyespot centers and golden rings, but at this time point (4h post-wounding) it was not expressed at wound site (Figure 2.6A). In contrary, Antp was expressed at wound sites (Figure 2.6B). As a transcription factor this protein is active when it is expressed in the nucleus as it occurs at eyespot center (Figure 2.6B). Unfortunately, in this experiment our nuclear staining did not worked and at the wound sites the Antp staining is dispersed. We first hypothesized that Antp expression at wound sites was unspecific binding of the antibody to the wound site, but the negative result of En (an antibody also produced in a mouse, run according same IHC protocol) at wound sites indicates that this is not the case (Figure 2.6). We also observed spots of Actin at eyespot centers, wound sites and also spread in an apparent random pattern over the wing (Figure 2.6B). These Actin spots are located between epithelia and some of them co-locate with cells expressing Antp (Figure 2.6). The actin staining at wound site is very intense as well as Antp (co-localization in yellow, Figure 2.6B).

Antp is expressed in insect hematopoietic cells that can differentiate in plasmatocytes, crystal cells and in cases of injury or infection in lamellocytes (Mandal et al. 2007; Grigorian et al. 2011). In other experiments we saw that hemocytes isolated from young pupae strongly stain for Actin (Supplementary Figure S2.2). Together, this indicates that the expression of Antp at wound site 4h post-wounding is reflecting the presence of hematopoietic precursor cells and those might be essential in hemocyte differentiation and wound healing. In this experiment, we classified Antp as an eyespot gene (Saenko et al. 2011), but in fact this transcription factor is a pleiotropic protein with multiple function during limb development (Shiga et al. 2002),

neuronal network (Joliot et al. 1991) and also in hematopoiesis (Grigorian et al. 2011; Mandal et al. 2007). Early after wounding it might be necessary to promote hemocyte differentiation. The function of this transcription factor at eyespot centers to produce an organized pigmentation pattern is not known. The new methodologies of genome editing can be an important tool to uncover the biological function of Antp during eyespot development. Nevertheless, even without this tool further experiments can be performed including IHC for Antp and nuclei, and image acquisition with a higher magnification objective for more detail of cells expressing Antp at wound sites.

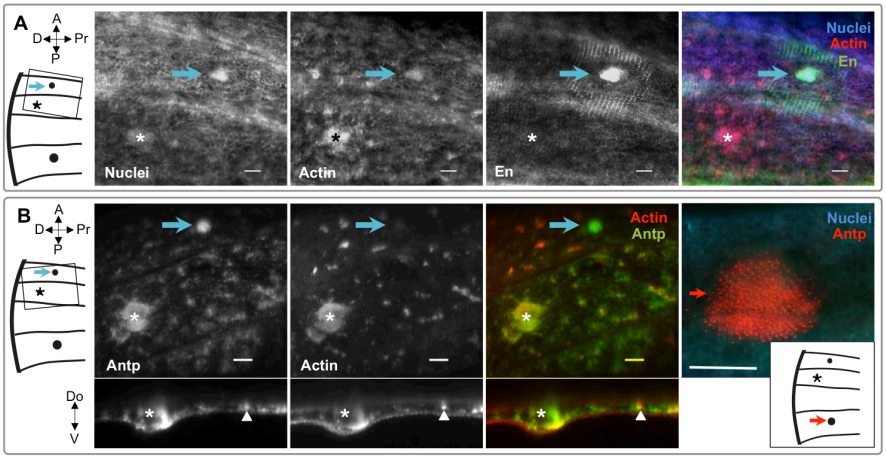

Figure 2.6- Antp, but not En, is expressed at wound site. A) En is expressed at presumptive eyespot center and golden ring but it was not detected at wound site. B) Antp is expressed at presumptive eyespot centers and wound sites. Actin and Antp are expressed at wound site (colocalization in yellow). Top images are a Z-projection and bottom images are orthogonal views of wound site. Blue arrows indicate the forewing anterior eyespot center, red arrow the posterior eyespot, arrowheads the actin spots, the asterisk (*) the wound site. The drawings indicate the approximate positions of the images and the crossed arrows the wing orientation; anterior (A), posteror (P), distal (D), proximal (Pr). Scale bars are 100μm.

2.4.4 The wound inhibits cell proliferation

The epithelium injury induces changes in cell and tissue organization (Razzell et al. 2011; Krautz et al. 2014). Our previous experiments (Figure 2.5 and 2.6) have suggested that presumptive eyespot centers and wound sites have higher cell density than other areas of wing epithelia. Higher cell density at wound sites can be due higher cell proliferation rate or cell migration towards wound site. Cell proliferation rate can increase at wound sites to restore and re-epithelize the wounded epithelium, generally this is the last phase of wound healing (Reinke & Sorg 2012; Razzell et al. 2011). To investigate whether more cells at wound sites and eyespot centers are a consequence of locally increased cell proliferation *vs.* cell migration, we used a mitotic marker. At both sites the epithelium was thicker than neighboring regions and had more cells (Figure 2.7A and B). At presumptive eyespot center there is an outgrowth towards the ventral epithelium in comparison with neighboring areas (Figure 2.7A). The same occurs at wound sites (Figure 2.7B).

To understand if were there higher cell proliferation we stained mitotic cells in wounded and non-wounded individuals from 30min to 4h post-wounding. Here, we are showing the staining at 1h30min (Figure 2.7C top), but we observed the same trend in all tested individuals. There are fewer proliferating cells around wounds in comparison with nearby wing. The wound was associated to inhibition of cell proliferation relative to the contra lateral non-wounded wing. To quantify cell proliferation we used five individuals dissected 4h post-wounding and compared the area of mitotic cells in wounded *vs.* control wing of same individual. Wounded wings had significantly lower area for mitotic cell relative to respective contralateral wings (lines in Figure 2.7C bottom). These results indicate that the higher

cell density around wound sites is likely due to cell migration, which is common in the inflammatory process after wounding (Wu et al. 2009; Williams 2007).

All nuclear RNA synthesis is repressed during the mitotic phase of the cell cycle (Hartl 1993; Spencer 2000). After wounding, cells have to readjust their transcription and initiate the synthesis of wound response genes such as AMPs and melanogenesis enzymes. It is possible that cells around wound sites are more transcriptionally active in comparison with other cells in the wing, which reduces the probability of mitosis. Double staining with a mitotic marker and a transcription marker, such as RNA polymerase II, can confirm this hypothesis.

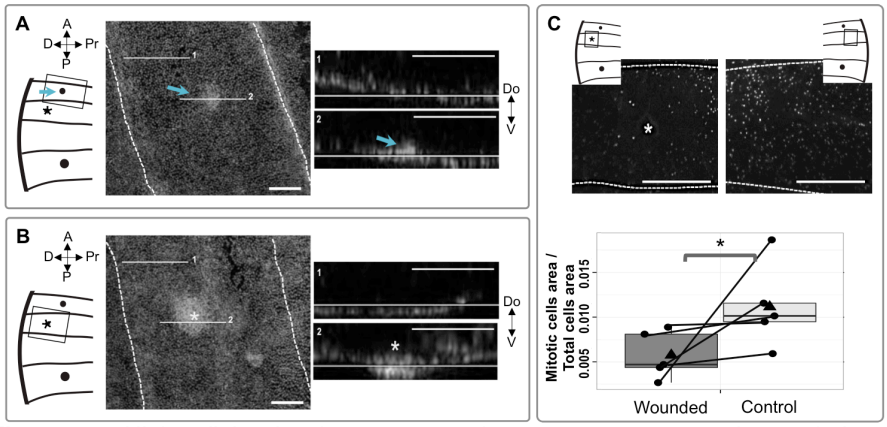

Figure 2.7- High cellular density at presumptive eyespot centers and wound sites is not consequence of higher cell proliferation. At presumptive eyespot centers (A) and wound sites (B) the nuclear staining is more intense relative to other wing areas. The orthogonal views in the right show the near wing epithelium (top; line 1) and the interest zone (bottom; line 2). C) Lower cell proliferation at wound sites. Top images are staining mitotic cells in the wounded (left) and the contralateral non-wounded wing of the same individual (right) (1h30min post-wounding). Bottom graphic is the quantification of mitotic cells in wings pairs (connected with a line) 4h post-wounding. There are fewer mitotic cells around wound site in comparison with same area in control wing (glm model with total cells area imaged as covariant; F=7.34, p-*value*=0.035). Blue arrows indicate the forewing anterior eyespot center, the asterisk

(*) the wound site and dashed lines the wing veins position. Drawings indicate the approximate positions of the images and the crossed arrows the wing orientation; anterior (A), posterior (P), distal (D), proximal (Pr), dorsal (Do), ventral (V). Scale bar in A and B is 100μm and in C is 500μm.

2.4.5 There are cellular similarities between wound sites and presumptive eyespot centers

The presence of more cells and lower cell proliferation rate (Figure 2.7) indicate that increased cell density at wound sites likely results from cell migration, which is consistent with cellular immune response (Strand 2008). Indeed, analysis of gene expression spatial patterns revealed the presence of cells that might be hemocytes (Figure 2.5), with similar shape to plasmotocytes and granolocytes (Kavanagh & Reeves 2004). The presence of plasmatocytes is especially intense after a parasitizing wasp that induces the migration of plasmatocytes towards parasitic egg (Mortimer; Russo et al. 1996). Our wounding treatment might be compared to the wasp ovipositor wounding; this physical damage can be sufficient to induce the same type of cellular immune response. In drosophila, studies during pupal stage have demonstrated that after laser epidermal damage there were active migration of hemocytes under the epithelium, often from the so-called 'sessile patches' (Regan et al. 2013). However, the cellular identity of such cells might be confirmed to confirm this hypothesis.

Hemocyte-like cells were also present at the presumptive eyespot centers forming clusters (Figure 2.5). At eyespot centers and wound sites Actin staining was more intense relative to other wing areas (Figure 2.6). Actin is a molecule involved in cell cytoskeleton architecture, when cells need to readjust their shape as in wound healing they change actin location and polarization (Wood et al. 2002;

Razzell et al. 2011). Motile cells, such as hemocytes, are rich in actin (Supplementary Figure S2.2) and also activate the same kind of processes to move towards wound sites (Sampson et al. 2013; Wood et al. 2006). Eyespot centers have more Actin staining but also have more cells; these Actin-rich cells can be hemocytes. Nevertheless, Actin-rich patches of cells are not exclusive of wound sites and presumptive eyespot centers; they are spread throughout the wing (Figure 2.6). Still, hemocyte-like cells expressing *Glov2* aggregated in patches were observed only at wound sites and presumptive eyespot centers. This can indicate heterogeneity of hemocyte-like cells in developing wings that express different combination of genes. Altogether, wounding induces an inflammatory response with migration of hemocyte-like cells expressing *Glov2* to the wound site, which increases the cell density. The same type of cells is also present at the presumptive eyespot centers, which also have higher cell density with a similar cell organization as at the wound sites as exemplified in scheme of Figure 2.8.

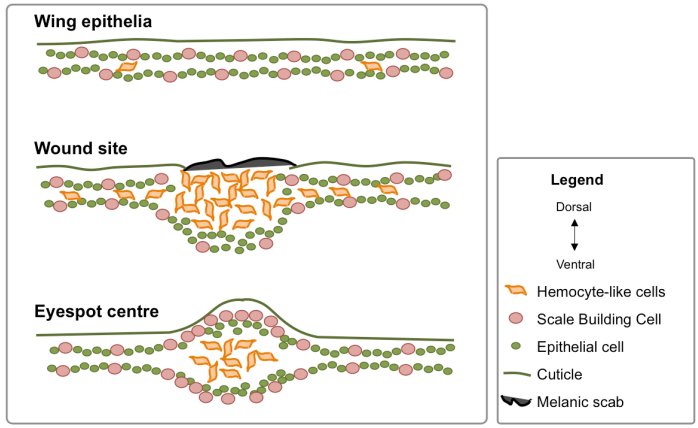

Figure 2.8- Scheme of cellular structure of wing epithelia, wound site and presumptive eyespot center. At wound sites and eyespot centers the thickness of wings is higher because they have hemocyte-like cells between dorsal and ventral epithelia.

2.5. Conclusions

Butterfly eyespots are evolutionary novelties and represent an excellent opportunity to understand the evolutionary origin of novel traits. In this chapter we aimed to understand if there were cellular and genetic commonalities between wound response and eyespot formation. The existence of such commonalities supports the hypothesis of co-option of wound response genetic circuitry to develop butterfly eyespots. Our results reinforce this hypothesis; we demonstrated that the wound response and the development of eyespots share cellular and genetic mechanisms.

2.6. Acknowledgements

We would like to thank Anthony Long and Nicolien Pul for help with obtaining the microarray data. Daniel Sobral, Paulo Almeida, and Renato Alves (IGC's Bioinformatics Unit) for gene annotation and enrichment analysis. Jorg Becker (IGC) and Adeline Simon (ANAIS project) for advising in the microarray analysis. Marta Marialva for the guidance in qPCR, David Duneau and Nelson Martins for the discussions and suggestions about statistical analysis. The Unit of Imaging at IGC for all the assistance during image acquisition and analysis, in particular to Emilio Gualda in Lightsheet SPIN microscope assistance. Élio Sucena, Marta Marialva, Elvira Lafuente, Alexandre Leitão and Magda Atilano for discussions throughout this project.

Chapter 3 – Immunity regulates the size and scale composition of wound-induced pigmentation patterns

3.1. Summary

The early development of organisms involves a series of tightly regulated processes that determine the adult phenotype. The diversity across species and also the variation of a species is very striking in butterfly wing color patterns, which are formed by single color scales organized in a mosaic. The scale development and the determination of its pigments occur during pupal development. Eyespots are butterfly color patterns elements combining different color rings organized around a central pupil. During pupal stage the wing cells are fated to produce different scale morphologies and pigments. In some butterflies an epithelial wound during early pupal development can change the fate of wing cells, which produce scales with different colors around wound sites, wound-induced eyespots (WIE). Here, we used the lab model *Bicyclus anynana* to investigate the effects on cell fate after inducing different levels of immune system activation. We observed that the treatment with heat-killed bacteria at wounding is very efficient to activate local and systemic immunity. In contrast with previous studies inducing different levels of wounding severity, the activation of higher immunity levels did not induced more, but induced larger WIP. This indicates that immunity affects the number of cells changeing their developmental program around wound sites, but it is

not affecting the initial signals triggering the development of WIE. We suggest that tissue repair/reepithelialization is affecting the early signals for eyespot development and immunity is affecting the production and/or migration a morphogen-like signal to the surrounding cells.

3.2. Introduction

The generation of cell diversity during development relies on mechanisms that provide spatial and temporal information to each cell. The establishment of morphogen gradients is an important strategy to achieve spatial information to the field of responding cells. Different morphogen concentrations are translated in different cell fates. The butterfly eyespot development is a classic and beautiful example of this process. Studies to date have allowed us to divide eyespot development into four major consecutive stages: focal determination, focal signaling, pigment positioning, and pigment synthesis (Brakefield et al. 1996). Focal determination refers to the developmental process that establishes which cell in the wing will be the organizing center of the future eyespot (the white pupil), and occurs during the last larval instar (Brakefield et al. 1996). The focal signaling stage occurs in young pupae. Experiments with grafting or destruction of focal cells, during early pupae stage, lead to misplacing or eliminating, respectively, of the corresponding eyespots. These experiments established the focal cells as the organizing center that establishes a morphogen-like gradient triggering the eyespot development (French & Brakefield 1995; Brakefield & French 1995). The way of how the morphogen gradient is established (source or sink) and the identity of this signal is still not known (French & Brakefield 1992; Dilão & Sainhas 2004). The yet unknown morphogen (but see (Monteiro et al.

2006) for candidates) presumably establishes a concentration gradient in a threshold-like fashion, providing positional information to the surrounding epidermal cells. At this stage, rings of cells expressing different transcription factors become fated to produce a particular color (Nijhout 1991, Brunetti et al. 2001, Beldade and Wittkopp 2009). The last eyespot developmental stage, the pigment synthesis and scale maturation, occur shortly before pupa eclosion in a stereotypical order (Koch et al. 2000; Wittkopp & Beldade 2009).

During last decades the butterfly *B. anynana* have been used as lab model to understand the development and evolution of eyespots (Brakefield & French 1999; Beldade & Brakefield 2002; French & Brakefield 1992). In this species and also in other eyespot-bearing species, wounding inflicted during pupal development can lead to the formation of WIE that resemble color rings of native eyespots (Brakefield & French 1995; French & Brakefield 1992; Monteiro et al. 2006). This resemblance suggested that the wound response genetic circuitry, ancestral in insects, might have been co-opted for eyespot development in butterflies (Monteiro et al. 2006). In fact, it is well established that wound sites do behave like organizing centers in that they release chemical signals that can change the fate of neighboring cells and trigger a fast wound response (Niethammer et al. 2009). A wound typically activates mechanisms of tissue repair and immunity, which induce reepithelialization of the tissue closing the opening and fight possible invading pathogens (Neves et al. 2015; French & Brakefield 1992).

In Chapter 2, we showed that wounding early pupal wings of *B. anynana* induces the up-regulation of genes related with insects' innate immune response encoding for antimicrobial peptides (AMPs) and melanogenesis enzymes. These genes integrate both the humoral and cellular immunity on insects and can be activated

according to the immune challenge faced by the organism (Lemaitre & Hoffmann 2007; X. X. Xu et al. 2012; Ling & Yu 2005). Upon mild immune challenge, the local (immune challenged tissue) and systemic (general/whole body) immune response is also mild, but when the immune challenge is high the up-regulation of immune pathways is massive and can even kill the organism (Ishii et al. 2010; Nappi & Christensen 2005). The mechanisms of activation, regulation and functions of these genes in a context of insects' immunity are largely studied (Lemaitre et al. 1997; Neyen et al. 2014; Flatt et al. 2008). However, we do not know if different expression levels of these genes upon wounding in Leptidopterans can lead to different cell differentiation around wound sites. Here we used manipulation of immune system activation in early pupal *B. anynana* wings to investigate the possible involvement of immune-related mechanisms/processes in early pupa cell fate determination.

3.3. Materials and Methods

3.3.1 Biological Material

B. anynana inbreed line (a sub population from Antónia Monteiro's lab; used for whole genome sequencing) was reared at 27° C as described elsewhere (Brakefield et al. 2009). Briefly, the butterflies were maintained at 27°C (+/- 0.5°C) with 65% (+/-1%) relative humidity with 12hrs cycle light/dark. Eggs were collected from adult cages with approximately 400 individuals (45x45x45cm; BugDorm-44545) in a very young maize plant. To reduce the probability of parasite transmission, we bleached eggs (5 min in a 20% bleach solution) immediately after collection. Adult butterflies were fed with fresh banana on top of wet cotton and larvae were fed with fresh young maize plants and maintained in cages identical of

those used for adults at a density of 150 to 200 individuals per cage. Larvae were sexed and only females were used in this study. Pre-pupae were collected onto 25 well plates and pupation time was recorded during the night via time-lapse photography with a photo taken each 10 min; Canon 1000D digital camera, Hahnel Giga T Pro 2.4GHz wireless timer remote control. For this work we did three different batches of experiments: first batch we only analyzed WIE phenotypes on the wounded (right) wing; second batch we analyzed gene expression upon treatments (wounded and control wing), survival and adult WIE phenotypes on wounded wing; and in third batch we analyzed WIE phenotypes (on left and right wings) to distinguish the effect of local versus systemic immune response on eyespot-like formation.

3.3.2 Wounding and Immune system activation

Wounds were inflicted with a tungsten needle (cat. no. 501317; World Precision Instruments) in the dorsal surface of the right forewing. We induced this mild damage in the wing compartment below anterior eyespot, which is defined by adjacent veins, approximately halfway between the wing margin and the normal location of the eyespots (Figure 3.1). Pupae were returned to 27°C until dissection, for quantification of immune system activation, or until adult stage, for quantification of adult wound-induced eyespots.

To activate different levels of immune system we used heat-killed *Escherichia coli* (DM09-CFP) obtained from overnight liquid culture from a single colony. Bacteria were collected after heat shock treatment (80°C during 30 min) and dissolved in sterilized PBS in three different stock solutions concentration: 10^5, 10^6, or10^7 cells/µL. To the fresh wound, we added 0.5 µL of a different solution for each of

four treatments: 1) non-sterilized wound (NS) with sterilized PBS, 2) 10^5 cells/μL (Ec5), 3) 10^6 cells/μL (Ec6), and 4) 10^7cells/μL (Ec7). An additional group of non-wounded individuals (NW) were used as reference in qPCR experiment. In phenotypic analysis we added a group in which we sterilized the pupa cuticle before wounding, to minimize the probability of infection, and added 0.5 μL of sterilized PBS (S).

3.3.3 Melanotic Spots

Four hours post-wounding, the wounded wings of four biological samples were dissected, fixed (9% formaldehyde for 30min) and mounted in 100% glycerol. Images were acquired through a Zeiss stereoscope (Zeiss Stereoscope Stemi SV6) attached to a camera (UEye Cockpit software) under standardized light conditions. We loaded images onto Fiji software (Schindelin et al. 2012), selected the same rectangle area (1.60 x 1.20 mm) in the two distal wing compartments below anterior eyespot, which are defined by adjacent veins, and counted the number of darker points that correspond to melanotic spots.

We used R software (R Development Core Team 2015) for graphical representation and statistical analysis and we tested for the effect of treatment on number of melanotic spots using an ANOVA (aov(Melanotic spots ~ Treatment)). We first confirmed that the residuals of the data or logarithmic transformed data showed no significant departure from normality (Shapiro-Wilk test) or from homogeneity of variances (Brown-Forsyth test). We then used ANOVA to test for the effect on number of melanotic spots of treatment (factor with four levels: NS, Ec5, Ec6 and Ec7). We used the

lsmeans R package (Lenth & Hervé 2015) (based on Tukey test) for pairwise comparisons considering different groups when *p-value*<0.01.

3.3.4 Survival

Seven days after wounding all survival individuals had reached the adult stage, the ones that were still like pupa were dead. We quantified the number of survival and dead individuals per treatment. These data were imported to R (R Development Core Team 2015) for graphical representation and statistical analysis. We did a contingency table with number of survival and death individuals and used a Chi-square test to determine if the proportion of individuals in both classes were different across treatments. After we run a pairwise comparison to know differences within treatment groups. In this experiment we only considered the individuals treated

3.3.5 Quantitative PCR

Both the wounded forewing and the control, contralateral non-wounded forewing of each individual pupae were dissected along with the overlaying pupal cuticle, at four or eight hours post-wounding. A distal and anterior section of each forewing and cuticle was used for RNA isolation (Figure 3.1). The wings were collected directly into a 2mL epp with a 7mm glass bead and 400uL of TRIzol (Invitrogen), kept at -20ºC for 0-8 hrs until tissue disruption and homogenization in Qiagen's TissueLyserII (5 min at max speed), and the homogenate was stored at -80ºC until RNA isolation.

RNA isolation was done using the Direct-zol™ MiniPrep Kit (ZIMO Research) according to the manufacturer's recommendations. The RNA was treated with DNase and diluted in 50ul of RNAse-free water. RNA was checked for yield and purity (A260/A280 ratio of > 1.8) in

NanoDrop, and for integrity by running in a 1% agarose gel. We synthesized the cDNA taking 400ng of RNA as template in a 10ul total volume reaction using 40U of the reverse transcriptase (M-MLV RNase H Minus, Promega) and 0.5µg oligo(dT) following manufacturer's instructions. The cDNA product was diluted for a final volume of 50µL and used as template.

We used the 7500 Real-Time thermal cycler (Applied Biosystems) to run all qPCR. The reaction mixes were optimized for a total volume of 10uL with 5uL iQTM SYBR Green supermix (BioRad), 3.6uM of each primer, and 1uL of cDNA template. The PCR program included an initial step of 95ºC for 10min, followed by 40 cycles of 95ºC for 20 sec, 59ºC for 20 sec, and 72ºC for 30 sec. The specificity of the qPCR reactions was monitored with melting curves obtained from the dissociation curve (59-95ºC), using SDS software (version 1.4; Applied Biosystems). We quantified the expression for three target genes: one antimicrobial peptide (AMP), *Gloverin2* (*Glov2*), a melanogenesis enzyme, *pale* (*ple*) and a potential melanogenesis-related enzyme, *primo1* (*pri1*) (see Chapter 2). We designed primers to amplify amplicons spanning an intron for these genes and also an endogenous control gene, Ribosomal-like protein 10A (RpL10A)(primer sequences, amplicon size and homology described in Chapter 2- Supplementary Figure S2.1)

Gene expression levels were determined four and eight hours post-wounding in four replicate pupae (each with wounded and control wings) and for each biological sample were run three technical replicates. We had four wounding treatments (S, NS, Ec6, Ec7) and a reference group (NW). We quantified the expression levels in four biological replicates per treatment per time point using the mean of technical replicates (rejecting the biological samples in which the

repeatability of technical replicates were low: differences between technical replicates higher than 1.5 cycles). We used the ΔΔ Ct method to quantify the gene expression (Livak & Schmittgen 2001; Pfaffl & Pfaffl 2001). Briefly, with Ct values we first normalize the gene expression of target genes (*Glov2*, *ple* and *pri1*) relative to the internal control gene (*Rpl10A*), we obtained the ΔCt values and calculated the relative gene expression. After we compared the relative gene expression in each treatment (NW, S, NS, Ec6, Ec7) with the average of relative expression for NW group for each gene (*Glov2*, *ple* and *pri1*) in each time point (four and eight hours) and tissue (wounded and control wing), so the results are shown as fold change difference relative to NW group.

We imported the results to R software (R Development Core Team 2015) for graphical representation and statistical analysis. For each gene, time point and tissue we tested for the effect of treatment and technical replicate on gene expression using the model: Gene expression ~ Treatment * Technical replicate, which was simplified whenever the effect of technical replicates was not statiscaly significant. We transform our data to meet the Shapiro-Wilk normality test and Brown-Forsyth homogeneity of variance test (*p-value*<0.05) and after checking that there were no interactions between explanatory variables we used an ANOVA (aov(Fold Change ~ Treatment * technical replicate)). In cases where the variance was not constant we used a generalized linear model (GLM) with Gamma distribution. When there were significant differences among treatments (*p-value*<0.01) we used the lsmeans R package (Lenth & Hervé 2015) for post-hoc pairwise comparisons and considered different gene expression between treatments when *p-value*<0.01.

3.3.6 Phenotypic measurements

After stretching wings, adult butterflies were sacrificed (-20ºC for at least 2hrs). Wings were detached from the thorax and the dorsal side was scanned (Epson Perfection V600 Photo). Images were imported to Fiji (Schindelin et al. 2012) and wings were classified for presence/absence of WIE. After that, we measured the total area of WIE (response variable), as well as total wing and dorsal anterior native eyespot of control wing (used as covariants). We also measured the scar area (absence of color scales) at the wound site and calculated the color scales area subtracting the scar area to the total WIE area (Figure 3.1). All measurement data were imported to R (R Development Core Team 2015) to do their graphical representations and statistical analyses. We tested the effect of treatment on development probability, total area, scar area and total color scales area of WIE, taking in consideration possible covariants with wings area and dorsal native eyespot area, and also considering the batch of the experiment (two batches run in two different months). To know if the treatment has an effect on WIE formation (presence/absence) we used a GLM with a binomial error distribution and a logit link: glm(Presence WIE ~ Treatment + Wing Area + Dorsal native eyespot Area + Batch, binomial). In the WIE area traits we tested the effect of treatment on WIE taking in consideration possible covariants with wing area or native eyespot area and the experiment batch. In this analysis we confirmed that the residuals of the data or logarithmic transformed data showed no significant departure from normality (Shapiro-Wilk test) or from homogeneity of variances (Brown-Forsyth test). After we used ANOVA to test for the effect of treatment (factor with four levels: S, NS, Ec6 and Ec7) on these area traits: lm(WIE area ~ Treatment + Wing Area + Dorsal native eyespot Area + Batch). Whenever the Treatment had a statistical significant

effect on WIE we performed a pairwise comparison between treatment groups through lsmeans R package (Lenth & Hervé 2015).

3.3.7 Local and Systemic effect of immune system activation

Instead of wounding one forewing and having the contra-lateral forewing as the control, in this experiment we wounded both wings. We compared the WIE in two treatment groups: Control and Test group. The wounding treatment in the right wing is different in Control, NS-like wound and Test group, Ec7-like wound, which according to gene expression results (Figure 3.3) do activate different levels of local and systemic immunity, but the wound on the left side is similar in both Control and Test groups. Thus, if the components of systemic immunity were essential to increase the WIE size, the WIE on the right wing and also in the left wing of Test group are larger than WIE in Control group. After wounding, pupae were returned to 27ºC until eclosion. Adults were sacrificed, wings collected, images were acquired and WIE were measured as before (Figure 3.1). We tested the effect of Treatment (Control and Test group), Wing side (Right and Left) and the interaction of Treatment*Wing side on the WIE size, taking the wing size as a possible covariate, using a GLM with a normal distribution (residuals with normal distribution tested with Shapiro test): glm(WIE ~ Treatment * Wing Side + Wing Size). We used the lsmeans R package for post-hoc pairwise comparisons (Lenth & Hervé 2015) considering different groups when $p\text{-}value<0.01$.

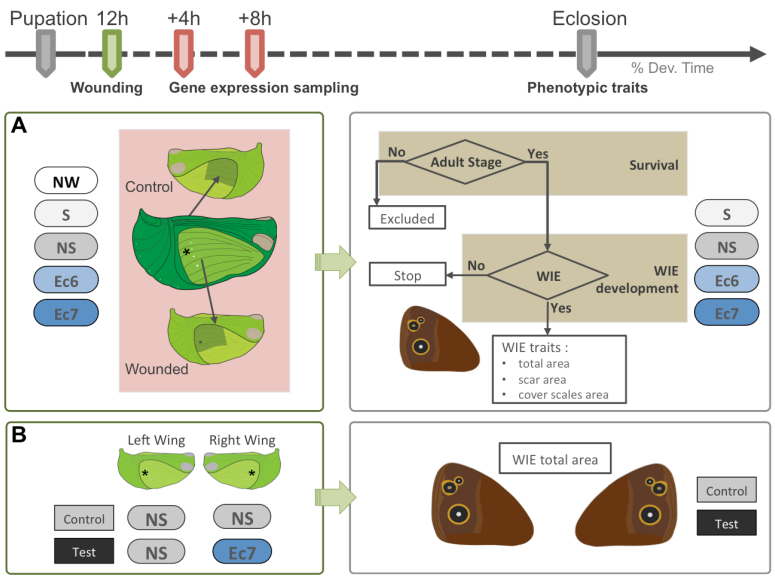

Figure 3.1- Experimental design. A) Effects of immune system activation on gene expression, survival and WIE formation. In a time line we first wounded (green arrow) and applied a drop of PBS (S and NS) or heat-killed *E. coli* solution (Ec6 and Ec7) (for a better description of treatments see the main text)), after we collected samples for gene expression analysis (red arrows) and the remaining individuals were used to analyze the treatment effects on survival and WIE (after eclosion). For gene expression quantification we collected from the same individual the most anterior and distal wing portion of wounded and control wing (dark green area), which was used for RNA isolation. B) Effects of local and/or systemic immune activation on WIE. Control and Test groups were wounded on both wings, the control group with NS-like wounds on left and right wings and Test group with NS-like wound in the left and Ec7-like wound on the right wing. The effect of systemic immune system activation was measured as the size of WIE on left wings of adult butterflies. Treatment groups are ordered by the increasing probability of immune system activation from the lighter to the darker box colors. NW – non-wounded, S – sterilized, NS – non-sterilized, Ec6 – 106 cells/µL E. coli, Ec7 –107 cells/µL E. coli.

3.4. Results and Discussion

Previous studies have shown that wounding butterfly pupal wings can induce the formation of eyespot-like patterns (Nijhout 1991; Brakefield & French 1995; Otaki 2011). These observations indicate

that wound response induces cell fate changes in pupal wing epithelial cells that otherwise would develop brownish background cover scales. In this case, processes involved in wound response, such as immunity and tissue repair might impact eyespot formation around wound sites. Brakefield and French had reported that the probability to induce an eyespot-like pattern was higher upon a severe epithelial damage, but the size of that eyespots was not affected (Brakefield & French 1995). Here we manipulated the immunity activation at the wound site and analyzed the eyespot-like patters in adult wings to investigate the role of immunity on cell fate determination upon wounding. Non-sterilized conditions (NS) have been used to induce the formation of eyespot-like patterns by pricking pupal wings (Nijhout 1991; Brakefield & French 1995; Otaki 2011), so we took this wound type as reference and compared other treatments thought to induce higher and lower immune response. We show that a treatment with heat-killed bacteria activates innate immune system in *B. anynana* (Figure 3.2 and 3.3) and that treatment induces the development of larger eyespot-like patterns (Figure 3.4C), but was not affecting the probability of its development (Figure 3.4A). We also demonstrated that the enlargement of these patterns is related with local, but not systemic immune response (Figure 3.4D).

3.4.1 The number of melanotic spots and the mortality increase upon treatment with heat-killed bacteria

There are multiple ways to activate the immune system: with live, killed or cell wall components of microorganisms, as well as with mechanical damage (Lemaitre et al. 1997; Rao & Yu 2010; Clark et al. 2011). Insects that are immune-challenged activate the innate immunity, and if the immune challenge is high it is possible detect

changes in hemolymph color and the presence of melanotic spots with a naked eye (Lavine & Strand 2002) (Figure 3.2A). To induce different levels of the immune system activation post-wounding, we first tested if a treatment with heat-killed *E. coli* was effective. Immediately after wounding, we applied on top of the wound 0.5 µL either of sterile PBS1X, in the NS control group or of a solution with three different concentrations of heat-killed *E. coli*, 10^5, 10^6, and 10^7 cells/µL for the Ec5, Ec6, and Ec7 groups, respectively. With a naked eye, it was visible that wings of the Ec7 treatment had more melanotic spots (Figure 3.2A). The quantification revealed indeed that melanotic spots number was higher in treatment groups stimulated with higher concentration of bacteria (Ec6 and Ec7) (F=230, d.f.=3, p-*value*<0.0001)(Figure 3.2B). Ec5 group was not statistically different of NS. Therefore, to increase the immune system activation after wounding we select the two higher heat-killed bacteria treatments, Ec6 and Ec7.

This simple methodology can be an alternative approach to quantify the immune response on butterfly pupal wings without the traditional gene expression quantification, which requires more time, human and economic resources. Quantifying the melanotic spots through cuticle is also possible because we can see darker areas under the cuticle (Figure S3.1). Since this methodology does not require pupal sacrifice, we can correlate the immune response upon wounding on pupal stage with adult phenotype for each individual in a population, which might allow, for example, artificial selection on intensity of immune response upon challenging.

The balance between immune system activation and inhibition is vital to maintain homeostasis. Upon an immune threatment, the absence of an immune response can allow pathogens to proliferate

uncontrollably inducing septic shock and eventually kill the host, while an excessive immune response can lead to anaphylactic shocks with deadly consequences for the host (Cauwels 2007). In insects also occur similar scenarios of septic and anaphylactic shocks. For example, several studies had demonstrated that the number of pathogens increases over time in immune challenged individuals (Atilano et al. 2011; Quiroz-Castañeda et al. 2015; Singh et al. 2014), and in silkworm was demonstrated that after challenge with heat-killed bacteria or cell wall components the individuals induced an excessive activation of the innate immunity, which increased the host mortality risk (Ishii et al. 2010). In this study the authors demonstrated that treatment with melanogenesis inhibitors increased the host survival, which shows that melanin pathway over-activation is harmful to the host (Ishii et al. 2010).

Here, we saw that the Ec7 treatment induced higher mortality during pupal stage (χ^2 = 31.8, d.f.=3, *p-value*<0.001) (Figure 3.2C). This result suggests that heat-killed bacteria induced an exaggerate immune response. We did not use live bacteria in order to avoid the septic shock-like scenario, but not the anaphylactic shock-like scenario. Typically, Ec7 individuals had darker hemolymph (observed during dissections for qPCR sampling), turning the pupa a dark green color. In general, dark green pupae revert to the normal color in one or two days, those that do not revert the color usually ever reach the adult stage. All together these observations suggest that, as in silkworm experiments (Ishii et al. 2010), the heat-killed bacteria treatment induced the over-activation of melanogenesis. Some individuals decreased the melanin production, restoring the homeostasis, but some individuals maintained the melanin production longer increasing the reactive oxygen species (ROS) levels. High

levels of ROS are necessary to kill invader pathogens, but also induce apoptosis in host cells that, if generalized in whole body, deregulate the internal homeostasis and lead to the host death (Ishii et al. 2010; Nappi & Christensen 2005).

3.4.2 Heat-killed bacteria treatments increase local and systemically the expression levels of immune-related genes

The immune system activation can be quantified through different methods, such as enzymatic activity, number of immune cells, and gene expression (Neyen et al. 2014). Here, we quantified the expression of immune-related genes after different wounding treatments. To induce higher levels of immune system we selected the two higher heat-killed bacteria dosages tested in previous experiment (Ec6 and Ec7) and to induce a lower activation we sterilized the cuticle of wounded pupae to minimize possible natural infections. After wounding we collected wings at two different time points (4 and 8h) to quantify the extent of local (wounded wing) and systemic (control wing) immune system activation in all treatment groups (S, NS, Ec6 and Ec7) and compare it with non-manipulated individuals (NW) (see experimental design Figure 3.1). We measured the expression of three immune related genes, which were overexpressed after wounding around wound sites (see Chapter 2 - Figure 3.3): *Gloverin 2* (*Glov2*), *pale* (*ple*), and *primo-1* (*pri1*). In general, the expression levels increased after wounding relative to NW individuals: a higher heat-killed bacteria dosage added to the fresh wound induced higher gene expression of immune related genes in both wounded (Figure 3.3A) and control wings (Figure 3.3B) at 4 and 8h post-wounding. This analysis revealed that S and NS treatments activated immunity to similar levels (Figure 3.3A and B). Thus, the cuticle sterilization does

not decrease significantly the immunity activation upon wounding, which indicates that wounding *per se* is activating immunity pathways. It had been shown before that the mechanical damage of pricking an epithelium induces a basal activation of the immune system (Márkus et al. 2005). This basal activation of an immune response might be sufficient to deal with potential opportunistic pathogen invasions at wound sites. In contrast, the Ec7 treatment was statistically different from NS treatment (except for the expression of *pri1* at 4hrs and *ple* at 8hrs) leading to higher up-regulation of immunity-related genes, both locally in the wounded wing, as well as in the contra-lateral control wing (Figure 3.3 A).

The gene expression dynamics of *Glov2* and *pri1* was similar: local, expression levels were already increased at 4h and are still high at 8h post-wounding. Systemic expression levels are similar, but higher at 4h than at 8h. The *ple* expression dynamics is slightly different: at 8h local expression levels are already decreasing and systemic expression levels are already in basal levels (Figure 3.3A and B). This indicates that in *B. anynana* during early pupal stage the local response is longer than systemic response and the systemic response might have two phases: first phase with activation of genes related with melanogenesis, and the second phase with activation of genes related with AMP and other peptides/enzymes production.

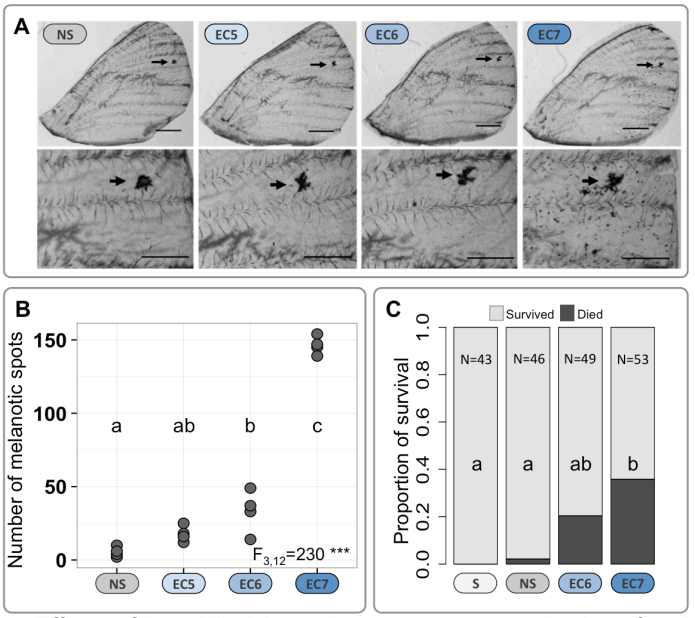

Figure 3.2- Effects of heat-killed Bacteria treatment on production of melanotic spots and mortality during pupal stage A) Formation of melanotic spots after addition 0.5 uL of different Bacterial solutions at wound site: PBS1x (NS); 10^5 heat-killed bacterial cells/uL (Ec5), 10^6 cells/uL (Ec6), and 10^7 cells/uL (Ec7). Arrows indicate wound site (black scab); scale bars are 1mm and 0.5mm in wings and magnifications, respectively. B) Quantification of melanotic spots. The number of melanotic spots increased as the number of heat-killed bacteria increased. Different letters indicate pairwise comparisons that were statistically different (lsmeans *p-value*<0.01); N=4. C) Survival after heat-killed bacteria treatment. The proportion of survival individuals was reduced in heat-killed bacteria treatments and the same in individuals wounded in sterilized conditions (S) treatment relative to NS treatment. We used a Chi-square test (χ^2 = 31.4, d.f.=3, *p-value*<0.001) and different letters indicate differences in pairwise comparisons (*p-value*<0.05). N is the total number of individuals used in each treatment group.

3.4.3 Immune stimulation at wound site does not increase the probability of WIE development

After wounding two major processes are activated: tissue repair and immunity. To what extent these two processes are involved, if at all, in butterfly WIE development is poorly understood. Moreover, the

butterfly eyespots development is not completed known, but we can distinguish three very different stages: the focal establishment, focal signaling and cell differentiation (Brakefield et al. 1996). To understand if immunity could affect the cell decision of establishment of an eyespot-like center that leads to the development of an eyespot-like pattern, we manipulated the immune system activation during pupal stage and classified the adult wounded wings for presence or absence of WIE. We saw that activating higher levels of immune system did not affect the likelihood of WIE development after wounding; $\chi^2 = 1.02$, d.f.=3, *p-value*>0.05 (Figure 3.4A). This indicates that the immune stimulation at wound site does not affect the genetic network/signaling that determines formation or non-formation of WIE. Moreover, even the basal immunity stimulation induced in S group was sufficient to induce same proportion of WIE (Figure 3.4A).

A previous study comparing mild (normal needle) and severe (heated needle and deep pricking) wounds showed that severe wounds, that might activate higher levels of tissue repair and also slightly immunity levels, were more likely to induce WIE formation (Brakefield & French 1995). This suggests that the number of damaged cells at wounding might be crucial to trigger the genetic network determining the wound site as an eyespot-like organizing center. In our experiments, we minimized possible differences in wounding (all wounds were done with the same type of needle and by the same person). We did not quantify whether and to what extent our different immune-stimulation treatments differ in tissue damage, and tissue repair mechanisms activation. However, we do know that any possible differences in tissue damage and/or tissue repair mechanisms among treatments were not enough to replicate the effects of damage severity on the likelihood of WIE formation. Thus, we suggest that the number of damaged cells during wounding might

be the key signal triggering the cell fate decision of formation or non-formation of WIE. To test this hypothesis, we could quantify the development of WIE in pupae wounded with different thickness needles.

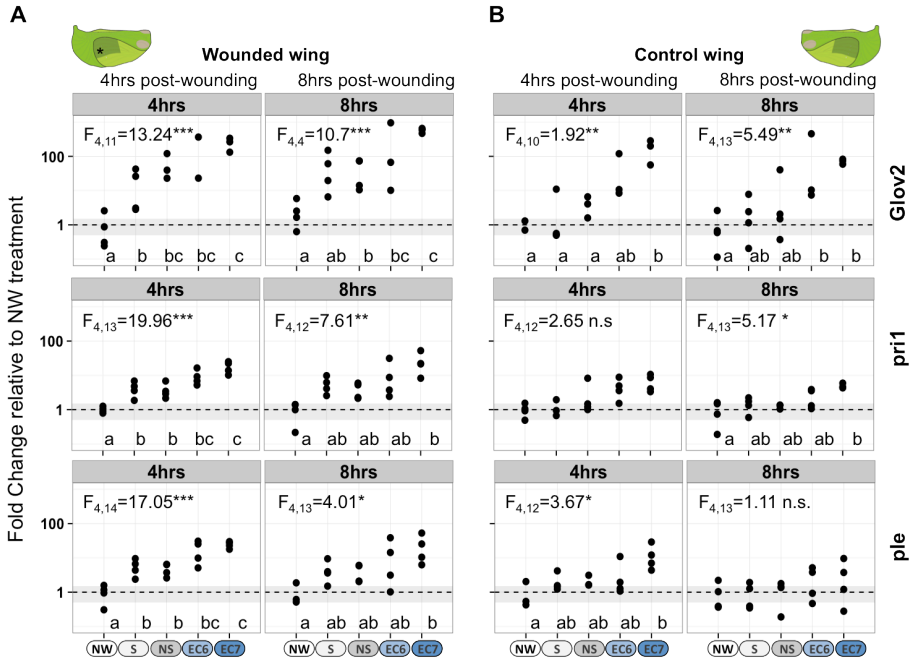

Figure 3.3- Application of heat-killed bacteria to fresh wounds activates the immune system, local (wounded wing) and systemically (non-wounded, contralateral wing). A) Local immune system activation. The gene expression of immune related genes was higher in groups treated with heat-killed bacteria (Ec6 and Ec7) in both time points (4 and 8hrs). B) Systemic immune system activation. Gene expression in non-wounded wings was higher in groups treated with heat-killed bacteria. Each dot represents the mean fold change of technical replicates per biological replicate, which was calculated relative to the NW group. The dashed horizontal line is a fold change equal to one that correspond to the mean relative gene expression in NW group, the surrounding gray area correspond to a ±0.5 fold change difference in gene expression. Statistical results for effects of treatment on gene expression in each time point are indicated on the bottom of each graphic: n.s. (non-significant) and ****p-value*<0.001. Different letters indicate differences across treatments (lsmeans *p-value*<0.01). Sample size

was three or four biological replicates, only for Ec6 in wounded wings for the Glov2 quantification were considered only two.

3.4.4 Activation of local immune system increases the morphogen-like signaling affecting the cell fate decision of cover scale

Transplant experiments had shown that during early pupal development the eyespot center (focus) determines the cell fate of surrounding cells (Nijhout 1991; French & Brakefield 1992; French & Brakefield 1995). Eyespot development models suggest that a diffusible morphogen-like molecule is produced in focal cells and it is released to surrounding cells (Nijhout 1991; Beldade & Brakefield 2002; French & Brakefield 1995). The size of eyespots is correlated with the number of cells in the focus: more cells might produce more morphogen-like signal inducing the development of larger eyespots (French & Brakefield 1995). The cell fate of surrounding cells is determined according to the morphogen-like molecule concentration sensed in each cell (Nijhout 1991; French & Brakefield 1995; Beldade & Brakefield 2002). The identity of these morphogen-like molecules is still unknown. Well known drosophila wing patterning morphogens, such as Wingless (Wg), Decapentaplegic (Dpp) and Hedgehog (Hh) have been suggested as candidates (D N Keys et al. 1999; Monteiro et al. 2006). To understand if immunity activation can affect this signaling, we induced distinct immune challenges and measured the adult WIE. We quantified the wing area producing different color from brownish background, including a scar area (only ground scales) and the eyespot-like color rings (ground and cover scales) (as exemplified in Figure 3.4B). The immune challenge treatment affected the size of WIE ($F_{3,162}$=15.38, *p-value*<0.001) (Figure 3.4B and C). Wounds treated with heat-killed bacteria induced the development of larger

WIE (Figure 3.4C). This larger eyespot-like patterns area includes a larger scar area, ($F_{3,162}$=17.97, *p-value*<0.001) (Figure 3.4E) and a larger area of eyespot-like color rings ($F_{3,162}$=10.80, *p-value*<0.001) (Figure 3.4F).

The bacteria treatments activated higher levels of immune system both in wounded (local activation) and in contralateral non-wounded wings (systemic activation) (Figure 3.2). Thus, the enlargement of WIE can result from the local, systemic or both immune system activations. To understand if systemic immunity was the immune system component contributing for the enlargement of WIE, we designed a new experiment with two groups (Test and Control) (Figure 3.1B): we wounded pupae on both wings, the Control group with NS wounds on both left and right wings, and the Test group with a NS wound on the left and Ec7 on the right forewing. If systemic immune system activation had an effect on WIE size, the eyespot on the left wing (induced by a NS wound) should be larger in Test than in to Control group. This was not the case: WIE on right wing, but not on the left wing was larger for Test than Control individuals (effect of Group*Wing Side, $F_{1,107}$=9.57, *p-value*<0.01) (Figure 3.3C). Therefore, it is the local and not the systemic activation of immune system that mediates the enlargement of WIE. These results suggest that the local immune activation, possibly the cellular immune response, is 1) increasing the morphogen-like signal and/or 2) increasing the cellular permeability to this signal.

In favor of the first hypothesis, well known morphogen molecules have been detected at wounding sites, promoting wound healing, tissue regeneration and immunity. For example, Hh and Wg are required for tissue regeneration and Dpp is necessary to modulate the immune response upon wounding (Gibson & Schubiger 1999;

Schubiger et al. 2010; Clark et al. 2011). The calcium ion and hydrogen peroxide concentration are also signals acting as concentration gradients released at wounding sites (Razzell et al. 2013; van der Vliet & Janssen-Heininger 2014). However, their involvement during eyespot development was still not proved. One or more of these wound-signals might also be the morphogen released from the eyespot center. In this case the wound-signals promoting the immune activation, such as TGF-β superfamily (Clark et al. 2011), might be good candidates. To test this hypothesis, we can apply at the wound site and eyespot centers drugs/proteins known to agonize and/or antagonize their effects, and observe the impact on WIE and on native eyespot size (Yu et al. 1996; Pelletier et al. 2009; Frank-Kamenetsky et al. 2002).

For the second hypothesis, it is known that the immune process integrates to major responses: the cellular and the humoral response (Lemaitre & Hoffmann 2007; Krautz et al. 2014). The cellular response promotes the migration of immune cells, hemocytes, towards damaged sites (Strand 2008). Hemocytes are guided through chemoattractant signals released upon wounding (Evans & Wood). Mechanisms allowing the infiltration of hemocytes into tissues might also increase the migration rate of molecules through intracellular space – hindered diffusion (Müller et al. 2013). To test this hypothesis, we can add known drugs that decrease the hemocyte migration towards wounding (Merchant et al. 2008). and quantify the size of WIE.

3.4.5 Severe wounding and activation of local immune system inhibit the development of cover scale

Butterfly wing color patterns are formed by single color scales displayed as tiles in the wing epithelium. Colored wing scales are also

known as cover scales because they are covering another scales layer, ground scales, which are lighter in color and smaller than cover scales (Nijhout 1991). Frequently, at the wound site there is no development of colored cover scales, only ground scales do develop, the scar area (Figure 3.4B, solid line). Thus, during the wound healing process wing cells at wound site lose their ability to develop cover scales or switch their developmental program to develop only ground scales instead. This phenotype was also observed by Brakefield and French, they observed that after severe wounding the scar area was larger than in mild wounding (Brakefield & French 1995). In our experiment, infected-like wounds also developed larger scars than NS wounds (Figure 3.4E). This implicates immune system and/or tissue repair related pathways impact the type of scales that develop upon wounding. In *B. anynana*, around 40 hours post-pupation actin-rich structures start to be secreted in scale building cells, which are the future wing scales (Supplementary Figure S3.2). Scale production requires high quantities of actin (Dinwiddie et al. 2014). After wounding an actin rich cable is formed, which also requires high levels of actin and is critical to generate a pulling force that contracts the wound edges to close the wound (Wood et al. 2002; Bosch et al. 2005; Krautz et al. 2014). The actin requirements for wound healing (12-20h post-pupation) might decrease the available actin levels for scale development (36-48h post-wounding) and triggering the development of small ground instead of large cover scales at the wound site.

In severe wounds this hypothesis can be easily explained: the wound is larger and to close the wound it is necessary more time and high actin levels to form the actin cable, so the actin availability to build scales will be less and scar area larger. In infected-like wounds we do no expect a larger actin cable since the hole has the same size

as in NS wounds. However, the inflammatory response is longer (Figure 3.3) and can delay the healing process (Diegelmann & Evans 2004), which might extend in time the presence of the actin cable at wound site. Another hypothesis to explain the larger scars in infected-like wounds is the wing cellular dead at wound-site, which can be induced after melanogenesis over-activation (Nappi & Christensen 2005). Melanogenesis pathway is necessary during wound healing and also to neutralize pathogens (Binggeli et al. 2014; Nam et al. 2012). During melanin synthesis there is production of cytotoxic byproducts, which kill invader cells, but they are also harmful to host cells (Nappi & Christensen 2005; Ishii et al. 2010). We saw that 1) infected-like wounds had larger melanization areas at wound site (Figure 3.2A), 2) *ple* expression, a melanogenesis pathway gene, was eight times higher than in NS (NS=3 and Ec7=26, fold change relative to NW at four hours post-wounding) (Figure 3.3A), and 3) high expression levels of *ple* are maintained in wounded wing at least during more four hours (until eight hours post-wounding) (Figure 3.3A). In infected-like wounds melanogenesis over-activation might induce host cell death increasing the opening size, and consequently higher actin levels are required and also the wound healing process is delayed. This and previous experiments by Brakefield & French (Brakefield & French 1995) indicate that inhibition of cover scale development might be related with the time necessary to restore the wing epithelium, which might be proportional to the number of damaged cells, acting requirements and to the extent of inflammatory response.

In our experiments we did not explore in detail the scale composition of the scar area, so future experiments are necessary to understand whether in scar area we do have less and smaller scales or same number of scales but smaller. To quantify it it's necessary to

peal the wing scales and count the insertions (socket cells) of the scales in the wing.

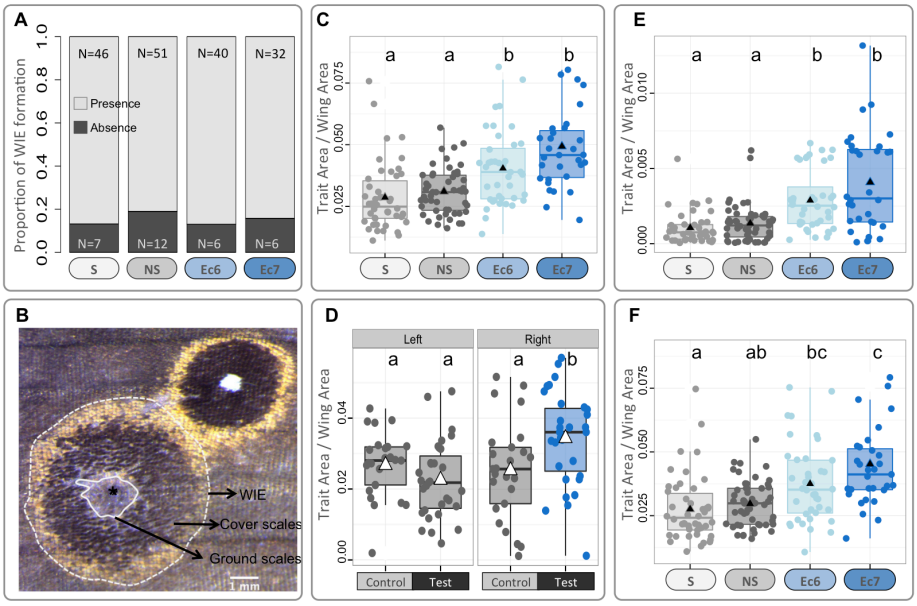

Figure 3.4- Local immune system activation induces larger, but not more WIE. A) Probability of WIE development. The immune system manipulation did not affected the likelihood of WIE development; (χ^2 = 1.02, d.f.=3, *p-value* >0.05. B) Section of anterior distal dorsal wing with anterior native eyespot and the WIE. We measured three traits of WIE: total area (dashed line), scar area (full line) and cover scales area (space between dashed and full line). (*) wound site; scale bar = 1mm. C)Total size of WIE. Higher bacterial dosage induces larger WIE; $F_{3,162}$=15.4, d.f.=162, *p-value* <0.001. D) Local, but not systemic, activation of immune system leads to enlarged WIE. The Test group produced larger WIE on right wing, but not on left wing; $F_{1,107}$(Group*Wing Side)=9.57, *p-value* <0.003, Control: N=25; Test: N=31. E) Ground scales area. High bacterial dosages inhibit the development of cover scales; $F_{3,162}$=18.0, d.f.=162, *p-value* <0.001. F) Cover scales area. Higher bacterial dosage transformed more background brownish scales into black or golden scales; $F_{3,162}$= 10.8, d.f.=162, *p-value*<0.001. Each dot represents the area of a biological replicate and triangles are the mean of each treatment, the horizontal line in the boxplot is the median, boxplot limits are the upper and lower quartiles and error bars are the maximum (upper) and minimum (lower) values excluding outliers. Different letters indicate treatment pairwise comparisons statistically different (lsmeans *p-value*<0.05). The sample size in C), E) and F) were the individuals producing WIE on A).

3.4.6 Reepithelialization and immunity related-genes might have distinct roles in WIE development

Wounding an early pupal developing wing affects the cell fate of wounded and surrounding wing cells in two ways: 1) scale-type development (ground or cover scales in focus-like cells), and 2) pigment-type production (black or golden instead around wound site). Here we quantified the area of 1) non-background scales around wound site, total WIE area (Figure 3.4C), 2) the scar area, only ground scales (Figure 3.4E), and the black and golden cover scales area, the difference between total and scar area (Figure 3.4F). All three traits were larger in groups with stronger activation of immunity (Ec6 and Ec7 groups) (Figure 3.4C, E and F). These results indicate that the immunity-associated genetic pathways impact both cell fate decisions: scale-type development and pigment-type production. As referred before, severe wounds without additional immune challenge affected the probability of eyespot-like pattern and scale-type development, but not the total number of cells with different pigmentation (Brakefield & French 1995). Therefore, factors increasing the scar area are equivalently activated in severe and infect-like wounds, but factors determining formation or not formation of an eyespot like pattern and the total number of cells changing the cell fate are stronger in severe wounds and in infected-like wounds, respectively.

The formation of an eyespot is tightly correlated with the expression of several transcriptional factors during late larval and early pupal development (Brakefield et al. 1996; Brunetti et al. 2001; Saenko et al. 2011). Antennapedia (Antp) in one of these transcription factors and we saw in previous chapter that some cells were expressing it at the wound edge 4h post-wounding. The expression of Antp at wound site can be correlated with the severity of wounding

and with the number of cells damaged and also with the cell fate decision of develop or not an eyespot-like pattern. To test this hypothesis it is necessary quantify the number of cells expressing Antp at wound site in mild and severe wounds.

Several studies in Drosophila have shown that severe epithelial damage activate higher levels of melanin pathway enzymes relative to mild injuries (Nam et al. 2012; Binggeli et al. 2014). Other study had demonstrated that after injury *Dpp*, a TGf-β signal, acts as an anti-inflammatory to decreases the expression of AMPs, this down-regulation of immune system is particularly strong in sterile injuries (Clark et al. 2011). *dawdle* (*daw*), another TGf-β signal, also inhibit the immune response, repressing the melanogenesis pathway, specially after infection (Clark et al. 2011). Thus, mild wounds reduce AMPs expression and infected-like wounds repress the over-activation of the melanogenesis pathway. Severe wounds presumably stimulate higher levels of melanogenessis than mild wounds, but AMPs levels might be similar, or only slightly high, because in absence of infection *Dpp* represses the AMP production. Infected-like wounds induced larger WIE and severe wounds did not, both wound types can activate high levels of tissue repair mechanisms (explained above) and melanogenesis, but only infected-like wounds can induce high levels of AMPs. In eyespot development models a morphogen-like signal regulates the eyespot size; higher levels produce larger eyespots (French & Brakefield 1992; Nijhout 1991). Therefore, morphogen-like signals regulating the production of AMPs might be good candidates to be the morphogen-like signal produced at the eyespot center that control the pigment-type development. Furthermore, the cytotoxic effects of melanogenesis, which might be correlated with the time required to restore of epithelium, regulate the scale-type development. Together, it suggests that different processes of wound healing

response are affecting different aspects of eyespot like patterns development. We propose that the number of damaged cells at wounding controls the establishment of an eyespot-like organizing center (Figure 3.5B); the duration of tissue reepithelialization affects the scale-type development (Figure 3.5C) and the level of immunity activation affects the pigment-type production (Figure 3.5D).

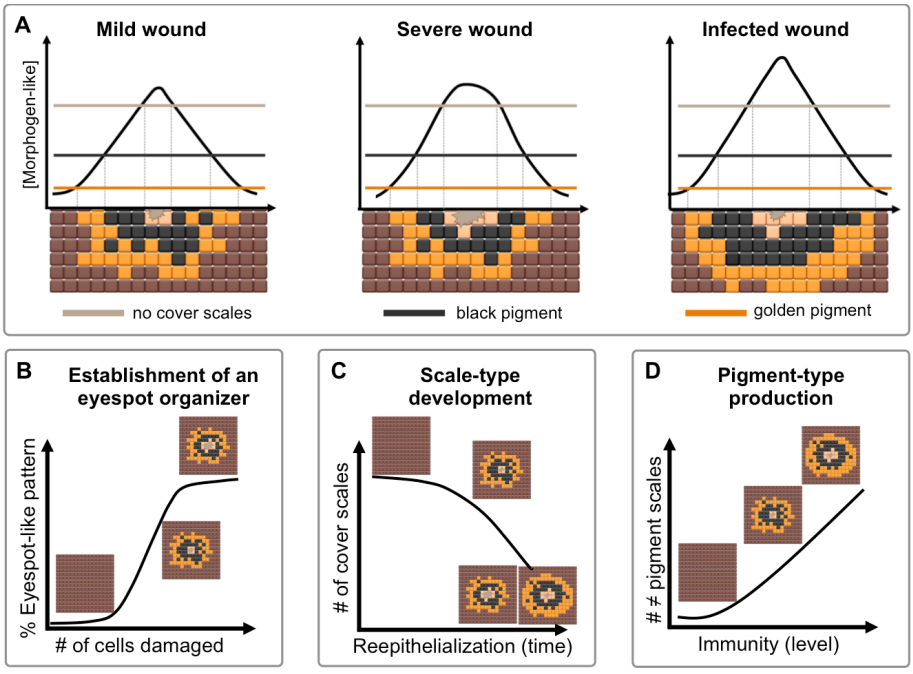

Figure 3.5- Possible models for morphogen-like molecule(s) production upon different wound types and cell fate determination on early pupal wing cells. A) Model of development of WIP after mild, severe and infected wounds. Black curve represents the concentration of morphogen-like and other lines represent the threshold-like response in wing epithelium. B-D) cell fate decisions upon wounding to establish an eyespot-like center (B), the scale-type (C) and the pigment-type (D) might rely on number of damaged cells, duration of epithelium reepithelialization and immunity level, respectively.

3.5. Conclusions

For simplicity, biologists always try to compartmentalize genetic networks, for example, as developmental or immune networks. However, the cases of blurring frontiers between both are quite common. For example the Toll pathway, which was first described as a developmental pathway essential to establish the dorsoventral axis in invertebrates, was lately described to be also essential in immune processes (Valanne et al. 2011).

Here, we studied another case of blurring frontiers, between eyespot development and wound response, where the genetic circuitry described as wound-related might be essential during butterfly eyespot development. Our and also previous results indicate that the number of wounded cells might establish an eyespot-like center; the duration of reepithilialization process might affect the type of scales produced; and the level of immunity activation affects the color of cover scales. During evolution Lepidopterans might have co-opted the initial wound signaling to establish eyespot-organizing centers, the tissue repair genetic circuitry to control the scale morphology; and immunity genetic circuitry to regulate eyespot size. Fine-tune adjustments of these gene networks might have been crucial for differentiation of wing cells through evolution and contribute for diversification of eyespot-like patterns in terms of its size, color, number, position, number of rings and also scale morphology.

3.6. Acknowledgments

We thank Antónia Monteiro for the *B. anynana* lab stock and Isabel Gordo for the *E. coli* bacterial strain used in these experiments, EVO-DEVO IGC community for the useful discussions, Luis Teixeira for the suggestions in experimental designto test the effects of local vs.

systemic effect of immune system and David Duneau and Jorge Carneiro for the suggestions to analyze the qPCR.

Chapter 4 – Immunity up-regulation in pupae phenocopies effects of low temperature on development time, wing patterns, and pupal ecdysone levels

4.1. Summary

In seasonal environments, fluctuations are predictable and multicellular organisms with seasonal polyphenism can cope better. Seasonal polymorphic organisms sense abiotic and biotic cues associated with a specific environment and change their development to produce the most adjusted phenotype. Changes in body pigmentation are common responses in this developmental process and usually they are regulated through changes in hormonal levels. In insects, pigmentation is tightly associated with the environmental temperature and internal immune state sensed during development. Here, we used a butterfly model system (*Bicyclus anynna*) to explore the effects on pigmentation after manipulation of internal immune state on a pre-adult stage. We saw that immunity phenocopied partially the effects of low developmental temperature and that this effect was independent of the immune challenge tissue/organ and bacterial-type. High systemic immunity induced 1) longer pupal developmental time, and reduced 2) eyespot size, 3) overall wing darkness, 4) wing color contrast and 5) pupal 20-hydroxyecdysone (20E) levels. These results demonstrated that immunity also induce

phenotypic plasticity in *B. anynana*. Future experiments exploring the interaction between pigmentation, temperature and immunity, and its regulation through hormones might shed light into the diversification of butterfly wing patterns.

4.2. Introduction

Many multicellular organisms have multiple life cycles during one-year length and different generations have to survive in completely different environmental conditions. Environmental fluctuations can affect drastically the availability of different nutrients, the presence of detrimental substances or other external abiotic and biotic factors like temperature and pathogens (Beldade et al. 2011). However, multicellular organisms have evolved mechanisms to cope with this environmental variation in order to survive and assure phenotypically robust developmental outcome (Braendle & Félix 2009). Thus, the external environment can affect development and lead to the production of distinct phenotypes from the same genotype, this mechanism is called phenotypic plasticity (Pigliucci 2001; Beldade et al. 2011). Seasonal polyphenism, in which different forms of a species are produced at different times of the year, is a common form of phenotypic plasticity among insects (Hazel 2002). In seasonal habitats, phenotypic plasticity may evolve as a result of contrasting but predictable seasonal selection pressures, resulting in different phenotypes being expressed in each season (Roskam & Brakefield 1999; Oostra et al. 2014). The environmental cues inducing seasonal polyphenism can be very diverse. For example, abiotic cues: temperature, photoperiod, and salinity; and biotic cues: nutrition, crowding, presence of predators and pathogens (Beldade et al. 2011; Poinar & Yanoviak 2008).

Body pigmentation is among the most common phenotypic traits that depend on developmental temperature and is relatively easy to quantify (Watt 1968; Rajpurohit et al. 2008; Gibert et al. 2004). However, body pigmentation also can change with variations in biotoc factors, such as crowding and presence of pathogens (Hassall 2014; Barnes & Siva-Jothy 2000; Galko & Krasnow 2004). In insects, low temperatures and high immune function both induce the development of darker body pigmentation through up-regulation of melanin pathway (Nishikawa et al. 2013; Binggeli et al. 2014).

Like many butterflies from highly seasonal environments (examples in (Beldade & Brakefield 2002)), *B. anynana* exhibits clear seasonal polyphenism, developing darker wing pigmentation patterns at low temperatures (Roskam & Brakefield 1999). In sub-Saharan Africa, larvae that develop during the wet season produce adults with conspicuous wing patterns that include large marginal eyespots, while those that develop during the dry season produce adults with dull brown colors and very small eyespots (Figure 4.1). These alternative wing patterns correspond to alternative strategies to avoid predation. While the marginal large eyespots of the wet-season butterflies are thought to attract the predator's attention to the wing margin and away from the vulnerable body, the all-brown dry-season butterflies are cryptic against a background of dry leaves (Brakefield & Frankino 2009; Olofsson et al. 2010). Laboratory studies showed that the temperature sensed during development, which predicts the natural seasonal fluctuations in precipitation, determines the production of the alternative wing pattern phenotypes (Brakefield & Frankino 2009). Curiously, only the wing pattern on the ventral side of the wings (the surface exposed at rest) shows plasticity in relation to developmental temperature (Brakefield et al. 1998) and has been associated with predator avoidance (Prudic et al. 2015).

The seasonal polyphenism is hormone-mediated, 20-hydroxyecdysone (20E) (the molting hormone) dynamic also varies with rearing temperature (Koch et al. 1996; Oostra et al. 2011; Mateus et al. 2014). Individuals reared above 23°C have earlier hormone titers peak, whereas individuals reared below 19°C the hormonal peak occurs later (Oostra et al. 2011). Hormonal manipulations of individuals reared at low temperatures induced the development of wing patterns more conspicuous with larger eyespots, demonstrating that 20E is mediating, at least partially, seasonal polyphenism in this butterfly (Koch et al. 1996; Mateus et al. 2014). Several studies have been implicating this hormone also in immune processes in which it is critical to regulate the gene expression of antimicrobial peptides (AMPs) after immune challenge (Tian et al. 2010).

Here, we explored the triad temperature-pigmentation-immunity in *B. anynana*, a model of seasonal polyphenism with well characterized mechanisms for temperature-induced changes in wing pattern (Roskam & Brakefield 1999; Koch et al. 1996; Mateus et al. 2014; Monteiro et al. 2015). In previous experiments, we showed that the immune system was involved in size regulation of eyespot-like patterns induced by wounding (Chapter 3 - Figure 3.4C). Moreover, even at naked eye, it was clear that those adults that had experienced higher bacterial dosage as pupae (Ec7) had smaller native eyespots and different wing color tones on ventral wing side (Figure 4.1). Ec7 wing patterns were less conspicuous than in control group, and the marginal and submarginal bands and also all patterns elements in border ocelli were very easy to distinguish in PBS, but not in Ec7 individuals (Figure 4.1). The bacterial treatment affected native eyespots in the opposite direction of wound-induced eyespot-like patterns, phenocopying the effect of low developmental temperature. Nevertheless, the effect on wing patterns of low developmental

temperature is more drastic than after bacterial challenge (Figure 4.1). In this chapter, we investigated the effects on developmental time (Figure 4.3), wing patterns after bacterial treatment 1) on different positions (wing and thorax) (Figure 4.4) and 2) different bacteria-types and dosages (Figure 4.5 and 4.6) and the effects on hormonal dynamics after bacterial treatment (Figure 4.7). We saw that ventral eyespots were smaller independently of the position and bacterial-type, and that immune-challenge individuals had similar 20E levels to low developmental temperature individuals.

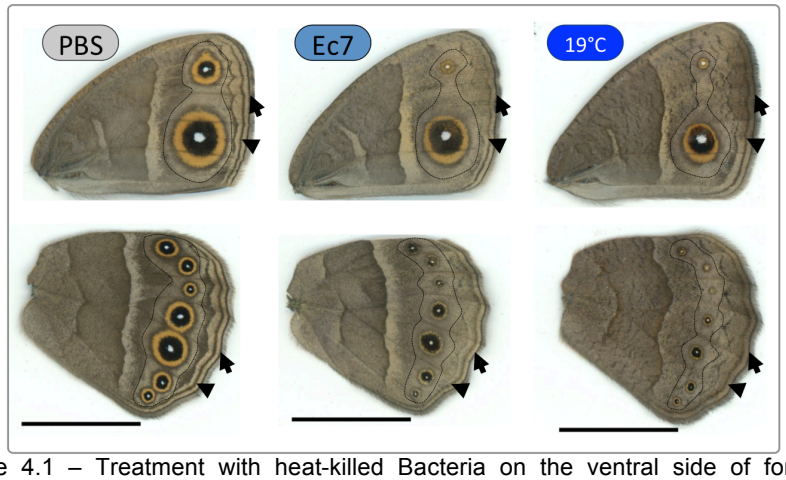

Figure 4.1 – Treatment with heat-killed Bacteria on the ventral side of forewing phenocopies low developmental temperature effects on ventral wing patterns. Ventral surface of fore- (top) and hindwing (bottom) of females reared at 27°C and wounded with application of PBS (left) or solution of heat-killed bacteria (Ec7) (center), or non-wounded female reared at 19°C (right). In Ec7 as well as in low developmental temperature, border ocelli elements (dashed line) are smaller, the marginal (arrow) and submarginal (arrowhead) bands are reduced and the overall wing pigmentation is dull brown. Scale bar 1 cm.

4.3. Materials and Methods

4.3.1 Biological Material

B. anynana butterflies from an inbreed line (a sub population from Antónia Monteiro's lab; used for whole genome sequencing) were

reared at 27 or 19°C as described elsewhere (Brakefield et al. 2009). Briefly, the butterflies were maintained at 27 or 19°C (+/- 0.5°C) with 65% (+/-1%) relative humidity and 12/12hrs light/dark cycle. Eggs were collected on a very young maize plant from net cages (45x45x45cm; BugDorm-44545) with approximately 400 adult individuals. Eggs were collected and bleached (5 min in a 20% bleach solution) during the first day after laying Adult butterflies were fed with fresh banana on top of wet cotton, and larvae were fed with fresh young maize plants and maintained in cages identical of those used for adults at a density of 150 to 200 individuals per cage. Larvae were sexed and only females were used in this study. Pre-pupae were collected onto 25 well plates and pupation time was recorded during the night via time-lapse photography with a photo taken each 10 min (Canon 1000D digital camera, Hahnel Giga T Pro 2.4GHz wireless timer remote control). We stimulated the immune system of 12hr old female pupae (cf. below) and then returned them to 27°C until wing dissection, hemolymph extraction, or adult eclosion.

3.3.2 Immune challenge treatments

We induced immune challenge treatments using heat-killed bacteria and differing in: 1) place of application of heat-killed bacterial solutions: wing versus thorax (Figure 4.2A), 2) bacteria used: Gram negative (Gram-) *Escherichia coli* (DM09-CFP) (Ec), Gram positive (Gram+) *Staphylococcus aureus* (NCTC8325-4) (Sa), or a balanced mix of both (ES), and 3) bacterial doses: 0 (control), $0.5x10^5$, $0.5x10^6$, or $0.5x10^7$ total bacterial cells in PBS (Figure 4.2B). We used heat-killed bacteria obtained from overnight liquid cultures from a single colony. Bacteria were collected after heat shock treatment (80°C during 30 min) and dissolved in sterilized PBS in three different

concentrations stock solutions: 10^5, 10^6, or10^7 cells/μL. Directly to the fresh wound, we added 0.5 μL of different stock solutions: 1) non-sterilized wound, sterilized PBS (NS), 2) 10^5 cells/μL (Ec5 and Sa5), 3) 10^6 cells/μL (Ec6 and Sa6), and 4) 10^7cells/μL (Ec7 and Sa7). Wounds were made with a tungsten needle (cat. no. 501317; World Precision Instruments) either on the right forewing wing (cf. Chapter 3) or on the thorax (in the middle of the dorsal part of the third thoracic segment) of 12hr old pupae reared at 27°C. Pupae were then returned to 27°C until hemolymph extraction or until adult eclosion.

4.3.3 Measurement of adult wing eyespots

After stretching and drying their wings, adult butterflies were sacrificed (-20°C for at least 2hrs), fore and hindings were detached from the thorax and both their dorsal and ventral surfaces were scanned (Epson Perfection V600 Photo). Images were imported to Fiji (Schindelin et al. 2012) and various wing pigmentation traits were measured. First, we adjusted the threshold brightness and took the measure of the respective areas: fore and hindwing areas (threshold brightness = 200) and eyespot color rings, external golden ring, middle black disc, and central white focus (threshold brightness = 120). In the forewing we measured the most posterior eyespot traits on dorsal and ventral sides, and in hindwing the fifth eyespot traits of the ventral side (Figure S4.1A).

Data were imported to R and we used ANCOVA, using wing size as covariante, to test for immune challenge effects on position and side (model: lm(Trait size ~ Treatment * Position * Side + Wing size) and bacteria type and dosage (model: lm(Trait size ~ Treatment + Wing size). We tested for the normality of residuals (Shapiro test) and constant variance (Brown-Forsyth test), whenever it was necessary

data were transformed to fit both ANCOVA assumptions. We considered significant effects when *p-value*<0.01. We used the lsmeans R package for post-hoc pairwise comparisons (Lenth & Hervé 2015) considering different groups when *p-value*<0.01.

4.3.4 Quantification of adult wing overall darkness and color contrast

We developed a protocol to quantify the overall darkness and color contrast of hindwings. Images were imported to ImageJ software (Schindelin et al. 2012) and there we obtained the gray values for each pixel (ranging from black with gray value of zero to white gray value of 255) and calculated the average gray value *per* hindwing (Figure S4.1B), it was the distance of this value to the white (255) that we took as a measure of wing overall darkness. To analyze the color contrast in proximal-distal wing axis we draw one transect crossing the wing (from pint 1 to point 2 in Figure S4.1B and C) in ImageJ software (Schindelin et al. 2012) and took the gray values of each pixel in this transect. These values can be graphically represented as exemplified in Figure S4.1C. Curves of gray values in higher dosage immune challenged individuals seemed more flat that in control individuals. To quantify the flatness of gray values throughout transect, we counted the number of “contrast points”. We considered “contrast points” tow points that differing the same distance (10 pixels in xx axis) were different between each other in at least 30 gray value units (values on yy axis) using the formula: GrayValue(pixel(X))-GrayValue(pixel(X-10)≥30) (Figure S4.1C, note that the example of to pixels pointed on xx axis (black bar) are not necessarily 10 pixels). Transects with higher number of contrast points have more acute differences in color and consequently the color contrast is higher.

To validate these two methodologies, we measured the overall darkness and color contrast in non-wounded individuals reared at 19C and 27C. The low developmental temperature phenotype is considered to be darker and with less color contrast (Beldade & Brakefield 2002). We observed the same pattern for these two traits using these new methodologies (see Figure 4.6A).

Data were imported to R and we used ANCOVA taking the total number of pixels and the transect size as covatiantes for overall darkness and color contrast, respectively. To see the effects of temperature on these two traits we used the following models: lm(overall darkness ~ temperature + total number of pixels) and lm(color contrast ~ temperature + transect size). The effects of bacteria type and dosage were accessed through these models: lm(overall darkness ~ bacteria * dosage + total number of pixels) and lm(color contrast ~ bacteria * dosage + transect size). Residuals were normal (Shapiro test) and variance was constant (Brown-Forsyth test), so we used ANCOVA without data transformation. We considered significant effects when *p-value*<0.01, and we used the lsmeans R package for post-hoc pairwise comparisons (Lenth & Hervé 2015) considering different groups when *p-value*<0.05.

4.3.5 Quantification of 20E levels

We measured internal levels of 20E in immune challenged (control and treatments with 10^7 heat killed *E. coli* or *S. aureus* as explained above) and non-manipulated pupae reared at 27°C and 19°C at 8.5, 12 and 24% of total pupal developmental time (Figure 4.2C red square). We extracted hemolymph by smashing the pupae with a pestle in an empty 1.5mL eppendorf tube pre-warmed to 60°C. The tube was immediately placed at 60°C for 20 min to inactivate the

hemolymph enzymes and avoid melanization processes (George & Cristofalo 1972). Tubes were after placed on ice and then centrifuged (10 min at 4C) at full speed to remove cell debris. The supernatant was collected into a new cold tube and 300µL of ice-cold 100% methanol were added for protein precipitation. Samples were again centrifuged and the supernatant placed in a new cold tube. This process was repeated until no pallet was deposited upon centrifugation (typically, three times) and the samples were stored at -80°C until further processing. Before hormone quantification with EIA enzyme immunoassay (Cayman Chemical Co., Ann Arbor, MI, USA), the methanol was eliminated from the samples by using a rotary evaporator, at maximum speed (RT). During this process we checked the samples every 30 min to remove the dried ones, typically the methanol evaporation required 1h ± 30 min. Dried samples were then dissolved in assay buffer. According to the manufacturer's instructions, the quantification of 20E levels requires controls (blanks) and standard calibrator samples, to generate a calibration curve. Standard calibrator samples were generated using serial dilutions of commercially available 20E (SciTech chemicals, ref: S5314-001; 0.5 µg/µL in 100% ethanol) (six on Plate 1 and eight on Plate 2). The ethanol from standards was eliminated as methanol in hemolymph samples, and after dried standards was dissolved also in assay buffer. Absorbance for controls, standards, and hemolymph samples was measured in triplicated at a wavelength of 405 nm (VICTOR Multilevel Plate Reader spectrophotometer). We calculated the average of absorbance for controls, standard and hem lymph samples. According to manufacture instructions, we removed the blanks absorbance to all samples and used the standard samples to do a calibration curve (Figure S4.2), which was used to calculate the 20E concentration in hem lymph samples.

Data were imported to R and we used an ANOVA statistical test to see the effects of immune challenge on 20E levels, which were normalized for the minimum 20E levels in each plate. We used the following model: avo(20E levels ~ Treatment * developmental time + plate) and the leans R package for post-hoc pairwise comparisons (Lenth & Hervé 2015) considering different groups when *p-value*<0.05.

4.3.6 Manipulation of 20E levels

To the immune-challenged pupae (cf. methods described above), we also applied 0.5 µl of a solution of 20E in PBS. We first tested a dosage that had previously been used successfully to partly rescue effects of low developmental temperature: 250pg injected into the abdomen of pupa at 8% of their pupal life duration (Mateus et al. 2014). In our experiment, application of 250 pg to wing or thorax wounds lead to 100 % pupal mortality. We then tested a series of lower doses: 250, 125, 62.5 and 31.25pg of 20E *per* pupa. 62.5pg was the highest dose that did not lead to 100% mortality. To test if this dosage could restore the phenotype of high developmental temperature, we measured three wing pattern traits (size of hindwing fifth eyespot, overall darkness and color contrast) in tree different treatments 1) wound with PBS (PBS), 2) solution with 10^7 heat-killed *E. coli* (Ec7), and 3) same bacterial solution supplemented with hormone (HOR) (Figure 4.2C gray square). The hormone stock solution was dissolved in ethanol, so we added to PBS and bacterial solution the same volume of ethanol. Treated pupae were left to complete their development at 27°C, adult wings were removed, and wing pattern traits were measured and analyzed for as explained above.

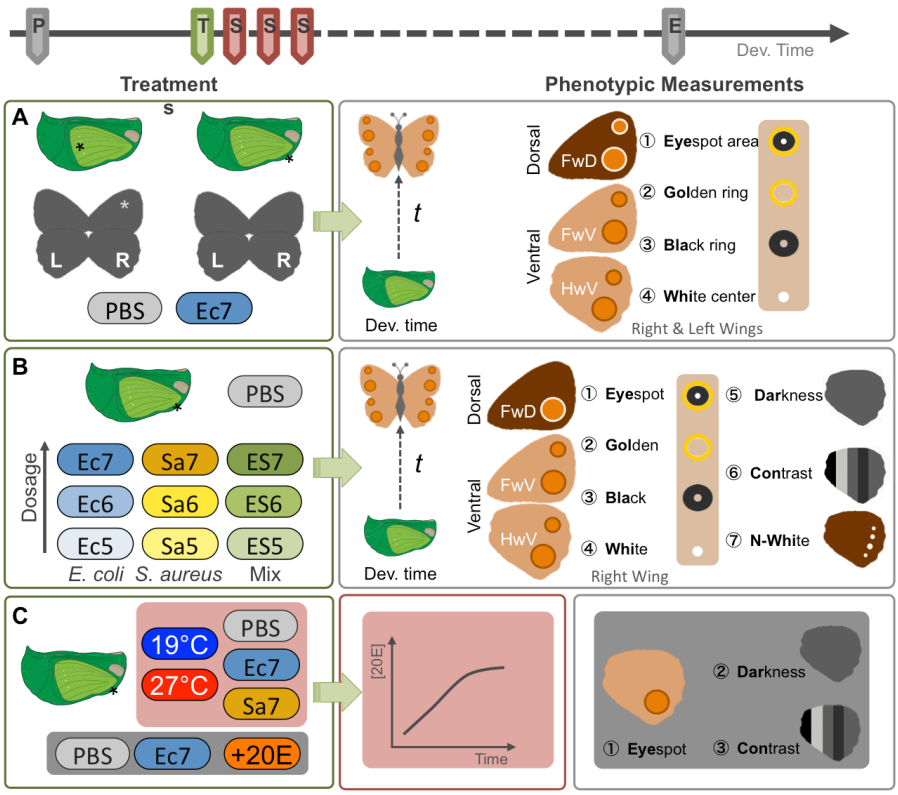

Figure 4.2- Experimental design to understand the A) treatment position effects; B) bacteria type and dosage effects and C) to measured and manipulate 20E levels. Top arrow represents developmental time from pupation (P) to eclosion (E) with treatment (T) and sampling (S) time points. In these experiments we treated the individuals always at 12hours post-pupation. To analyze treatment position effects (A) we treated individuals on wings or on thorax (position is indicated with (*) on pupae scheme) with control (0.5µL of sterile PBS – PBS) or immune challenge (0.5µL of 10^7 *E. coli* solution – Ec7) solutions and measured the pupal developmental time and six eyespots (with four eyespot traits each) on both sides (L-left and R-Right). We evaluated the effects of bacteria type and dosage (B) after treatment on thorax. We used three different bacteria types: *E. coli* (Ec – blue); *S. aureus* (Sa – yellow) and a balanced mix of both bacteria solutions (ES – green); in three different dosages: application of 0.5 µL of 10^5, 10^6 and 10^7 bacteria cells solutions (darker colors represent higher dosages). Each treatment group is identified with a combination of the bacteria type and the dosage; e.g. treatment with 0.5µL of 10^5 *E. coli* solution – Ec5. We analyzed the effects on pupal developmental time, on five eyespots (with four eyespot traits each) on the right side, on hindwing colors (overall darkness and

color contrast) and on number of dorsal hindwing white pupils. 20E levels were quantified in non-wounded individuals reared at 19°C and 27°C and in thorax-treated individuals with PBS (control group) and Ec7 and Sa7 (reddish squares). Effects of 20E manipulations were analyzed on fifth eyespot of the hindwing and also in color traits (overall darckness and color contrast). FwD-Forewing dorsal surface; FwV-Forewing Ventral surface; HwV-Hindwing Ventral surface.

4.4 Results and Discussion

The thermal developmental plasticity in *B. anynana* is well-known (Brakefield et al. 1998; Oostra et al. 2014; Mateus et al. 2014). However, to our knowledge, other environmental cues inducing developmental plasticity in this species are not described. Our results showed that immune challenged early pupae phenocopy the low developmental temperature effect in four different aspects: 1) longer pupal developmental time (Figure 4.3), 2) reduced eyespot size (Figure 4.1, 4.4, 4.5), 3) reduced color contrast (Figure 4.6B2) and 4) reduced levels of 20E (Figure 4.7). These effects were independent of the immune-challenged organ (here only tested wing and thorax) (Figure 4.4), and despite only Gram- Bacteria induced an extended response, Gram+ Bacteria had similar effects on wing patterns (Figure 4.5) and 20E levels (Figure 4.7)

4.4.1 High bacterial dosage treatment reduces the number of "fast-living" individuals

The presence of parasites and pathogens cause substantial fitness costs to their hosts. Thus, hosts have evolved effective immune systems, which are energetically expensive to maintain and to activate (Saastamoinen & Rantala 2013). Trade-offs between immune defense and other life-history traits are common (Saastamoinen & Rantala 2013; Valtonen et al. 2010). For example,

individual's nutritional resources and body condition can influence immune investment directly, in this case individuals with fewer resources being able to allocate less to immunity (Valtonen et al. 2010). Here, we investigated the effects of internal immune state on pupal survival and developmental time. We considered the effects of 1) the immune challenge position (wing and thorax), 2) the bacteria type (Gram-:Ec, Gram+:Sa and both Gram+ and Gram- together: ES), and 3) the bacteria dosage (10^5,10^6,10^7 bacterial cells)(Figure 4.2). We quantified the number of pupae that reached the adult stage in each day and several times during a day (each ~20min after light time). For same age pupae, eclosion occurred during two days (classified as fast-development (FD) (first day) and slow-development (SD)(second day). Pupae that did not eclosed during this time window were dead (classified as non-adult (✝)). Among eclosed pupae there were individuals that started the metamorphosis process but could not completed it, and others that could not stretch correctly the wings. Those individuals were also classified as non-adults. Regardless the wounding position (Figure 4.3A; Eclosion Day*Treatment: χ^2 = 43.129, d.f.=2, *p-value*<0.0001) and bacteria type (Figure 4.3C; Eclosion Day*Treatment: χ^2 = 20.63, d.f.=6, *p-value*=0.002), high bacterial challenged pupae eclosed preferentially on the second day. Only very few individuals from higher bacteria dosage groups were FD (Figure 4.3A and C). The proportion of SD was not different in comparison with control individuals (Figure 4.3A and C). If mortality among FD and SD was equivalent and both had delayed the developmental time (according to classic trade-off theory (Anderson & May 1982)), we should observe pupae eclosing on a third day, which did not occurred. Thus, our results are consequence of higher mortality among FD and same developmental time of SD or increased developmental time of FD and higher mortality of SD..

The pace of life theory predicts that “fast-living” individuals have high energy turnover, short developmental time and invest relatively little in immune defense in favor of growth and early reproduction (Niemela et al. 2013; Reznick et al. 2002). On the other hand,,“slow-living” individuals have lower energy turnover, long developmental time and invest more resources into costly immune defense (Niemela et al. 2013; Reznick et al. 2002). According to this theory, the “slow-living” animals use more slowly-deployed while “fast-living” use more rapidly-deployed immune process (Previtali et al. 2012). Melanogenesis is a fast immune response that occurs in arthropods after a wounding or immune challenge it is essential for wound healing and control of invaders (Eleftherianos & Revenis 2011; Binggeli et al. 2014). Nevertheless, if over activated it can induce the host death (Ishii et al. 2010). During the experiment we observed that after high bacterial dosage treatment, there was an intense darkening at wound site and pupae were darker, especially during the treatment day. Two days after treatment, there were pupae that had already recovered the original green color and others that were still darker. Usually, these darker pupae (still alive by the third day post-pupation) never reached the adult stage. Thus, after bacterial treatment “fast-living” pupae might have over activated melanogenesis producing higher levels of cytotoxic by-products, which induced developmental defects and consequently the pupae death.

There were more pupae eclosing on the first day in wing- than in thorax-wounded individuals in PBS treatment, for Ec7 individuals the differences were not significant, but still the proportion of first day eclosions was lower (Figure 4.3B; Position: χ^2 =97.57, d.f.=1, *p-value*<0.0001). In *Drosophila* it was shown that mortality is higher after immune challenge (in aseptic conditions and with infection) on thorax than in abdomen (Chambers et al. 2014). This indicates that the

wound healing process is different in different organs, and can result in differences in survival (Chambers et al. 2014) and perhaps in developmental time.

We saw that thorax-wounded individuals developed one day faster (four to five days) than wing-wounded individuals (five to six days)(Figure 4.3B). This experiment was done in two different phases: first we run the experiment wounding individuals on wings (during winter) and second on thorax (summer). We saw that non-wounded individuals had similar developmental time as the PBS treated individuals (personal observations) in both experimental batches. Thus, it is not the wounding position that is inducing such developmental differences. This might be a consequence of butterfly feeding system in the lab. Butterflies were fed on young maize plants growing in a greenhouse, which at the time had not very strict temperature control. In summer maize plants grew faster than in winter and the nutrient composition on plant leaves might be slightly different. This hypothesis was not tested in our lab yet, but it was shown in other Lepidoptera species that different grown conditions of host-plants can greatly influence developmental time (Bauerfeind & Fischer 2013).

Treatments with different bacteria-type did not induced differences on eclosion day (Figure 4.3D; Eclosion Day*Bacteria Type: χ^2 =0.44, d.f.=2, *p-value*= 0.8020). However, higher bacterial dosages groups eclosed preferentially on the second day (Figure 4.3D; Eclosion Day* Dosage: χ^2 = 43.57, d.f.=3, *p-value*< 0.0001). The lowest bacterial dosage did not induced differences relative to PBS treatment group and the intermediated dosage only induced differences with Gram- bacteria (*E. coli*, Ec). This might indicate that

Gram- Bacteria are more efficient to overactivate the immune system in this butterfly,

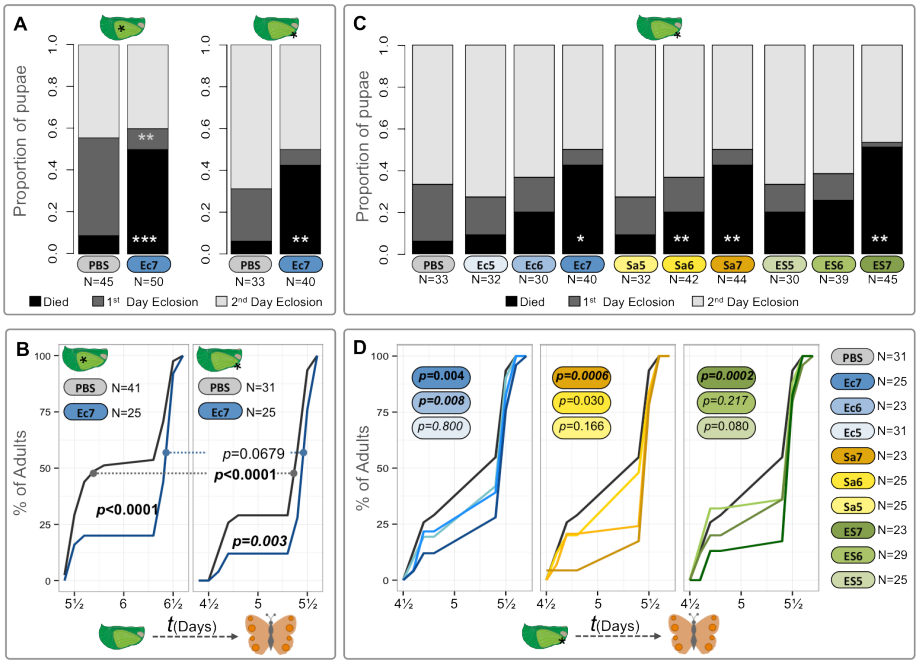

Figure 4.3- Effects on survival and pupal developmental time after different immune challenges. The mortality and developmental defects were increased in immune-challenged individuals independent of the treatment position (A) and bacteria type (B), but they were significant only in higher dosages. Among the individuals that had reached adult stage, the total developmental time was different in immune-challenged individuals. This effect was independent of the treatment position (C) and bacteria type (D), and it was statically significant in higher bacterial dosages (10^7 bacteria cells in all bacteria types and also in10^6 for Ec). *p-value* <0.001***, *p-value* <0.01**, *p-value*<0.05*; sample sizes (N) are indicated for each treatment group in each experiment; treatment position is represented by an asterisk (*) on pupae scheme; Ec: *E. coli*; Sa: *S. aureus*; ES: balanced mix of both bacteria (Ec and Sa) solutions; treatment with 0.5 µL of 10^5, 10^6 and 10^7 bacteria cells solutions are represented as 5, 6 and 7 numbers after bacteria type, with darker colors representing higher dosages.

4.4.2 Systemic immunity is a developmental plasticity trigger

After Chapter's 3 experiments, we noticed that individuals treated with Bacteria on dorsal wings had changed their ventral wing patterns

(Figure 4.1). Wing patterns were similar to those of low developmental temperature. (Figure 4.1). To understand if these phenotypic effects were a wing-specific response or a general response to internal immunity state, we induced wounds on thorax and compare phenotypes between wing- and thorax-treated groups (Figure 4.2A). We hypothesized that effects after wing-treatment were wing-specific if after thorax-treatment with same stimuli, there were no phenotypic differences between control (PBS) and treatment (Ec7) groups. For this comparison we measured the area of color rings in six eyespots *per* side (left and right) obtaining four eyespot traits *per* eyespot: golden, black, and white areas and total eyespot area (sum of golden, black and white areas) (Figure 4.2). Results are show in Figure 4.4 and are represented as the percentage of difference relative to PBS. There are significantly different responses (red circles in Figure 4.4; dotplots graphics in Supplementary Figure S4.3), in which the size of eyespot traits were smaller, in wing- and in thorax-treated groups. Thus, reduction of native eyespot size is a result of differences in internal immune state and can be induced in different organs other than wings.

Previous studies have shown that the eyespot center produces one (or more) morphogens that diffuse to the surrounding cells which, depending on the morphogen concentration they experience, become fated to producing different colors (Brunetti et al. 2001; French & Brakefield 1992). The centers of larger eyespots presumably produce higher quantities of morphogen that spread through more cells (Monteiro et al. 1997; Patrícia Beldade et al. 2008; Beldade & Brakefield 2002). In native eyespots, systemic immunity might have reduced the production and/or migration of this focal signal inducing the formation of smaller eyespots. On the other hand, on wound-induced eyespot-like patterns, the local immunity had the opposite

effect enlarging them (Chapter 3 – Figure 3.4). Thus, it seems that no mater the type of eyespot patterns, immunity processes are crucial for eyespot size regulation.

4.4.3 Local and systemic immunity has an additive effect on native eyespot size regulation

Local immunity, i.e. the locally increased immune resistance/tolerance of a tissue or organ without the participation of the organism as a whole (Frisch 1930), is very common in epithelial tissues that are in direct contact with the external environment (Ferrandon et al. 1998). In these barrier tissues AMPs expression helps multicellular organism to prevent pathogen infections (Davis & Engström 2012). In *B. anynana*, we have shown before that in wounded wings the activation of immune related genes is higher and longer than in contralateral wings (Chapter 3 - Figure 3.3). Higher gene expression might be the cumulative effect of two different immune responses: local and systemic immunity, but only systemic immunity affects contralateral non-wounded wings. Those differences might be enough to induce distinct responses between both wings in wing-treated group. We analyzed eyespot traits on left and right wings to distinguish possible effects of local and systemic (wounded side - right) *vs.* only systemic (Non-wounded site – left) immunity. If local immune response, which regulates the size of wound-induced eyespots (Chapter 3 - Figure 3.4), also regulates the size of native eyespots, the right side might have higher number of smaller eyespot traits than left side in wing-treated group. On the other hand, the number of smaller eyespot traits might be the same on both sides of thorax-treated group. Indeed, this was the case (Figure 4.4). After wing treatment, there were 14 traits decreasing the size on the right *vs.*

seven on the left side (Figure 4.4). After thorax treatment there were no differences between both sites; same seven traits responded on right and left sides (Figure 4.4). Therefore, in wounded side of wing-treated individuals it might occur a cumulative effect of local and systemic immunity, which induced higher immunity levels on this side. This effect did not occur in contralateral wings of wing-treated and both wings of thorax-treated individuals.

In previous chapter we saw that local immunity was enlarging wound-induced eyespot-like patterns (Chapter 3 – Figure 3.4D) and here it is reducing the native eyespots, how this contradictory effects can be triggered by same type of immune response we do not know. Nevertheless, we can pointing three hypothesis: 1) different phases of local immune response affect each type of eyespot; e.g. first signals affect wound-induced and later signals the native eyespots, 2) the same immune-related signals are interpreted differently in each type of eyespot, and 3) systemic immunity is not homogeneous in all pupae with higher levels on immune affected and surrounding body compartments, so the wounded side (right side) in wing-wounded individuals reduced more eyespot traits.

4.4.4 Different sets of eyespot traits were affected after wing and thorax immune challenge

The immune system detects pathogen invasion, tissue damage, abnormal cell growth, and also participates in wound healing and tissue remodeling. During development the risk of such factors is variable, for example, in insects after metamorphoses the tissue remodeling is high and also the immune cells activity (Altincicek & Vilcinskas 2006; Lanot et al. 2001). Metazoans have compartmentalized bodies, which necessarily leads to the

compartmentalization of immune responses. Cells of the immune system have the ability to circulate between body compartments and inevitably the local environments in these compartments influence them (Hu & Pasare 2013). Thus, different organs also can induce different immune responses, for example in drosophila the immune response after immune challenge on abdomen and in the thorax is different inducing higher mortality on thorax (Chambers et al. 2014). Here, we saw that after immune challenge on wing and on thorax there were reduction of native eyespot traits, but the set of native eyespot traits responding was different. There were traits that responded always independent of the treatment position (FwVAnt-Eye, FwVAnt-Bla, FwVPost-Gol, HwVPost-Gol), and others that only responded after wing (FwVPost-Eye, HwVAnt-Eye, HwVAnt-Gol) or thorax treatment (HwVAnt-Bla, HwVPost-Eye, HwVPost-Bla) (Figure 4.4). We classified these traits as systemic, systemic-wing and systemic-thorax responses, respectively. Therefore, the eyespot size regulation mediated by immunity can occur 1) systemically and tissue specific: the response observed in left wing of wing- but not in thorax-treated wings or the other way around; and 2) systemically and tissue independent: the response observed in left and right sides of both wounding positions (Figure 4.4). This suggests that different organs might induce different systemic immune responses, such as different immune activation levels (more cells and/or higher production of immune proteins) or different cellular immune responses (different immune cells producing different immune proteins). Nevertheless, we saw and discussed above (Figure 4.3) that total developmental time in wing- and thorax-treated individuals was different. Thus, these differences can result from differences in developmental stage at immune treatment of wing- and thorax-treated individual cohorts. If this hypothesis is true, not only the immunity thresholds are specific

for each trait (or each trait set) but also they have different sensitive periods to respond, heterochrony, to immunity levels. In this case, the sensitive period for traits on systemic – thorax is early, followed by systemic (tissue non-specific) and after by systemic – wing response (Figure 4.3). To test this hypothesis, different time points must be used to induce the immune challenge, early time points might induce similar differences as on systemic-thorax responding traits and later time points as on systemic-wing responding traits.

4.4.5 Traits related with natural selection are more sensitive to internal immunity state during development

It was demonstrated in *B. anynana* that the dorsal and ventral surfaces of same wing have different sensitivities to temperature: the dorsal surface barely responded (non-plastic) and the ventral surface very responsive (plastic) (Mateus et al. 2014; Brakefield et al. 1998). Here, we saw the same pattern; some of dorsal eyespot traits only responded in wounded wing, but almost half (seven) of ventral surface traits responded on both wings in wing- and thorax-treated individuals (Figure 4.4).

Dorsal traits on forewing are associated with sexual selection (Robertson & Monteiro 2005; Breuker & Brakefield 2002), they are more robust to temperature oscillations (Mateus et al. 2014) and here we also saw to internal immune variations. High levels of immunity, such as in wounded wings (Chapter 3 - Figure 3.3), reduce dorsal eyespots, especially the black ring area, but not the trait associated with sexual selection, the white pupil of dorsal posterior eyespot (Robertson & Monteiro 2005) (Figure 4.4). On the other hand, ventral patterns are under natural selection by predators (Prudic et al. 2015). In our experiments the ventral traits were more responsive,

independently of the wounding position (Figure 4.4). Golden and black rings were not significantly smaller for the in the same eyespot. There were differences in responding rings between 1) treatment positions (wing *vs.* thorax), 2) wings (forewing versus hindwing) and 3) wing compartments (anterior versus posterior). On thorax-treated individuals, anterior eyespots reduced the black ring and posterior eyespot the golden ring. The same was true for wing-treated individuals, but only in forewing, in hindwing only golden rings responded (Figure 4.4).

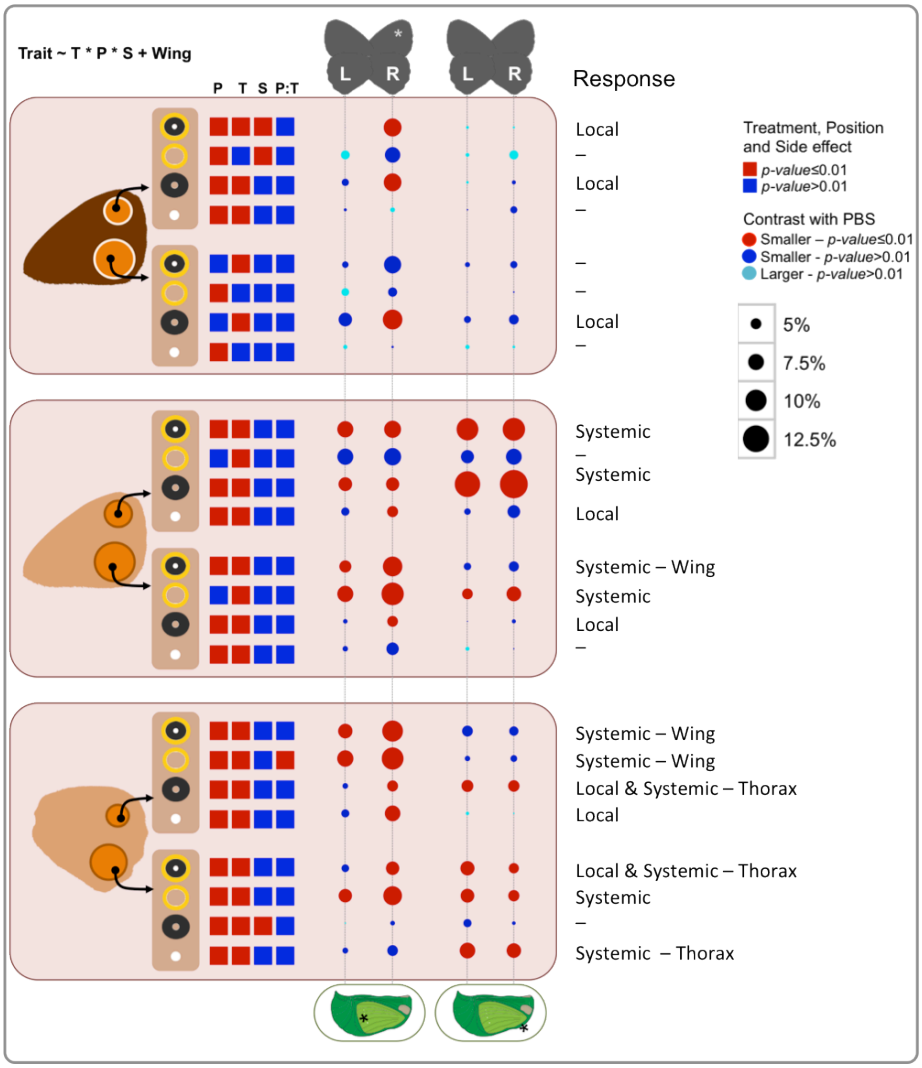

Figure 4.4 - Effect of treatment position and wing side on different eyespot traits. For each trait, side and treatment-position combination, the circles represent the magnitude (circle size; scale on right side), the colors represent the direction of size variation (red and dark blue for smaller eyespots and light blue for larger eyespots relative to PBS) and statistical significance (red for significant differences (*p-value*<0.01)) of the difference between immune- *vs.* control-treated individuals. We tested the model lm(trait size ~ treatment (T) * position (P) * side (S) + wing size); color squares represent the effect of model terms (red significant (*p-value*≤0.01) and blue non-significant). Eyespot traits are organized *per* wing: dorsal forewing, ventral forewing and ventral hindwing eyespot traits. Traits were classified according to its

response: no response, local or systemic response. The systemic response was subdivided in two classes: independent (systemic) or dependent of wounding position (systemic-wing or -thorax). See data point distribution in Supplementary Figure S4.3. Sample sizes are between 23 and 60.

Previous experiments testing for the effect of developmental temperature and hormone manipulations on eyespot color rings had shown differences in developmental plasticity among different rings between dorsal and ventral eyespots and between anterior and posterior wing compartments (Mateus et al. 2014). It has been shown that butterflies with dry season phenotype (smaller eyespots) in a wet season environment dye more after a predator attack (Prudic et al. 2015). Thus, an infection during early pupal development might have two fitness costs associated: 1) the resources used during development in immunity cannot be later used on reproduction or locomotion and 2) the risk of predation during adult stage might increase.

4.4.6 Immune challenge level, but not type, affected eyespot size

Different types of bacteria activate preferentially different immune system pathways. Most Gram- bacteria are rich in meso-diaminopimelic acid containing peptidoglycan (DAP-PGN), while Gram+ bacteria in lysine-containing peptidoglycan (Lys-PGN). DAP-PGN and Lys-PGN preferentially activate the IMD or Toll pathways, respectively (Tanaka & Yamakawa 2011). However, there is cross talk between both pathways that act synergistically after an immune challenge (Tanji et al. 2007). We tested if immune challenge with three different heat-killed bacteria solutions (Gram-: Ec, Gram+: Sa, and a mix of both bacteria: ES) in different dosages (0.5 µL of a solution with

10^5, 10^6 and 10^7 bacterial cells) induces different phenotypic responses in wing pigmentation (Figure 4.2). We saw that despite Gram+ bacteria had induced more significant differences relative to control group (Figure 4.5). This might indicate that the pathways controlling Gram- pathogens, e.g. IMD, are more involved in eyespot development than pathways controlling Gram+ pathogens, e.g. Toll.

Lower experimental dosages (ca. 10^5 and 10^6 bacterial cells) did not significantly decrease the size of eyespot traits (dark blue circles, Figure 4.5), but higher dosage (ca. 10^7 bacterial cells) resulted in smaller eyespots (red circles, Figure 4.5). Moreover, lower dosages had the opposite effect increasing the size of some eyespot traits (light blue circles, Figure 4.5). This indicates that activation of immune system does not always mean smaller eyespots. Testing different bacterial dosages and also different time points can clarify this hypothesis.

The role of Toll and IMD pathways after infection is well documented (De Gregorio et al. 2002; Lemaitre & Hoffmann 2007; Tanaka & Yamakawa 2011). Toll pathway were also described having a crucial role in dorsal/ventral patterning during embryonic development (Belvin & Anderson 1996). IMD pathway is more described in regulation of immune-related processes (Costa et al. 2009; Myllymäki et al. 2014), but *relish* a transcription factor involved in IMD signaling has shown to be involved in aging and neurodegeneration developmental processes (Seroude et al. 2002; Chinchore et al. 2012). In *B. anynana*, Toll and IMD pathways (or related pathways) might be crucial in eyespot size regulation. Our results indicate that IMD might decrease eyespot size and both IMD and Toll together might increase it.

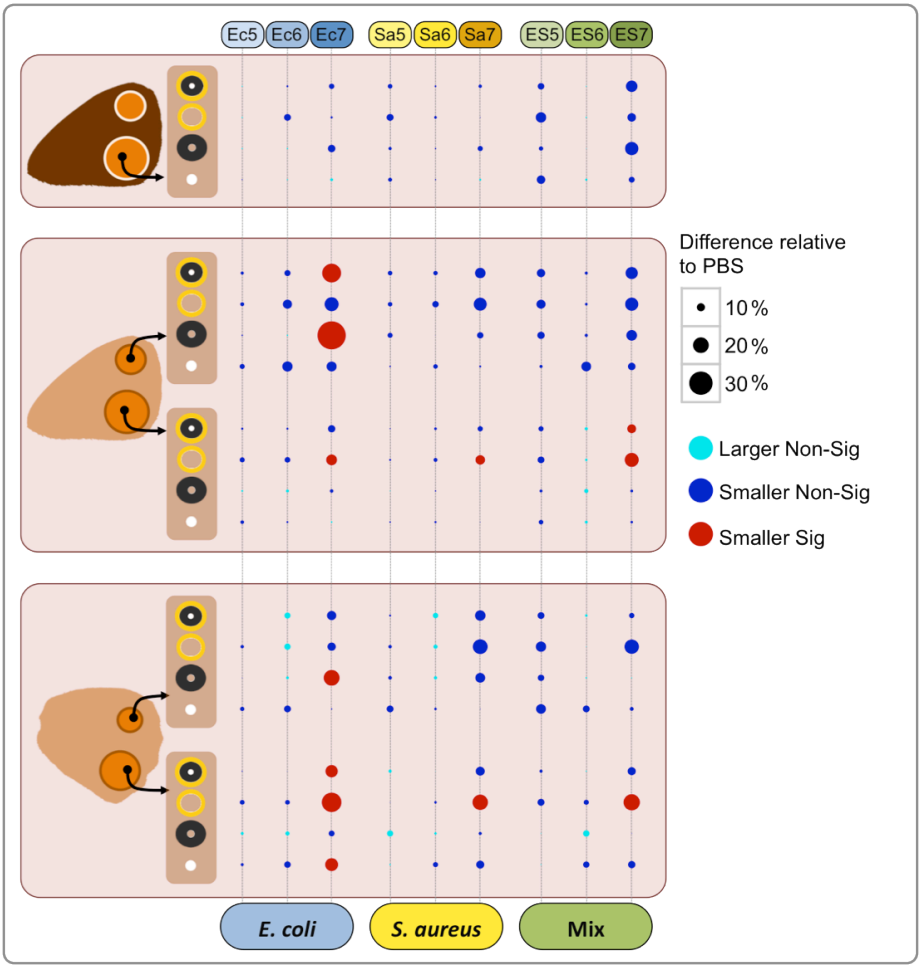

Figure 4.5- Effect of bacteria type and dosage on different eyespot traits. For each trait, bacteria type and dosage combination, the circles represent the magnitude of different relative to PBS (circle size; scale on the right side), Different colors represent different directions of eyespot size variation (red and dark blue for smaller and light blue for larger eyespots) and statistical significance (red significant and two shades of blue for non-significant differences; lsmeans *p-value*≤0.01). We used an ANCOVA statistical test to test the model: lm (trait size ~ Treatment + wing size). Eyespot traits are organized per wing: dorsal forewing, ventral forewing and ventral hindwing eyespot traits. See data point distribution in Supplementary Figure S4.4. Sample sizes are between 23 and 31.

4.4.7 Immunity up-regulation only partially phenocopies the low developmental temperature syndrome

In insects, pigmentation plays essential role in thermoregulation, sexual selection, species recognition and immunity (Wittkopp & Beldade 2009). Melanin pigments play a key role in both coloration of the insect integument and in defense against pathogens and an increasing body pigmentation is costly and associated with higher resistance to infection (Dubovskiy et al. 2013; Hassall 2014; Barnes & Siva-Jothy 2000). Here, we observed that the wing patterns of *B. anynana* changed dramatically after an immune stimulation (Figure 4.1). We started analyzing changes in eyespot size, because differences were obvious and eyespots are easy to measure. However, this treatment also induced other changes in wing pigmentation that were not so easy to measure. We tried to find some methodologies to quantify possible differences in general wing pigmentation, such as the overall darkness of the wing and the color contrast over proximal-distal axis (for a better explanation see Materials and Methods). To validate this methodologies we used non-manipulated individuals reared at 19°C and 27°C and compared them, expecting low temperature individuals to have darker and less color contrast phenotypes. Indeed, this was the case (Figure 4.6A_1 and A_2).

The highest dosages of bacteria decreased the overall wing darkness, contrary to low temperature individuals (Figure 4.6B_1). On the other hand, the color contrast of same individuals decreased as in low temperature, both presented less color contrast (Figure 4.6B_2). Melanic strains are usually more resistant to parasites, but in the absence of pathogens, the heavy defense investments result in a lower biomass, decreased longevity and lower fecundity (Dubovskiy et al. 2013; Barnes & Siva-Jothy 2000). Melanin production after immune

challenge and those used for wing pigmentation require prophenoloxidases (Cerenius & Söderhäll 2004). Deployment of phenoloxidases for immune defense could come at the cost of their availability for producing body colors. However, both processes in our experiments are occurring in different times: immunity during the first day and pigmentation during the last two days of pupal development.

We also analyses the number of dorsal hindwing white pupils. This trait is involved in sexual selection: in butterflies reared at low temperatures males prefer to mate with females more dorsal hindwing white pupils (Westerman et al. 2014). The number of such pupils was shown higher in females reared at 17°C than at 27°C (Westerman et al. 2014). In our study, we found the same trend between low (19°C) and high (27°C) temperature reared females (Figure 4.6C). In immune treated groups there were no significant differences in this trait, and contrary to low temperature effect dorsal white pupils decreased in higher bacterial dosage independently of the bacteria type (Figure 4.6D).

4.4.8 Higher immune challenge reduces 20-hydroxyecdysone to levels closer to those characteristic of lower developmental temperatures

Thermal plasticity is correlated with, and mediated by changes in 20-hydroxyecdysone levels (Koch et al. 1996; Oostra et al. 2011; Mateus et al. 2014). This hormone is also known to regulate insect immunity (Regan et al. 2013; Rus et al. 2013; Tian et al. 2010), promoting both cellular and humoral immune responses (Regan et al. 2013; Rus et al. 2013; Ahmed et al. 1999). Here, we saw that lower developmental temperatures induced development of smaller eyespots (Figure 4.1) and darker wings (Figure 4.6A_1) with lower

contrast (Figure 4.6A_2). The immune challenge applied to pupae phenocopies the effects on eyespot size (Figure 4.4 and 4.5) and contrast (Figure 4.6B_2), but not wing overall-darkness (Figure 4.6B_1). We hypothesized that the mechanism mediating the wing pigmentation changes induced by immune challenge was also altered levels of 20-hydroxyecdysone (20E). We induced immune challenge at 8% of pupal developmental time (12h post-pupation at 27°C) with PBS (control for wounding), Gram- (Ec) and Gram+ (Sa) bacteria. After, we collected hemolymph to quantify hormone levels at 8.5, 12 and 24% of developmental time in treated individuals, as well as in non-wounded individuals reared at 27°C or 19°C.

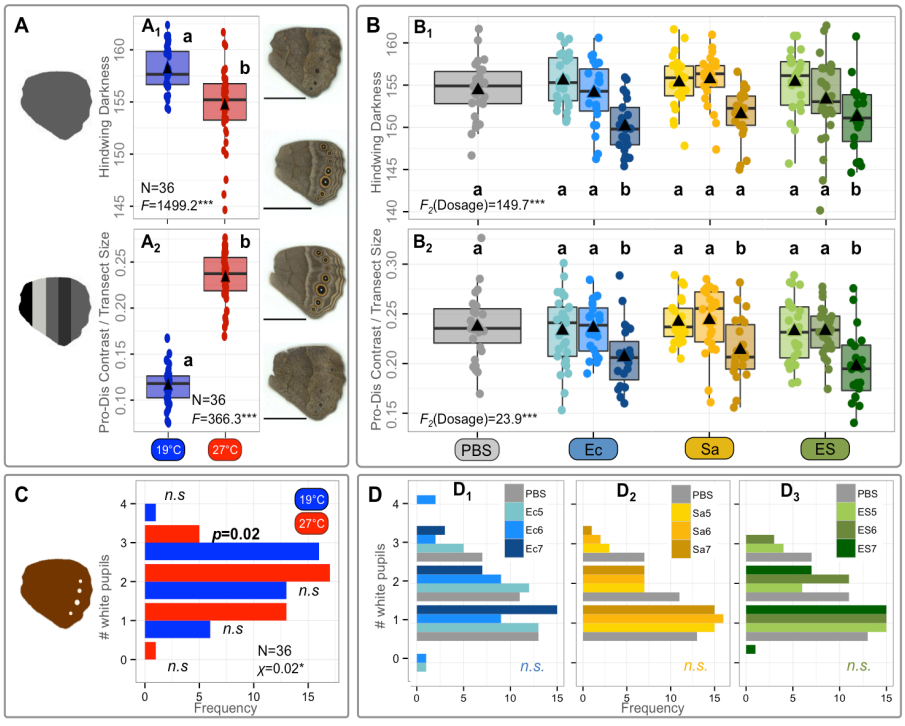

Figure 4.6 –Higher bacterial dosage induce same effect on wing color contrast but opposite effect on overall darkness and dorsal hindwing white pupils relative to low developmental temperature. A) Low developmental temperature individuals have overall darker hindwings (A_1) with lower color contrast over proximal-distal axis (A_2) relative to high developmental temperature individuals. B) High dosage immune-

challenge individuals have overall lighter hindwings (B_1) with lower color contrast over proximal-distal axis (B_2) relative to control group. C) Low developmental temperature increases the number of dorsal hindwing white pupils, the number of individuals with three white pupils is higher at 19°C than at 27°C. D) Immune challenge did not affected the number of dorsal hindwing white pupils, but if there is a trend on this trait it is opposite to low developmental temperature individuals. *p-value*<0.001***, *p-value*<0.05*, *p-value*>n.s.; same letter indicates no significant difference (*p-value* >0.05), while different letters indicate significant differences (*p-value* <0.05); sample sizes in A and C are indicated (N), and in B_1 and in D were the same as indicated on Figure 4.3 (N), but in B_2 we removed outliers, so sample size in this analysis was different: PBS=30, Ec5=28, Ec6=24, Ec7=23, Sa5=23, Sa6=24, Sa7=21, ES5=23, ES6=28, ES7=19.

One hour post immune challenge (8.5% of pupal developmental time) there were no differences among pupae reared at 27°C. 4h later (corresponding to 12% of pupal development), immune challenged pupae reared at 27°C had 20E levels closer to those of non-challenged pupae from lower developmental temperatures (Figure 4.7). One day after bacterial treatment (24% of pupal developmental time), pupae had intermediate 20E levels: lower than 27°C and higher than 19°C (Figure 4.7). The control treatment *per se* did not affected 20E levels in any of tested time points (Figure 4.7). This result indicates that 20E is mediating the immune-induced developmental plasticity.

In several insects, such as *D. melanogaster* (Diptera) and *Helicoverpa armigera* (Lepidoptera), increased levels of 20E induce higher expression of AMP (Flatt et al. 2008; Wang et al. 2014). However, it was reported that in *B. mori* 20E levels decrease the AMP gene expression (Tian et al. 2010; Tanaka & Yamakawa 2011). We know from previous chapter that AMPs levels are high in Gram-treated pupae, at least until eight hours post-immune treatment (see

Chapter 3 - Figure 3.3). Here, we saw that six hours post-immune challenge the levels of 20E were already reduced, indicating that in *B. anynana* the production of AMPs do not require higher levels of this hormone. In this case, the immune system regulation in *B. anynana* through 20E might be similar to *B. mori*. Nevertheless, to confirm this hypothesis further quantifications are required: 1) 20E levels in time points between zero and six hours post-immune challenge; and 2) AMPs gene expression levels, in 20E manipulated individuals.

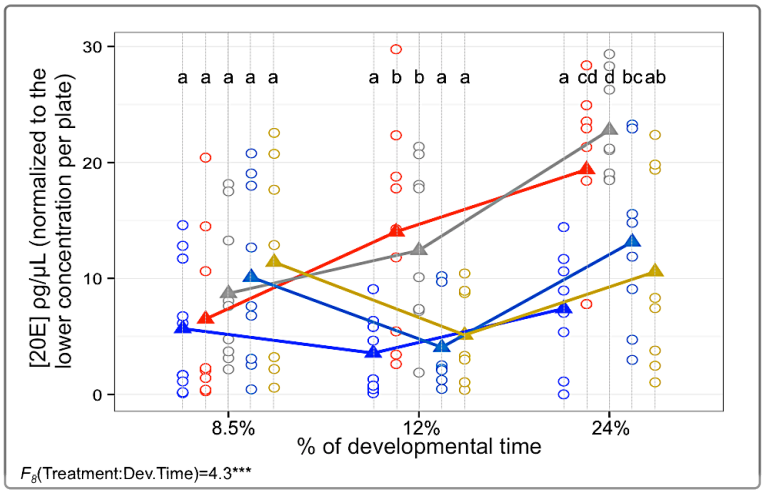

Figure 4.7- 20E levels decreased in immune-challenged pupae towards levels that are similar levels of low developmental temperature pupae. *F*(Treatment : Developmental time)=4.3, d.f.=8, *p-value*= 0.0001, followed by multiconparison analysis, alpha=0.05: same letter indicates no significant difference (*p-value* >0.05), while different letters indicate significant differences (*p-value* <0.05)

4.4.9 Hormonal treatment of immune-challenged pupae induced high mortality

The hormonal levels in *B. anynana* are responsible (at least partially) for wing pattern differences between individuals reared at 19°C *vs.* 27°C (Koch et al. 1996; Mateus et al. 2014). Studies have demonstrated that low temperature individuals injected with 20E had

increased eyespot size relative to control injections (Mateus et al. 2014; Koch et al. 1996). Because immune challenged pupae have phenocopied the effect of low developmental temperatures in wing pigmentation (Figure 4.1) and in internal 20E levels (Figure 4.7), we hypothesized that the immune challenge-induced changes in the later could be the cause for the former. We designed an experiment with application of the same dose of hormone as tested in (Mateus et al. 2014) that had been shown to cause wing phenotype of low temperature individuals to look like those of high temperature. However, our experimental design was different in where (thorax instead of abdomen) and how (topic application on wound instead of injection) and when (8% of development instead of 3%) the hormone was applied. Surprisingly, regardless whether 20E was applied with PBS or solution of dead bacteria, we had 100% pupal mortality. The 20E used here was purchased from a different company, we wondered if differences in purity might result in differences in effective dose and tried different doses for our assay. We found that application of 62.5 ρg per individual was the highest of our tested dosages that did not result in 100% mortality (Fig 8A). Even though mortality was still high for this dose (Fig 8B), we could obtain adults to score wing pigmentation phenotypes. Phenotypic measurements showed that this hormonal treatment was not sufficient to restore the eyespot size of immune-challenged individuals. To confirm this first interpretation the 20-hydroxyecdysone levels need to be measured in controls, and hormone treated individuals to know if internal levels of treated individuals at 12% of development are at least as higher as PBS controls. However, this interpretation even if 20E levels were confirmed is quite risky with such high mortality.

A previous study has demonstrated that same immune challenge induced on thorax and on abdomen have different impacts on flies:

thorax injury is more severe than abdomen injury (Chambers et al. 2014). During these experiments we got the idea that the melanization after a thorax immune challenge was faster and more extent than an abdomen or wing immune challenge. Even if this cannot explain everything it might be explaining part of it. In other insects was shown that 20E regulates drastically the immune system (Flatt et al. 2008; Wang et al. 2014; Tian et al. 2010). For example higher 20E levels in two different Lepidoptera have opposite consequences: in *Helicoverpa armigera* there is an increase and in *B. mori* a decrease of AMPs production (Wang et al. 2014; Tian et al. 2010). Because we saw that six hours post-immune challenge 20E levels were reduced, it is very likely that in *B. anynana* 20E is regulating the immune response as in *B. mori*. In this scenario, it is not obvious the reason of such a high mortality after an immune challenge with a non-infectious agent. We observed that three days after treatment, pupae that had not restored the original greenish color maintaining the blackish color did not managed to reach adult stage. The blackish pupae color we think was related with the hemolymph melanization, and consequently those pupae had over activated this pathway to harmful levels for the host. If this hypothesis is true low levels of 20E are not limitative to produce high levels of AMPs (Chapter 3 - Figure 3.3), but they might be crucial for melanogenesis down regulation.

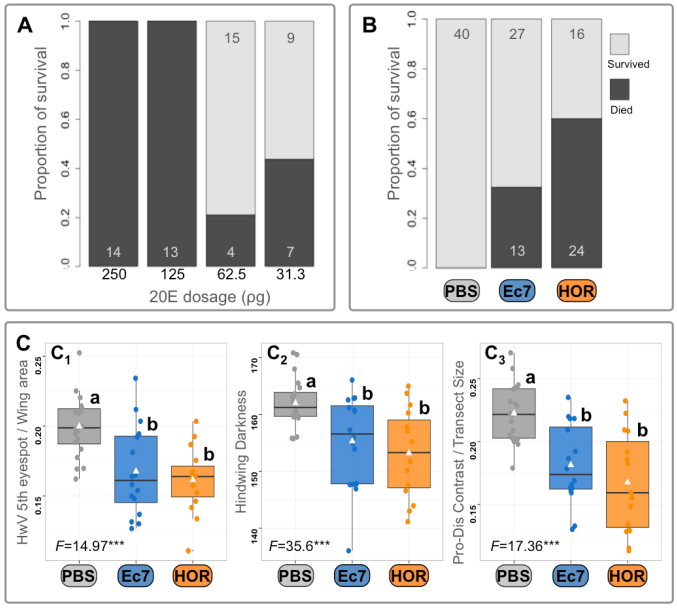

Figure 4.8- Hormone manipulation during immune treatment on thorax induced high mortality and did not restored the high temperature phenotype. A) Mortality in Ec7 individuals after treatment with 20E serial dilution dosages. B) Survival after hormone manipulation. C) Wing pigmentation traits after hormone treatment did not recovered the high temperature phenotype in eyespot size (C1), overall darkness (C2) or wing color contrast (C3). *p-value*<0.001***; multiconparison analysis, alpha= 0.05: same letter indicates no significant difference, while different letters indicate significant differences (*p-value* <0.05).

4.5. Conclusion

A possible role of immune genes during Lepidoptera pigmentation have been pointed in several wide genomic analysis, where immune-related groups of genes were up regulated in pigmentation mutants or in certain pigmentation patterns (Hines et al. 2012; Nishikawa et al. 2013). For example, in *Papilio polytes* genes related with Toll pathway are upregulated in red areas indicating a possible regulation of a very well-known immune pathway with a specific wing pigmentation pattern (Nishikawa et al. 2013). Studies on *Pieris brassicae L.*, revealed that immune-challenged pupae tended to have larger and darker forewing

black tips (Freitak et al. 2005). Our results, confirm the involvement of systemic immunity regulators and/or effector playing a key role during early pupal development, and triggering the development of a distinct adult wing patterns. This work opens up new questions about immunity and 1) pigmentation, 2) developmental temperature, 3) pathogens associated to different seasonal environments and 4) their hormonal regulation (Figure 4.9). Future experiments, focusing on how immunity impact life history traits, natural and also sexual selection will help us to understand the ecological "meaning" of this immune-mediated phenotypic variation.

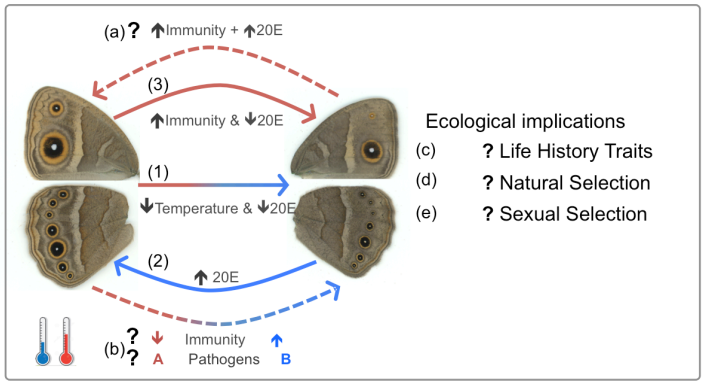

Figure 4.9- Model of wing pigmentation variation mediated by temperature, immunity and hormones, and open questions. Before this study we already knew that temperature induce phenotypic plasticity (1), low temperature individuals have lower hormonal levels and that hormonal treatment in low developmental temperature individuals restores the high temperature phenotype (2). With this work we saw that immunity also induce phenotypic plasticity and immune-challenged individuals have lower hormonal levels (3). Future experiments will clarify if it is possible to restore the high temperature phenotype through hormonal manipulations (a), if the internal immune levels are different at different temperatures (b), which life history traits are affected after immune challenge (c), and if immunity-mediated phenotypic variation affects natural (d) and sexual (e) selection.

4.6. Acknowledgements

We thank Antónia Monteiro for the *B. anynana* lab stock; Isabel Gordo and Magda Atilano for bacterial strains used in these experiments; Pedro Castanheira for maintaining the butterfly lab populations, helping on separation of wings from thorax in adult butterflies and wing scanning; Filipa Alves for the scanner, and EVO-DEVO IGC community for the useful discussions.

Chapter 5 – Immune and thermic stress induce similar changes in wing shape

5.1. Summary

Shape is an important element in biological systems providing a link between genotype, environment and function. Trait morphological variation results from the combination of genetic and/or environmental factors, depending on the degree of phenotypic plasticity of each trait. In this experiment we explored the effects on wing size and shape of biotic (immunity) and abiotic (temperature) environmental factors that induce phenotypic plasticity in *Bicyclus anynana*. We manipulated the immune system with heat-killed bacteria on wing and thorax of early pupae and measured the size and shape of adult wings. We found that treatment position had different effects on wing size: the size decreased in all wings on wing-treated individuals, but there were no changes in thorax-treated individuals. Wing-treated individuals had allometric and non-allometric differences in wing shape. Individuals treated with bacteria had fewer mitotic cells relative to controls. Temperature also induced allometric and non-allometric wing shape changes. Low temperatures and immune challenge changed the wing shape in a similar direction. This study has shown that the development of the four wings is tightly coordinated in terms of size and shape and that different stress conditions induce similar non-allometric wing shape. Future studies with this model can provide a better understand of ecological effects of wing shape variation and

signaling mechanisms underlying the interorgan developmental coordination.

5.2. Introduction

During development, a multitude of cellular processes are coordinated to give rise to a viable organism of proper size and shape. The size of organs are proportioned to total body size indicating regulatory mechanisms of organ to the body growth (Mirth & Shingleton 2012). The size and shape of an organ can be affected during development; different environmental conditions can produce organs of different size and shape, phenotypic plasticity (Whitman & Agrawal 2009; Pigliucci 2001). Deregulation in the mechanisms controlling organ growth induces variation in organ size and shape impacting (positively or negatively) the fitness of adult individuals (Andersen et al. 2013). For example the wing size and shape can affect flight performance affecting the individual ability to escape predation and find mate pairs (Sane & Dickinson 2001; Swaddle 1997; Bradley & Altizer 2005). Understanding the processes involved in the control of phenotypic variation, such as how growth is controlled and how it is integrated with other cellular processes to produce an adult organ with a correct size and shape is an important challenge in developmental biology.

The number of cells and/or the size of each cell impact the growth and size of an organ (Trumpp et al. 2001; Azevedo et al. 2002; Neufeld 2003). Organisms of a given species generally grow at a predictable rate and to a specific body size, but individuals can modify this program during development in response to environmental conditions (Neufeld 2003). A variety of environmental factors contribute to growth during development, including nutrition,

temperature, oxygen level, and crowding (Shingleton et al. 2009; Andersen et al. 2013; Neufeld 2003), but also genetic factors regulating the macromolecular synthesis and degradation, cell division and cell death (Neufeld 2003; Azevedo et al. 2002). For example, a decrease in rearing temperature increases the size of the wings, legs and eyes through an effect on epidermal cell size, with no significant change in cell number (Azevedo et al. 2002).

Low developmental temperatures in insects are associated with development of larger wings (Debat et al. 2003; Shingleton 2010; Mateus et al. 2014). In Drosophila, this is mainly due to changes in cell area, although temperature also affects cell number (Shingleton 2010; Azevedo et al. 2002). Low temperatures increase cell area, but reduce the cell proliferation rate (Watanabe & Okada 1967), this is thought to be a consequence of the effect of temperature on biochemical kinetics (Gillooly et al. 2002). Temperature also affects hormonal dynamics (Koch et al. 1996; Oostra et al. 2011), which is one of the physiological mechanisms regulating growth. Previous studies of drosophila wings demonstrated that extreme temperatures (high and low) induced opposite allometic variation (shape differences correlated with size; producing smaller and larger wings in high and low temperatures, respectively), and similar non-allometric shape variations (Debat et al. 2003). This suggests that thermal stresses, with high or low temperatures, might trigger same developmental shifts leading to similar adult wing shape. The effect on wing shape of other stressing factors is poorly understood.

Organ injuries during development can affect greatly the size and shape of the adult organ (Pesch et al. 2016; Díaz-García & Baonza 2013). In Drosophila the damage to individual imaginal discs (larvae and pupae tissues that originate adult organs in holometabolous

insects) causes a delay in metamorphosis (Stieper et al. 2008). This allows repair of the damaged disc, with its cells readjusting proliferation rates to regenerate two adult wings similar in size and shape (Smith-Bolton et al. 2009; Shingleton 2010). *In vitro* experiments with wing imaginal discs cultured in a growth-permissive environment showed that they autonomously stop cell division at approximately the same size as that in larval environment (Bryant & Levinson 1985). This supports the idea that each organ does have a target size that should be achieved before metamorphosis.

Here, we used a butterfly, *B. anynana*, as a model system to understand if immune stress (wounding with bacterial challenge) during pupal stage affects wing size and shape. We wounded one of the wings with different heat-killed bacteria, a treatment that activates immune system (Chapter 3 - Figure 3.3), and analyzed adult wings. With this experiment we were able to know if there was interorgan communication and developmental coordination of all four wings at this stage. Geometric morphometrics are analytical methodologies that allow researchers to analyze shape differences in its both components: allometric and non-allometric (Debat et al. 2003; Klingenberg 2011). Trait shape changes are very common and can be very drastic across species (Gidaszewski et al. 2009; Camargo et al. 2015; Outomuro et al. 2012). In contrast, within a population shape variations are rare and discreet (Debat et al. 2003; Blackstone et al. 2013). We used geometric morphometrics to analyze the contribution of allometric and non-allometric components of shape variation. A possible mechanisms contributing for wing size and shape variation is proliferation rate. In Lepidopterans, two to three cell divisions occur during pupal stage (Nijhout et al. 2014). To understand if treatment was affecting proliferation during this stage we quantified the number of mitotic cells in immune challenged and control individuals. Finally,

we quantify shape variation associated with different developmental temperature (a known environmental abiotic cue inducing wing size and shape differences (Debat et al. 2003)), and compared the direction of non-allometric shape changes of both stresses (temperature and immunity).

5.3. Material and Methods

5.3.1 Biological Material

B. anynana inbreed line (a sub population from Antónia Monteiro's lab; used for whole genome sequencing) was reared at 19 or 27°C as described elsewhere (Brakefield et al. 2009). Briefly, the butterflies were maintained at 27°C (+/- 0.5°C) with 65% (+/-1%) relative humidity with 12hrs cycle light/dark. Eggs were collected from net cages (45x45x45cm; BugDorm-44545) with approximately 400 adult individuals in very young maize plants. To reduce the probability of parasite transmission, we bleached the eggs (5 min in a 20% bleach solution) immediately after collection. Adult butterflies were fed with fresh banana on top of wet cotton and larvae were fed with young maize plants and maintained in cages identical of those used for adults at a density of 150 to 200 individuals per cage. Larvae were sexed and only females were used in this study. Pre-pupae were collected onto 25 well plates and pupation time was recorded during the night via time-lapse photography with a photo taken each 10 min (Canon 1000D digital camera, Hahnel Giga T Pro 2.4GHz wireless timer remote control).

5.3.2 Wounds and Immune Challenge

We wounded only females reared at 27°C. Wounds were inflicted with a 0.25mm diameter tungsten needle (World Precision

Instruments) in the right wing (in the wing cell (wing compartment between two adjacent veins) below the anterior eyespot, approximately halfway between the wing margin and the normal location of the eyespots) and in the thorax (in the middle (relative to left and right and anterior and posterior) of the third dorsal thoracic segment). Pupae were returned to 27°C until adult eclosion or until further manipulation for hemolymph extraction. The wing-wounded experiment was run on January and the thorax-wounded experiment on July of 2014.

We induced three different immune challenges: one control (PBS1X – PBS), one bacteria type (*Escherichia coli* – Ec (MC4100-CFP)) in two different dosages: 10exp6 (Ec6) and 10exp7 (Ec7) heat-killed bacteria cells/μL diluted in PBS). 0.5μL of each solution were added to the fresh wound. After immune challenge treatment individuals were returned to 27°C until adult eclosion or until dissection.

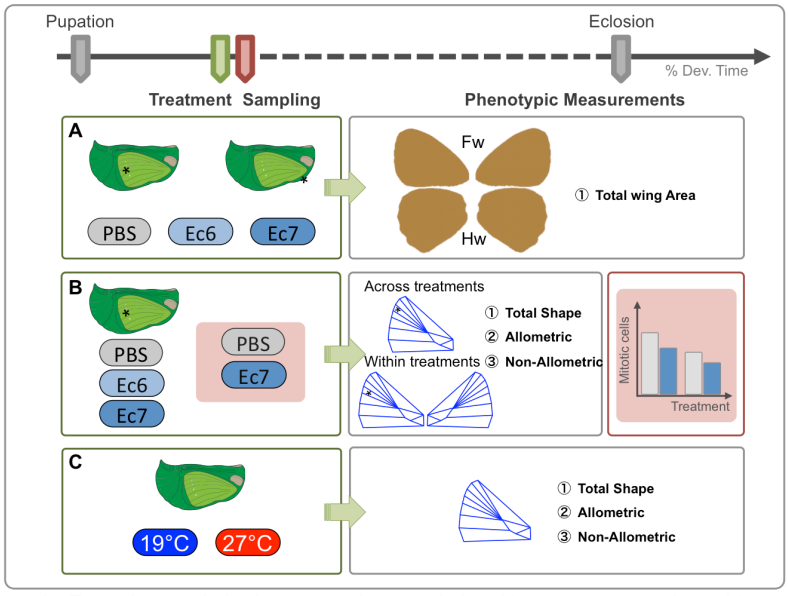

Figure 5.1- Experimental design to understand the A) treatment and position effects on wing size; B) the affect on allometric and non-allometric shape changes in wing-

treated individuals and the proliferation after bacterial treatment; and C) the affect on allometric and non-allometric shape changes in different rearing temperatures. Top arrow represents developmental time from pupation to eclosion with treatment (12 hours post-pupation) and sampling time points (four hours post-treatment). To analyze treatment position effects (A) we treated individuals on wings or on thorax (position is indicated with (*) on pupae scheme) with control (0.5µL of sterile PBS – PBS) or immune challenge (0.5µL of 10^6 – Ec6, and 0.5µL of 10^7 *E. coli* solution – Ec7) solutions and measured the total size of adult wings. Differences in wing shape were analyzed using geometric morphometrics methods. In wings-treated individuals (B), we analyzed effects of treatment in treated wings, the effect of treatment*wounding, and the effects of bacterial treatment on proliferation during pupal development (light red square). To analyze the effect of temperature on wing shape, we analyzed adult wings of individuals reared at 19°C and 27°C.

5.3.3 Wing Area and landmarks measurements

After stretching their wings, adult butterflies were sacrificed (-20°C for at least 2hrs). Wings were detached from the thorax and dorsal sides were scanned (Epson Perfection V600 Photo). Images were imported to Fiji (Schindelin et al. 2012) and the same color threshold was applied to all images, we selected whole wing area as measurement. Data were imported to R (R Development Core Team 2015) to do their graphical representations and statistical analysis.

We used an ANOVA to test if bacterial treatments had a significant effect on wing area (aov(wing area ~ Treatment*Side)). When ANOVA showed significant effects of treatment on wing area, we compared across treatments using a pairwise comparison test (lsmeans) (Lenth & Hervé 2015).

The shape analysis, geometric morphometrics, is based on the relative position of predefined landmarks, which can carry important phylogenetic, developmental, and functional information (Cardillo & Reyment 2010). In butterflies, and in insects in general, the landmarks most often measured are the locations where wing veins meet the

wing margin or other veins because they are easyer to identify (Figure 5.2A). In this analysis we followed the standard recommendations for selection of landmarks (13 in total) (Zelditch et al. 2012): 1) homology, landmarks number one to five are vein interceptions or bifurcations in the proximal side of the wing and from number six to 13 are vein interceptions with the distal margin; 2) adequate coverage of the form, landmarks covered proximal and distal parts of the wing; 3) repeatability, landmarks were easy to find in all individuals; 4) consistency of relative position; 5) coplanarity of landmarks (Zelditch et al. 2012) and 6) appropriated sample size (number of landmarks=< (N -4)/2), to maximize the wing shape information and the statistical power of this analysis) (Zelditch et al. 2012). Images were loaded to Fiji-ImageJ (Schindelin et al. 2012) and 13 landmark were placed for each wing. The landmark coordinates were loaded in MorphoJ (Klingenberg 2011) for geometric morphometric analysis. Variation in shape was examined by using geometric morphometrics based on generalized least squares Procrustes superimposition methods (Klingenberg & Mcintyre 1998), which analyze shape by superimposing configurations of landmarks of individuals to achieve an overall best fit.

To verify repeatability of the measurments, we took 10 butterfly wings (four PBS, three Ec6 and Ec7) and placed all landmarks three times independently. We quantified variance among treatments and between three sets of measurments through Procrustes ANOVA analysis in MorphoJ (Klingenberg & Mcintyre 1998; Klingenberg 2011). Results showed that the variance between measurments is negligeble (p-value>0.05) for centroid size (differences in shape correlated with size) and also proscustes distance (differences in shape without size effect) (Tab S1). Thus, since biological differences between wings are much higher than technical errors we can use this methodology in our

shape analysis. From the landmarck coordinates we obtained an average position for each ladmark (red dots on Figure 5.2B), which represents the wing shape without location, scale and rotation effects. This wireframe representation was used as wing shape reference in further analysis.

We analyzed shape variation to understand the effects of: 1) different immune challenged organs; right forewings of wing and thorax immune challenged individuals, 2) wounding and immune challenge in wing-treated individuals; right (wounded) and left (non-wounded) forewings, 3) developmental temperature; right forewings of non-wounded individuals reared at different temperatures (19 and 27°C). For these three comparisons we ran the following set of analyses: 1) detection of possible outliers for wing shape (e.g. wrong landmarks coordinates), 2) Procrustes best fit, 3) generation of a covariance matrix, 4) principal component analysis, 5) canonical variation analysis and 6) discriminant analysis (DA) (Klingenberg 2011). The output of DA is the comparisons between pairs of treatment for the Procrustes distance (shape difference) and the statistical significance of it is given after 1000 random permutation test. Variation in shape was determined as total (both components; black double arrow in Figure 5.2C), allometric (variation correlated with size; red double arrow in Figure 5.2C) and non-allometric (variation in shape not correlated with size; blue double arrow in Figure 5.2C). The total shape variation was calculated from the original landmark data. The covariance matrix of these data was used in a regression model (variation ~ wing size) to obtain the data for allometric shape variation (regression predicted values) and non-allometric shape variation (regression residuals values). All morphometric and statistical analyses were performed using MorphoJ software, including routines

for the Procrustes fit as well as the permutation and bootstrap procedures (Klingenberg 2011).

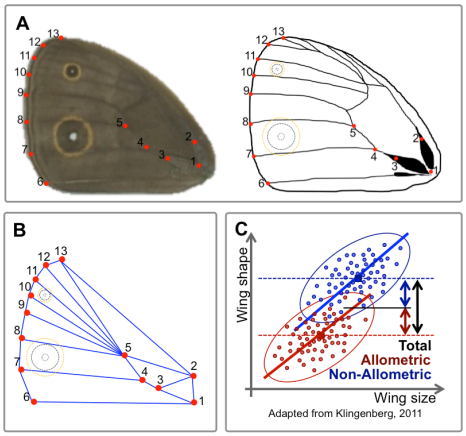

Figure 5.2- Landmark position in the forewing. A) Image of a dorsal forewing from *B. anynana* and respective scheme, with the 13 landmarks used in this study superimposed as solid red dots. B) Wireframe scheme of landmark position variation after procrustes superimposition of all 10 individuals used for error measurments (red dots represent the average for each landmark). The wing shape wireframe was drawn in MorphoJ and the relative wing position of anterior and posterior eyespot rings and wound site (*) were added manually. C) Graphical representation of total, allometric and non-allometric shape variation between two hypothetical populations. The difference between the average (ditched lines) of both populations is the total shape variation (black double arrow). Solid blue and red lines represent allometric shape variation. Shape variation in blue relative to the red population, it is explained by the allometric effect (red double arrow) and other remaining effects (residuals): non-allometric shape variation (blue double arrow).

5.3.4 Immunohistochemistry

We used wounded and control forewings with overlaying cuticle collected at 4 hours post-treatment to know if there was a reduction of mitotic cells in immune challenged individual (Ec7). The wings were fixed, dehydrated (5min sequential washed with 25%, 50%, 75% and 100% ethanol) and stored at -20°C until further processes.

Immediately before starting the immunohistochemistry protocol described in (Saenko et al. 2011; Brakefield et al. 2009), wings were rehydrated (5min sequential washed with 100%, 75%, 50% and 25% ethanol). We used DAPI (Invitrogen; 1(5mg/mL): 1000(PBS1X) and followed manufacturer's instructions to stain nuclei. To stain mitotic cells, we use the anti-phospho-histone H3 (Ser10) mouse antibody (1:500; Cell Signaling Technology) detected with an anti-mouse secondary antibody coupled with Alexa 647 (Invitrogen; 1:200 dilution). Confocal Z-series stack images were acquired on a Leica SP5 confocal, using 20x 0.7NA objective. Images were acquired taking the wound site or equivalent area in the non-wounded wing at image center. Z-stacks were then converted into a single image, and its brightness and contrast were adjusted in Fiji software (Schindelin et al. 2012). We quantified the wing area with fluorescence intensity above a certain color threshold (equal threshold for all images for each fluorescence staining) in total image area (2.4 mm^2). These fluorescent areas were taken as an approximation of total number of wing cells in the image (DAPI fluorescence) and number of mitotic cells in the image. DAPI area was taken as covariant and the anti-phospho-histone H3 (Ser10) as response variable in the statistic analysis. We used a GLM model to test if the number of mitotic cells was significant different in treatment and wing type taking total number of cells as covariant. The minimal model was (lm(number of mitotic cells ~ treatment + wing + total cell number)). After we then run pairwise comparisons (package lsmeans) to find differences across treatments and wings (Lenth & Hervé 2015).

5.4. Results and Discussion

Wing size and shape are crucial traits for flight (Sane & Dickinson 2001; Swaddle 1997), and are known to be affected by genetic and environmental factors (Zeng & Verheyen 2004; Debat et al. 2003). In previous chapters, we have shown that treatment with heat-killed bacteria increased the expression of immunity related genes (Chapter 3) and also saw that this treatment induced general wing pigmentation changes in all wings (Chapter 4 - Figure 4.1). Here, we investigate the effects of same treatments on wing size and shape. We saw that when bacterial treatment is applied on one wing during early pupal development all adult wings were smaller, but not when same treatment is applied on thorax (Figure 5.3). Thus, the response after wing treatment is a wing-specific response and implies interorgan communication/regulation. We hypothesized that immune stress on pupal wings might affect also adult wing shape. To address this hypothesis we analyzed wing shape in its two components: allometric (differences in shape in relation to size) and non-allometric (differences in shape not correlated with size) in wing-treated individuals comparing 1) wounded wings of different treatment pairs (Figure 5.4) and 2) wing pairs (wounded and non-wounded wings) of same treatment (Figure 5.5). These analyses revealed that the bacterial treatment affected wing shape in its both components and that the wing damage only affects the non-allometric shape component. To understand the possible mechanism underlying the development of smaller wings we quantified cell proliferation in wounded and contralateral wings in control and bacteria treated groups (Figure 5.6). We saw that bacterial treated group had lower mitotic density in both wounded and contralateral wing, relative to control group. Finally, we analyzed the wing shape of two different

developmental temperatures (Figure 5.7A) and saw that low developmental temperature induce similar non-allometric wing shape changes as in bacterial treatment groups.

5.4.1 Bacterial treatment, on developing wing, reduces the total area of all adult wings

In previous chapters, we have shown that treatment with heat-killed bacteria increased the expression of immunity related genes such as antimicrobial peptides and melanogenesis pathway genes (Chapter 3 - Figure 3.3). We also saw that this treatment induced local (Chapter 3 - Figure 3.4) and general wing pigmentation changes (Chapteer 4; Figure 4.1). Here, we investigate the effects on wing size of wing- and thorax- treated individuals with same bacterial treatment. Bacterial treatment reduced wing size relative to the control treatment (PBS), but only when bacteria were applied on developing wings (Figure 5.3). This suggests an interaction between treatment and affected organ and also an interorgan communication after wing treatment to develop same size of left and right wings. This also suggests that during this developmental stage the butterfly is no longer able to restore the target size of damaged wing, but it can still readjust the size of other wings, all reaching a new final size. The readjustment to a new adult size might be important to produce symmetric wings, which in turn, are important for flight performance (Hambly et al. 2004).

The readjustment of size for all wings can also reflect other phenomena; such as the reallocation of energetic resources. Immune system activation induces a battery of responses including the production of high concentrations of antimicrobial effectors (Wu et al. 2010; Ferrandon et al. 1998; Lemaitre et al. 1997). Mounting an

immune response is an energetically costly process that requires a shift in energy from nonessential functions to immune function (DiAngelo et al. 2009; Carré & Singer 2008). Our treatments did not induce infection, but did induce an immune response (see Chapter 3 - Figure 3.3). It might be that the butterfly had allocated less energy to wing development. Growth of organisms and their organs responds to both intrinsic and extrinsic cues during development, but individuals can modify their developmental program in response to environmental conditions.

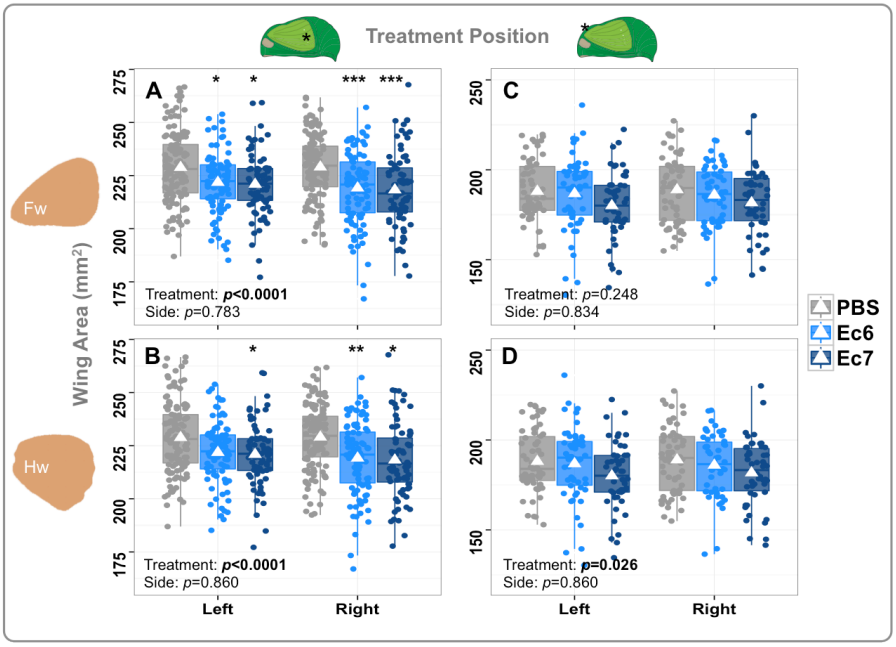

Figure 5.3- Immune treatment on wing-wounded individuals reduced the size of all wings. Bacterial wing-treated groups (Ec6 and Ec7) have smaller forewings (both wings: wounded, right; non-wounded, left) (A) and hindwings (both wings for Ec7 and only right wing for Ec6) (B) relative to control group (PBS). Same treatments on thorax-wounded group did not significantly decrease the size of forewings (C) or hindwings (D). Statistically significant differences relative to control group are indicated: p-value<0.05*; p-value<0.01**; p-value<0.001***.

Previous experiments have revealed the central role of insulin signaling network, which controls growth by coordinately regulating a large number of cell biological processes (Neufeld 2003). In Drosophila, it was shown that Toll but not IMD signaling (immune pathways) in the fat body suppresses insulin signaling both within these cells and non-autonomously throughout the organism, leading to a decrease in both nutrient stores and growth (DiAngelo et al. 2009). This suggests that communication between immune pathways and insulin signaling can coordinate the individual's energy between growth and/or immune function. Our treatments were induced with a heat-killed gram negative bacteria that mainly activates IMD signaling (De Gregorio et al. 2002; Myllymäki et al. 2014; Lemaitre & Hoffmann 2007). However, studies have demonstrated that both pathways act synergistically to activate and coordinate the immune response (Tanji et al. 2007), so our bacterial treatment also can induce expression of Toll. Nevertheless, other components of the immune system can be involved in fat body singling leading to reallocation of energetic resources.

5.4.2 Bacterial treatment induces allometric and non-allometric shape changes on wounded wings

The wing size in drosophila is partially regulated by short-range paracrine signals that define the pattern of the developing wings (Hariharan 2015). Changes in the expression of these morphogens and patterning genes alter the size and shape of the resulting organs (Zeng & Verheyen 2004; Bejarano et al. 2012). The wounding *per se* might disrupt cell-cell signals, and more severe wounds might disrupt larger areas having more severe consequences on organ shape. We saw that wing-treated butterflies had smaller wings (Figure 5.3). To

understand if the bacterial treatment induces shape changes more than total size we run geometric morphometric analyses and analyzed wing shape in its two components: allometric and non-allometric. The wing shape comparison between treatments of wounded wings revealed that, relative to PBS only the highest bacterial dosage induced significant changes in total shape (Figure 5.4B). However, all comparisons revealed statistically significant differences for non-allometric shape (Figure 5.4). Comparing wing shape wireframe diagrams differences were more evident in the wounded and neighbor wing compartments (Figure $5.4B_3$). This suggested that the conjugation of both wing damage and immune system induced wing shape changes.

Some of the morphogens required for wing development are also required for wound healing related processes. For example, Hh and Wg are required for tissue regeneration and Dpp is necessary to modulate the immune response upon wounding (Gibson & Schubiger 1999; Schubiger et al. 2010; Clark et al. 2011). The wing development after bacterial treatment has to be readjusted. Higher bacterial dosages might involve longer readjustment processes, inducing changes in morphogen distribution through the wing and leading to deeper changes in the adult wing.

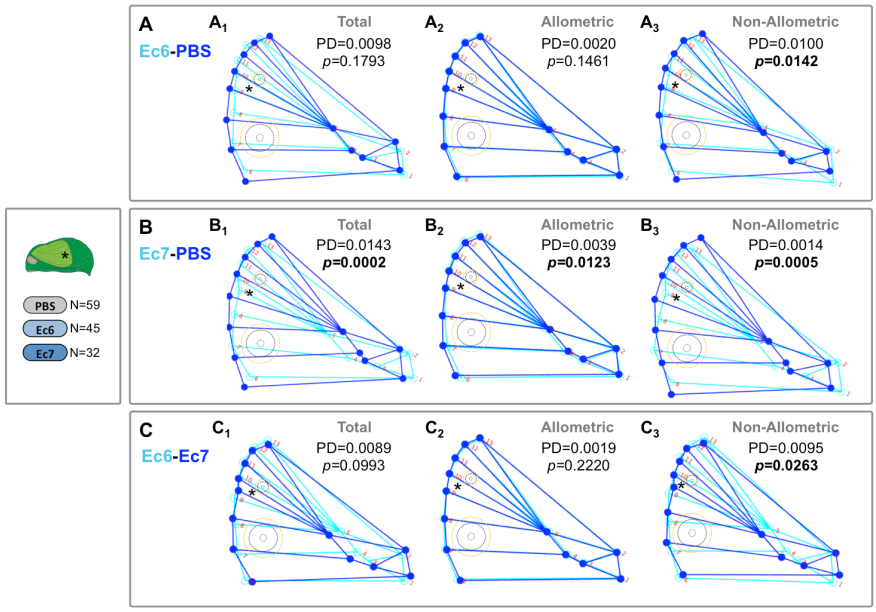

Figure 5.4- Bacterial treatment induced both allometric and non-allometric shape changes on wounded-wings. We analyzed wing shape differences of wounded wing between pairs of treatments: A) Ec6-PBS; B) Ec7-PBS; C) Ec6-Ec7. The magnitude of total shape variation and its allometric and non-allometric components are indicated in units of Procrustes distance (PD) and statistical significance is indicated (*p-val*). N is the sample size for each group; wounding site (*); pupae diagram indicate the type of comparison in this analysis: wounded wings.

5.4.3 Wing damage induces non-allometric changes in wing shape

Wing shape is a trait that affects the flight aerodynamics, and slight changes in wing shape can greatly impact an individual's flight performance (Sane & Dickinson 2001). Previously we saw that bacterial treatments induced smaller wings (Figure 5.3) and differences in wing shape relative to PBS controls (Figure 5.4). Here, to understand if growth readjustments were similar in both wounded and non-wounded forewings, we compared the wing shape between left and right side. Wings were different in shape for all treatments,

being more evident in bacteria treated groups (Figure 5.5). This indicates that wounding *per se* has a large effect on wing shape, even in control treatment (PBS) (Figure 5.5A_3). In bacterial treatments, differences were more evident (Figure 5.5B and C). This suggests that, as seen for wing size, wing shape also can be modulated at this developmental time. There were no differences in allometric shape variation (Figure 5.5; center). Differences in shape between wounded and contralateral non-wounded wings were essentially non-allometric, and more evident in wounded and neighbor wing compartments (Figure 5.5; right). This result suggests that growth readjustments regulating total wing area (the allometric component of wing shape) might be similar in both wings, since there were no differences in allometric wing shape component. However, the particular readjustments in each wing compartment might be different in each wing.

Mechanism such as cell proliferation, cell shape change, cell movement, and cell death can be modulating the wing size and shape through development. The healing process after wounding requires the first three mechanisms: in *B. anynana*, after wounding there is a reduction in cell proliferation around wounding site (Chapter 2 - Figure 2.7). In Drosophila, changes in cell shape and cell movements toward the wound edge have been reported (Wood et al. 2002; Losick et al. 2013; Galko & Krasnow 2004). The wing shape in Lepidoptera is tightly defined through apoptosis in specific wing regions during pupal stage (Macdonald et al. 2010). Thus, both processes wound healing and wing development are using the same mechanisms, which after wounding can impact the normal developmental progression of wing size and shape.

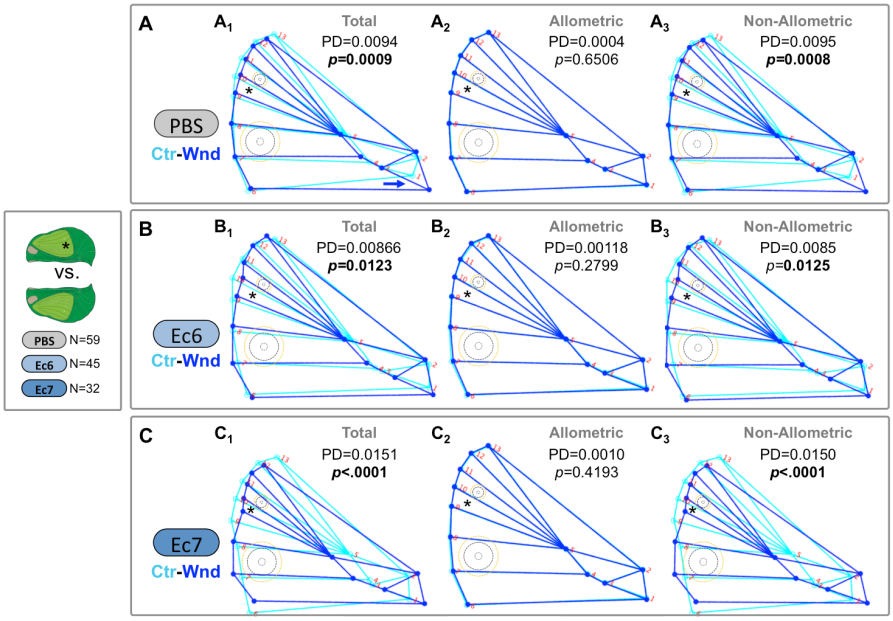

Figure 5.5- Wounding and bacterial treatment induced non-allometric shape changes in wounded wings (Wnd) relative to the contralateral non-wounded wing (Ctr). The shape of wounded and contralateral non-wounded wings was different for all treatments: PBS (A); Ec6 (B) and Ec7 (C). The magnitude of total shape variation and its allometric and non-allometric components are indicated in units of Procrustes distance (PD) and statistical significance is indicated (*p-val*). N is the sample size for each group; wounding site (*); pupae diagram indicate the type of comparison in this analysis: Wnd *vs.* Ctr.

5.4.4 Bacterial treatment reduces mitotic density locally and systemically

The mechanisms, by which tissues and organs acquire their size and shape during development, include cell proliferation, cell shape change, cell movement, and cell death. Changes in the shape of a tissue during development can be due to changes in the local patterns of one or more of these morphogenetic processes (Nijhout et al. 2014). In Junonia it was shown that differences in wing size and shape were correlate with mitotic density, but not with the orientation of cell division (Nijhout et al. 2014). On the other hand in Drosophila the

mitotic density was uniform and wing shape was determined entirely by the orientation of cell division (Baena-López et al. 2005; Bittig et al. 2009). In *B. anynana*, we have shown in previous experiments that around wounding sites there were more cells, but that those cells were not a consequence of higher proliferation; indeed the wounding *per se* induced inhibition of proliferation around wound size (Chapter 2 - Figure 2.7). Here we saw that individuals treated with bacteria have smaller wings (Figure 5.3A), so we hypothesized that in this case the mechanism to produce smaller wings was the reduction of mitotic density in both wounded and contralateral wings. Thus, Ec7 wings might have fewer mitotic cells in comparison with PBS wings, and this might be the cause of differences in wing size and shape. To test this hypothesis, we estimated the number of mitotic cells in pairs of wings in wounded individuals treated with PBS or Ec7. The immunohistochemistry showed clear differences between PBS and Ec7 wounded wings, around wound site; Ec7 wings have larger areas without mitotic cells (Figure 5.6A). In the contralateral wings, the number of mitotic cells in Ec7 also seemed to be lower than in PBS wings (Figure 5.6A). We quantified the wing area occupied by mitotic cells in five individuals taking the total cellular area in the section as a covariant. This experiment showed that wounded wings have fewer mitotic cells than contralateral wings in both PBS and Ec7 and that Ec7 wings (both wounded and contralateral) have fewer mitotic cells than PBS wings (Figure 5.6B).

These results suggest that butterflies regulate the mitotic density in both wings, which can lead to control the size and shape: local and systemically. A fine tune local regulation of proliferation might induce slight shape changes in specific wing areas, inducing non-allometric changes in wounded and neighbor wing cell compartments. Indeed, it was what we observed comparing wounded wings (Figure 5.4). A

systemic regulation of proliferation might be responsible for general changes in size affecting all wings (Figure 5.3), and inducing allometric shape changes. To test if allometric shape changes occurred in contralateral wings we compared its shape across treatments. We showed significant differences in both allometric and non-allometric components of shape. Still, the allometric shape variation is much higher (Procustes distance = 0.0264) than the non-allometric shape variation (Procrustes distance = 0.00839).

A possible mechanism controlling proliferation in a systemic manner might be hormonal. We have shown in previous work that 20-hydroxyecdyson levels drop after immune challenge in thorax-wounded individuals (Chapter 4 - Figure 4.7), which did not reduce wing size (Figure 5.3C and D). Thus, the differences in 20-hydroxyecdysone might not be the major signal synchronizing development between different wings. Nevertheless, further studies quantifying hormone levels in wing *vs*. thorax-wounded individuals might clarify this. Other hormones, such as juvenile hormone and insulin, and other regulators of cell death and wounding signaling, such as oxygen peroxidase, might also be considered (Shingleton 2010; Niethammer et al. 2009).

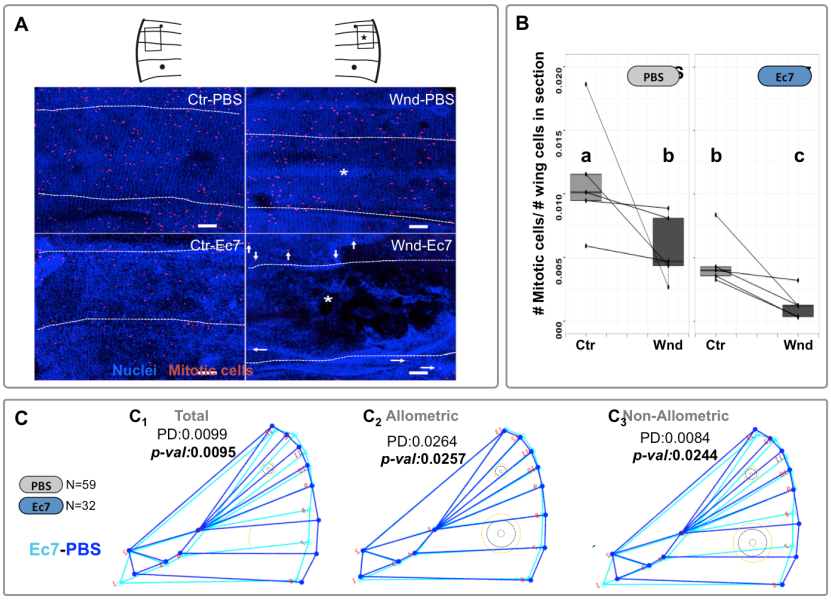

Figure 5.6- Bacterial treatment reduces the number of mitotic cells in developing wings, which develop to have different size and shape. A) Immunohistochemistry showing mitotic cells (red) and nuclei of developing wing epithelia 4h after bacterial treatment (blue). The number of mitotic cells is lower in Ec7 individuals especially around wound sites (*) in wounded wings (Wnd), but also in the contralateral non-wounded wing (Ctr). Black areas in Wnd-Ec7 are melanized. Dashed lines represent wing veins. The square section in the wing scheme (on top) represents the wing area imaged. Scale bar is 100µm. B) Quantification of mitotic cells per treatment and wing (N=5). Identical letters indicate no significant differences while different letters indicate significant differences between groups (*p-value*<0.05). Pairs of wings are linked with a line. C) Contralateral wing shape differences between treatments. There are allometric and non-allometric shape variations, but the differences are mainly allometric. The magnitude of total shape variation and its allometric and non-allometric components are indicated in units of Procrustes distance (PD) and statistical significance is indicated (*p-val*). N is the sample size for each group.

5.4.5 Thermal and immune stresses modulate the wing shape in same direction

Studies of wing shape variation in *Drosophila melanogaster* have shown that high and low developmental temperature also induce non-

allometric shape changes (Debat et al. 2003). The authors proposed that deviances of the optimal thermal condition, either with high or low temperatures, modulate wing shapes in the same way. Here, we saw that an immune stress induced allometric and non-allometric wing shape changes (Figure 5.4B_3). To understand if a thermal stress also induced non-allometric changes similar to the ones observed after immune stress, we conducted geometric morphometric analysis of high (27°C) and low (19°C) developmental temperatures individuals. Results showed that developmental temperature induced both allometric and non-allometric variations (Figure 5.7A). Major differences occur distally: low developmental temperatures "pull" the distal/anterior part and high temperatures the distal/middle part (Figure 5.7B). Non-allometric shape variations observed on contralateral wings (PBS-Ec7; Figure 5.6C_1) were similar but lower in magnitude (Figure 5.7C). These results indicate that very distinct stress conditions, such as low developmental temperature or immunity, switch the wing developmental program to produce similar wing shape.

Heat shock proteins (HSP) are mostly known to be up-regulated after changes in temperature (Feder & Hofmann 1999). However, these proteins are also up-regulated in response to other stresses as immune challenge and oxidative stress (de Morais Guedes et al. 2005; Landis et al. 2004). Genomic and proteomic studies have shown that HSP, insulin signaling, and immunity are involved in multiple stress responses (de Morais Guedes et al. 2005; Landis et al. 2004; Luckhart & Riehle 2007). This suggests that stress conditions lead to the activation of the same set of effector molecules, which switch the developmental program to produce similar stress-like phenotypic changes.

5.5. Conclusions

This study showed that an injured organ in post-critical size stage is able to readjust its developmental program, and signal to similar organs that readjust their developmental programs decreasing mitotic density. This developmental readjustment to an injury is organ-specific. Our experiments also have shown immunity induced allometric and non-allometric shape changes. The non-allometric shape changes after immune challenge and after low developmental temperatures were similar. This suggests that after an environmental stress there is a common developmental program determining wing shape, which is pulling the wing shape in a specific direction independent of the sensed stress.

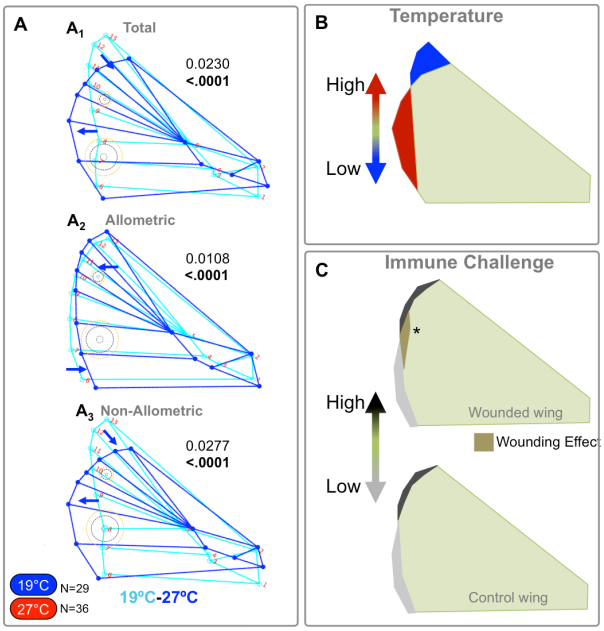

Figure 5.7- Low developmental temperature and higher immune challenge induce similar non-allometric changes in wing shapes. A) Wing shape differences between low and high developmental temperatures show allometric and non-allometric effects. The magnitude of total shape variation and its allometric and non-allometric

components are indicated in units of Procrustes distance (PD) and statistical significance is indicated (*p-val*). N is the sample size for each group. Schematic representation (qualitative) of non-allometric wing shape variation induced by developmental temperature (B), wing wounding (*) (C top) and immune system activation (C bottom).

All together these experiments open new perspectives in the wing size and shape regulation in *B. anynana*, and pinpoints the suitable of this model system to understand the organ size regulation, the interorgan communication during development, the mechanisms underlying these processes, and also the ecological effects of such phenotypic plasticity.

5.6. Acknowledgements

We thank Christian Klingenberg for MorphoJ software which was crucial for these analysis, Antónia Monteiro for the *B. anynana* lab stock; Isabel Gordo and Magda Atilano for bacterial strains used in these experiments; Pedro Castanheira for maintaining the butterfly lab populations, helping on separation of wings from thorax in adult butterflies and wing scanning; Filipa Alves for the scanner, and EVO-DEVO IGC community for the useful discussions.

Chapter 6 - General Discussion and Perspectives

In this thesis, we explored the hypothesis of co-option of wound-response genetic network for the evolutionary origin of butterfly eyespots. We began by characterizing wound response in our model system, *B. anynana*, with an analysis of gene expression profiles and gene expression patterns, as well as of the cellular organization to find commonalities between eyespot-inducing wounds and native eyespots (Chapter 2). This characterization showed a great number of immune-related genes overexpressed at wounded wings. To investigate the contribution of immune activation to the formation of wound-induced eyespots, we manipulated levels of immune activation following wounding (Chapter 3). This experiment demonstrated that immunity contributes to regulating wound-induced eyespot formation (Chapter 3), and it also affects the development of native eyespots. To understand the systemic effect of immune activation on butterfly wing development, we analyzed several wing traits on adult wings including wing pigmentation patterns (Chapter 4) and wing size (Chapter 5). In this final chapter, we review the main findings and conclusions of this work, discuss possible evolutionary and ecological scenarios for their interpretation, and propose future directions of research that could deepen our knowledge of how the evolutionary novel traits originate and diversify.

6.1. Wounds and pigmentation pattern formation

Wound response has been studied in insects for a long time, especially in Drosophila embryos and larvae (Lemaitre & Hoffmann 2007; Mace et al. 2005). The genetics of wound response during pupal stage, a post-growth and pre-adult stage in the life of insects, is much less understood (Regan et al. 2013). In Lepidopterans, several studies have described the ability of wings to form pigmentation patterns (ectopic eyespots) around wounds inflicted during pupal stage (Otaki 2011; Brakefield & French 1995; Nijhout 1985). The study of this particular wound response can help understand the development of eyespots, an evolutionary novel trait (Brakefield & French 1995; Monteiro et al. 2006; Otaki 2011). Here, we studied the pupal wing wound response in *B. anynana* to get new insight onto the evolutionary origin of butterfly eyespots (Chapter 2).

6.1.1. The "generalities" and the "particularities" of *B. anynana* wound response

To our knowledge, only one report tried to understand the genetics behind the development of ectopic eyespots and did so taking a candidate gene approach (Monteiro et al. 2006). More unbiased studies are necessary to understand this specific wound-response in its "generalities" with insects wound response; its "particularities" leading to the formation of an organized pattern; and its "commonalities" with the formation of other pigmentation patterns.

In a first experiment, we compared gene expression profiles of wounded *vs.* control wings to assess the wound-induced changes in gene expression putatively leading to the formation of ectopic eyespots. This analysis revealed that the majority of differently expressed genes were non-annotated (Figure 2.2). Even though the

majority of these is unlikely to be genes with no homolog in other insects (rather sequences too short for annotation to have been possible), it is possible the list includes genes that have not been implicated in wound response in other insects and possibly represent "particularities" of wound-response in Lepidopteran wings. To resolve the identity of the so far unnamed transcripts, we need additional sequencing effort. This could also help overcome another limitation of the microarrays we used to probe differences in expression between wounded and non-wounded wings. The custom-made array included genes from two EST projects mostly targeting un-manipulated developing wings but it almost certainly did not contain representatives of all *B. anynana* transcripts, including genes potentially involved in response to wounds.

Our gene enrichment analysis of the genes differentially expressed between wounded and non-wounded wings that were annotated revealed what I am calling "generalities" of insect's wound response. This corresponds to genes known to be involved in immune processes, such as AMPs and melanogenesis enzymes. We did not find enrichment for genes directly annotated as being involved in tissue repair or regeneration processes (Figure 2.2). Those are, perhaps, expressed soon after damage, at time points earlier that those we sampled, 4h and 8h post-wounding. In fact, wounded wings at 4h post-wounding have usually already closed the opening (personal observation). Identifying the genes involved in closing the wound would, thus, require sampling wings at earlier time points.

6.1.2. The "commonalities" of wound response and eyespot formation

Among genes involved in wound-response in this butterfly, we found that some were expressed at both sites: around wounds and at the presumptive eyespot centers in developing pupal wings. The AMP-encoding *Glov 2* gene was one of these genes seemingly "common" to the development both pigmentation patterns, ectopic and native eyespots (Figure 2.4 and 2.5). This result supports the idea that wound-response genes might have been co-opted to develop eyespots, and that immune-related genes might play a role during eyespot development.

We also investigated the cellular organization in early pupal wings around wound sites and presumptive eyespot centers. Both sites were characterized by increased cell density relative to neighboring wing regions, but we found no evidence for increased cell proliferation. On the contrary, there seemed to be inhibition of cell proliferation in the neighborhood of wound sites (Figure 2.7). We suggested that the increase in cell density was due to migrating cells such as hemocytes that would concentrate at wound sites and at presumptive eyespot centers. Expression of *Glov* has been reported for hemocytes of non-immunized *Manduca sexta* individuals (X.-X. Xu et al. 2012). We propose that *Glov2* detected in *B. anynana* eyespot centers might correspond to the accumulation of hemocytes at these sites. Aside increased cell density presumably corresponding to accumulation of hemocytes, we also found that both wound sites and presumptive eyespot centers showed higher levels of the cytoskeleton protein Actin (Figure 2.6). This protein is required for rearrangement of cell shape, such as that occurring in motile cells (Rosales 2011). Despite our attempts using hemocyte markers, we could not confirm the identity of

the *Glov2*-expressing cells as hemocytes. Those markers detected hemocytes in hemolymph samples, but never worked for wing samples. The antibody staining protocols used for hemolymph and wings were slightly different relative to fixation and sample storage. This might be enough to change the epitopes and consequently the affinity of the antibodies. To know if this is a technical problem, an antibody staining for hemolymph and wings should be run in parallel and also using additional/alternative hemocyte markers.

We also investigated the expression in wound sites of known eyespot development genes, *Antennapedia* (*Antp*) and *engrailed* (*en*). While we could detect Antp protein at both sites, En protein was detected around native eyespots but not around wound sites (at 4h and 8h post-wounding) (Figure 2.6). Expression in late larval wing discs had been documented for both Antp and En, while for pupal wings only En had been reported (Monteiro et al. 2006; Saenko et al. 2011; Brunetti et al. 2001). We found expression of Antp during pupal stages in the presumptive eyespot center (at least until 36h post pupation; personal observation). Given Antp's association with the establishment of eyespot foci in larvae of different Satyrinae butterflies (Shirai et al. 2012; Saenko et al. 2011), finding it around wound sites suggests it might play a role in wound-induced eyespot formation.

Monteiro and colleagues reported that en was expressed around wound sites but in later time points, at least 10h post-wounding, or 22h post-pupation (Monteiro et al. 2006). We found En in the presumptive native eyespot field between 12h to 20h post-pupation (Figure S5.1), corroborating previous studies of gene expression (Monteiro et al. 2006). It seems like 12h post-pupation at 27C is a key time period during pupal wing development; it is the time when wounds are more likely to induce the production of ectopic eyespots

(ref) and when eyespot ring patterning genes start to be expressed revealing future cell color fates.

6.2. Immune-related genes are key regulators of eyespot size

Transplant experiments with artificially selected lines have shown that eyespot size is correlated with the size of the eyespot center (Monteiro et al. 1994). Larger donor eyespot centers produce larger eyespots independently of the receptor tissue. Eyespot center cells presumably produce a morphogen-like signal that gives positional information to the surrounding cells (Nijhout 1991; Beldade & Brakefield 2002; Allen et al. 2008). The identity of this signal is unknown. Manipulating levels of immune challenge, we were able to change the size of both ectopic and native eyespots. Interestingly, the ectopic and native eyespots responded in opposite directions: increased immune challenge applied to wounds led to larger wound-induced eyespots (Chapter 3) and smaller native eyespots (Chapter 4).

6.2.1. High immune levels induce larger ectopic eyespots

Studies from the nineties characterized the sensitive period and wing area where wound to pupal wings induce the formation of ectopic eyespots centered at wound sites (Brakefield & French 1995; French & Brakefield 1992). They also have shown that severe damage increases the probability that an ectopic eyespot is produced, but does not affect ectopic size (Brakefield & French 1995). With our manipulations of the levels of immune challenge we did not affect the probability of ectopic development (Figure 3.4A). This suggests that the immunity-related genes are not implicated in the “first cell fate decision”, i.e., in determining whether or not an ectopic eyespot will be

formed around the wound site. The extent of tissue damage upon wounding, i.e. the severity of the damage is the factor affecting the likelihood of ectopic eyespot formation. I propose that the early wound response is responsible for the signaling that defines whether or not an ectopic eyespot-organizing center is established or not (Figure 6.1). Manipulating the level of immune activation at wounding, we demonstrated that the immune gene network is involved in eyespot size regulation. Higher local immune challenge induces larger ectopic eyespots (Figure 6.1 and 6.2). I propose that a signal (or signals) locally involved in activation/maintenance of the immune response act as important regulators of eyespot size (Figure 6.1). It is conceivable that such signal could be produced either by wounded epidermal cells or by the hemocytes that appear to converge into the wound site. The local cellular response is one of the components of wound response and also immunity (Krautz et al. 2014; Strand 2008). Experiments manipulating hemocyte migration to the wound site could help shed some light into the role of the cellular immunity in the development of ectopic eyespots.

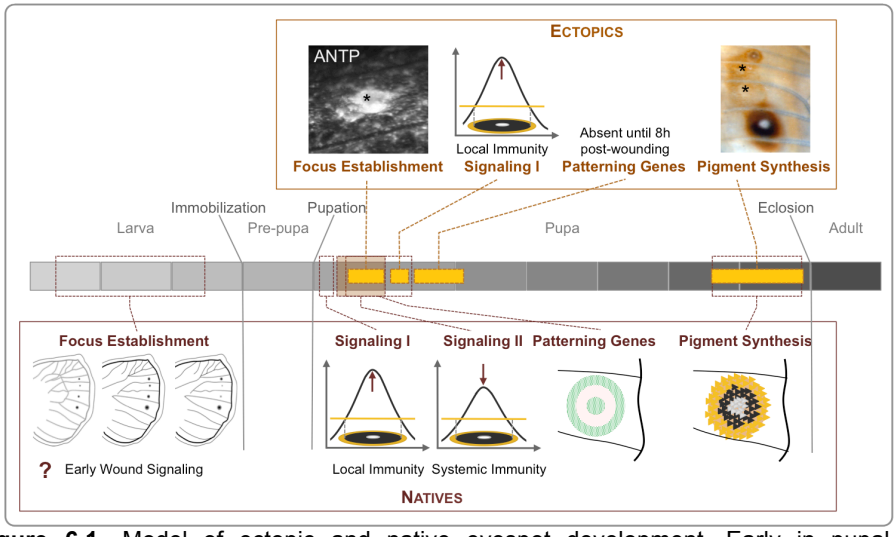

Figure 6.1- Model of ectopic and native eyespot development. Early in pupal

development immunity-related signals might contribute for the enlargement of eyespots (signaling I) and later the effect might be opposite (signaling II). Epidermal damage establishes a focus-like signal and might increase locally the effectors of signaling I.

6.2.2. High immune levels induces smaller native eyespots

The activation of the immune system decreased the size of ventral native eyespot. This result revealed the systemic effect of immunity activation in eyespot size regulation, but with opposite effects locally on ectopic eyespots (Figure 6.2). I propose that the gene networks involved in regulation of systemic immunity are regulating the size of native eyespots (Figure 6.1). The opposing effects could depend on differences between local and systemic immunity "signals" and/or on differences between native and ectopic eyespots in their sensitivity to systemic "signals". The development of native eyespots is "ahead" of that of the ectopic eyespots. At this time, one can typically already start seeing the rings of patterning genes around native eyespot foci (Monteiro et al. 2006). The corresponding phase for ectopic eyespots happens around 24h post-pupation (Monteiro et al. 2006). Whether an immune challenge done at this time would also reduce the size of ectopic eyespots is unknown.

We also observed differences in the systemic effect of immunity response on different color rings of different native eyespots. Specifically, we observed that anterior eyespots decreased more the black ring, while posterior eyespots decreased the golden ring (Figure 4.4 and 4.5). This, too, could result from differences in window of sensitivity to the systemic signals resulting from immune challenge, revealing possible heterochrony in the development of different eyespots and color rings.

6.3. Immune challenge and developmental plasticity

B. anynana is a well-known model for seasonal polyphenism, with distinct phenotypes corresponding to the tropical wet and dry seasons. In the lab, the temperature during development determines the production of what look like alternative seasonal wing pattern phenotypes, albeit never as extreme as those observed in the field (Brakefield et al. 1998). Temperature affects ecdysone dynamics and hormone titers in early pupal life affect a series of life history and wing patterns traits (Koch et al. 1996; Oostra et al. 2014; Mateus et al. 2014). Our experiments revealed that immune challenge imposed during early pupal life phenocopies the effect of development at low temperature on developmental time and on some, but not all, aspects of wing phenotype (Chapters 4 and 5).

At lower temperatures, *B. anynana* develop darker wings with low color contrast and smaller ventral eyespots. They also develop slower, having longer larval and pupal developmental time, and produce heavier adults with larger wings (Oostra et al. 2014; Mateus et al. 2014). Here, we demonstrated that higher levels of immune challenge also decreased wing color contrast and the size of ventral eyespots, and increased the duration of the pupal stage (Figure 6.2). However, the wings of immune challenged butterflies were overall lighter and not darker. It is well-known in *B. anynana* that low developmental temperatures induce a delay in the rise of ecdysone levels (Brakefield et al. 1998; Koch et al. 1996; Oostra et al. 2011). Our experiments also revealed similar effect of immune challenge on ecdysone levels (Figure 4.7). This suggests that the immune-induced plasticity is also mediated by ecdysone. We hypothesized that, similarly to what happens for cold-reared pupae which develop wing patterns more similar to warm-reared individuals when injected with the active form

of ecdysone (Koch et al. 1996; Mateus et al. 2014), ecdysone injections would rescue the effect of immune challenge. Our attempts to test this hypothesis were inconclusive as the doses of injected hormone that typically rescue the effect of low development temperature lead to 100% mortality. Several factors could explain this: we used the same hormone but from a different company (and they could differ in purity, for example), and we injected it in the thorax rather than the abdomen of the pupae. In future work, these should be taken into account and the hormone injection should follow more closely what has been done before to implicate ecdysone as a mediator of thermal plasticity in *B. anynana* eyespots (Mateus et al. 2014).

As is typical in insects (Debat et al. 2003; Lyimo et al. 1992), lower temperatures during development also lead to larger wing size in adult *B. anynana*. Our experiments revealed that dead bacteria applied to a wound on a pupal forewing, but not to a wound on the pupal thorax, affected the size of all wings (Figure 5.3). The resulting adults had smaller fore- and hindwings. The difference between wing and thorax applications of similar doses of dead bacteria suggests that the systemic effect of immune challenge on wing size regulation can only occur after wing damage. We also showed that the wound *per se* reduces the number of mitotic cells on the wounded pupal wing, and that the addition of suspension of dead bacteria to the wound further reduces the number of mitotic cells also in non-wonded wings of the same individual (Figure 5.6). I propose that in wing immune-treated individuals the wings are smaller because of this decrease in cell proliferation. This would imply that the wings of adults that were immune-challenged as pupae are smaller because they have fewer cells.

The natural wet and dry seasons differ not only for a number of abiotic environmental variables such as rainfall and temperature, but also in biotic factors. The latter include the abundance and quality of plant material for the larvae to eat, and possibly also the composition and size of the community of competitors, predators and pathogens. Whether or not the wet and dry season differ in parasite composition, the fact that dry-season butterflies typically delay reproduction and live longer might have as a consequence that they are more likely to be infected. If this is the case the risk of infection might be different between seasons and so, it is also expectable differences in immune investment between seasonal forms. Experiments measuring the risk of infection in each season, and quantification of immune investment in both seasonal forms can elucidate the existence and ecological significance of seasonal plasticity in immune function. Conversely, we can also ask about the putative ecological relevance of immune challenge affecting wing patterns. The adults that eclose from pupae that were exposed to an immune challenge carry a signature of this history on their wings. It will be interesting to explore whether this can be used as valuable information during mate choice.

After this work we shed some light into the possible role for immunity and early wound signals in the development of eyespots and also a new role for immunity in eyespot developmental plasticity in *B. anynana* (Figure 6.2). We answered some questions but we ended up with even more new questions that need an answer. In science as in life, success is not only the answers we obtain; it is also all the new questions that lead us to seek for new answers.

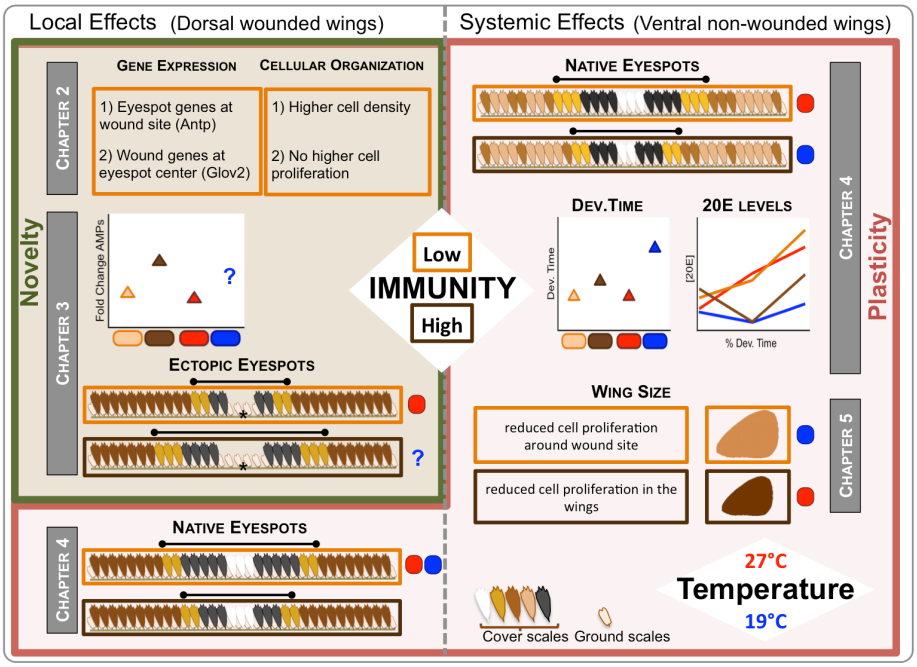

Figure 6.2 – Thesis overview. In Chapters 2 and 3 we tried to understand the role of immunity on ectopic eyespots development and its implications in the evolutionary origin of eyespots. In Chapters 4 and 5 we explored the role of immunity as an inducer of developmental plasticity.

6.4. Acknowledgements

I would like to thank the 'evo-devo' community at Instituto Gulbenkian de Ciência, including members of the labs headed by Patrícia Beldade, Christen Mirth, and Élio Sucena, especially Marta Marialva and Elvira Lafuente. I would also like to thank Magda Atilano for many fruitful discussions throughout my Ph.D.

Bibliography

Aggarwal, K. & Silverman, N., 2008. Positive and negative regulation of the Drosophila immune response. *BMB reports*, 41(4), pp.267–277.

Ahmed, A. et al., 1999. Genomic structure and ecdysone regulation of the prophenoloxidase 1 gene in the malaria vector Anopheles gambiae. *Proceedings of the National Academy of Sciences*, 96(26), pp.14795–14800. Available at: http://www.pnas.org/content/96/26/14795.short [Accessed July 23, 2015].

Allen, C.E. et al., 2008. Differences in the selection response of serially repeated color pattern characters: standing variation, development, and evolution. *BMC evolutionary biology*, 8, p.94.

Altincicek, B. & Vilcinskas, A., 2006. Metamorphosis and collagen-IV-fragments stimulate innate immune response in the greater wax moth, Galleria mellonella. *Developmental and comparative immunology*, 30(12), pp.1108–18. Available at: http://www.sciencedirect.com/science/article/pii/S0145305X06000656 [Accessed November 8, 2015].

Andersen, D.S., Colombani, J. & Léopold, P., 2013. Coordination of organ growth: Principles and outstanding questions from the world of insects. *Trends in Cell Biology*, 23(7), pp.336–344.

Anderson, R.M. & May, R.M., 1982. Coevolution of hosts and parasites. *Parasitology*, 85(April 2009), pp.411–426.

Atilano, M.L. et al., 2011. Wall teichoic acids of Staphylococcus aureus limit recognition by the drosophila peptidoglycan recognition protein-SA to promote pathogenicity. *PLoS pathogens*, 7(12), p.e1002421. Available at:

http://journals.plos.org/plospathogens/article?id=10.1371/journal.ppat.1002421 [Accessed November 12, 2015].

Azevedo, R.B.R., French, V. & Partridge, L., 2002. Temperature modulates epidermal cell size in Drosophila melanogaster. *Journal of Insect Physiology*, 48(2), pp.231–237.

Baena-López, L.A., Baonza, A. & García-Bellido, A., 2005. The orientation of cell divisions determines the shape of Drosophila organs. *Current Biology*, 15(18), pp.1640–1644.

Barnes, A.I. & Siva-Jothy, M.T., 2000. Density-dependent prophylaxis in the mealworm beetle Tenebrio molitor L. (Coleoptera: Tenebrionidae): cuticular melanization is an indicator of investment in immunity. *Proceedings. Biological sciences / The Royal Society*, 267(1439), pp.177–82. Available at: http://rspb.royalsocietypublishing.org/content/267/1439/177 [Accessed July 20, 2015].

Bauerfeind, S.S. & Fischer, K., 2013. Increased temperature reduces herbivore host-plant quality. *Global change biology*, 19(11), pp.3272–82. Available at: http://www.ncbi.nlm.nih.gov/pubmed/23775632 [Accessed August 9, 2015].

Beckstead, R.B., Lam, G. & Thummel, C.S., 2005. The genomic response to 20-hydroxyecdysone at the onset of Drosophila metamorphosis. *Genome biology*, 6(12), p.R99. Available at: http://www.pubmedcentral.nih.gov/articlerender.fcgi?artid=1414087&tool=pmcentrez&rendertype=abstract [Accessed July 22, 2015].

Bejarano, F. et al., 2012. A genome-wide transgenic resource for conditional expression of Drosophila microRNAs. *Development (Cambridge, England)*, 139(15), pp.2821–31. Available at:

http://dev.biologists.org/content/139/15/2821.full [Accessed August 20, 2015].

Beldade, P. et al., 2009. A gene-based linkage map for Bicyclus anynana butterflies allows for a comprehensive analysis of synteny with the lepidopteran reference genome. *PLoS genetics*, 5(2), p.e1000366. Available at: http://journals.plos.org/plosgenetics/article?id=10.1371/journal.pgen.1000366 [Accessed June 23, 2015].

Beldade, P. et al., 2006. A wing expressed sequence tag resource for Bicyclus anynana butterflies, an evo-devo model. *BMC genomics*, 7, p.130.

Beldade, P. & Brakefield, P.M., 2002. The genetics and evo-devo of butterfly wing patterns. *Nature reviews. Genetics*, 3(6), pp.442–452.

Beldade, P., Brakefield, P.M. & Long, A.D., 2002. Contribution of Distal-less to quantitative variation in butterfly eyespots. *Nature*, 415(6869), pp.315–318.

Beldade, P., French, V. & Brakefield, P.M., 2008. Developmental and genetic mechanisms for evolutionary diversification of serial repeats: Eyespot size in Bicyclus anynana butterflies. *Journal of Experimental Zoology Part B: Molecular and Developmental Evolution*, 310(2), pp.191–201.

Beldade, P., Mateus, A.R. a & Keller, R. a., 2011. Evolution and molecular mechanisms of adaptive developmental plasticity. *Molecular Ecology*, 20(7), pp.1347–1363.

Beldade, P., McMillan, W.O. & Papanicolaou, a, 2008. Butterfly genomics eclosing. *Heredity*, 100(2), pp.150–157.

Belvin, M.P. & Anderson, K. V, 1996. A conserved signaling pathway: the Drosophila toll-dorsal pathway. *Annual review of cell and*

developmental biology, 12, pp.393–416.

Benjamini, Y. & Hochberg, Y., 1995. Controlling the False Discovery Rate: A Practical and Powerful Approach to Multiple Testing. *Journal of the Royal Statistical Society. Series B (Methodological)*, 57(1), pp.289–300. Available at: http://www.jstor.org/stable/2346101.

Bidla, G. et al., 2009. Activation of insect phenoloxidase after injury: Endogenous versus foreign elicitors. *Journal of Innate Immunity*, 1(4), pp.301–308.

Binggeli, O. et al., 2014. Prophenoloxidase Activation Is Required for Survival to Microbial Infections in Drosophila. *PLoS Pathogens*, 10(5).

Bittig, T. et al., 2009. Quantification of growth asymmetries in developing epithelia. *European Physical Journal E*, 30(1), pp.93–99.

Blackstone, N.W. et al., 2013. Wing Shape Variation Associated With Mimicry In Butterflies. *Evolution*, 11(1), pp.235–247. Available at: http://link.springer.com/10.1007/978-3-540-95853-6%5Cnhttp://www.springerlink.com/index/10.1007/978-3-540-95853-6.

Boersma, M., Spaak, P. & De Meester, L., 1998. Predator-mediated plasticity in morphology, life history, and behavior of Daphnia: the uncoupling of responses. *The American naturalist*, 152(2), pp.237–248.

Bosch, M. et al., 2005. JNK signaling pathway required for wound healing in regenerating Drosophila wing imaginal discs. *Developmental Biology*, 280(1), pp.73–86.

Bradley, C. a. & Altizer, S., 2005. Parasites hinder monarch butterfly flight: Implications for disease spread in migratory hosts. *Ecology Letters*, 8(3), pp.290–300.

Braendle, C. & Félix, M.-A., 2009. The other side of phenotypic plasticity: a developmental system that generates an invariant phenotype despite environmental variation. *Journal of Biosciences*, 34(4), pp.543–551. Available at: http://link.springer.com/10.1007/s12038-009-0073-8 [Accessed April 23, 2016].

Brakefield, P.M. et al., 1996. Development, plasticity and evolution of butterfly eyespot patterns. *Nature*, 384(6606), pp.236–242.

Brakefield, P.M., Beldade, P. & Zwaan, B.J., 2009. The African Butterfly. , pp.291–330.

Brakefield, P.M. & French, V., 1999. Butterfly wings: the evolution of development of colour patterns. *BioEssays*, 21(5), pp.391–401.

Brakefield, P.M. & French, V., 1995. Eyespot Development on Butterfly Wings: The Epidermal Response to Damage. *Developmental biology*, 168, pp.98–111.

Brakefield, P.M., Kesbeke, F. & Koch, P.B., 1998. The regulation of phenotypic plasticity of eyespots in the butterfly Bicyclus anynana. *The American naturalist*, 152(6), pp.853–60. Available at: http://www.ncbi.nlm.nih.gov/pubmed/18811432 [Accessed July 16, 2015].

Breuker, C.J. & Brakefield, P.M., 2002. Female choice depends on size but not symmetry of dorsal eyespots in the butterfly Bicyclus anynana. *Proceedings. Biological sciences / The Royal Society*, 269(May 2002), pp.1233–1239.

Brunetti, C.R. et al., 2001. The generation and diversification of butterfly eyespot color patterns. *Current Biology*, 11(20), pp.1578–1585.

Bryant, P.J. & Levinson, P., 1985. Intrinsic growth control in the imaginal primordia of Drosophila, and the autonomous action of a lethal mutation causing overgrowth. *Developmental biology*, 107(2),

pp.355–363.

Bulet, P. & Stocklin, R., 2005. Insect antimicrobial peptides: structures, properties and gene regulation. *Protein and Peptide Letters*, (12), pp.3–11.

Camargo, W.R.F. de et al., 2015. Sexual Dimorphism and Allometric Effects Associated With the Wing Shape of Seven Moth Species of Sphingidae (Lepidoptera: Bombycoidea). *Journal of insect science (Online)*, 15(1), p.107. Available at: http://jinsectscience.oxfordjournals.org/content/15/1/107.abstract [Accessed July 29, 2015].

Cambi, A., Koopman, M. & Figdor, C.G., 2005. How C-type lectins detect pathogens. *Cellular microbiology*, 7(4), pp.481–8. Available at: http://www.ncbi.nlm.nih.gov/pubmed/15760448 [Accessed June 9, 2015].

Cardillo, M. & Reyment, R. a, 2010. Morphometrics for Nonmorphometricians. *Morphometric for Nonmorphometricians*, 124, pp.9–25. Available at: http://link.springer.com/10.1007/978-3-540-95853-6%5Cnhttp://www.springerlink.com/index/10.1007/978-3-540-95853-6.

Carré, J.E. & Singer, M., 2008. Cellular energetic metabolism in sepsis: the need for a systems approach. *Biochimica et biophysica acta*, 1777(7–8), pp.763–71. Available at: http://www.sciencedirect.com/science/article/pii/S0005272808000996 [Accessed August 20, 2015].

Casanova-Torres, Á.M. & Goodrich-Blair, H., 2013. Immune Signaling and Antimicrobial Peptide Expression in Lepidoptera. *Insects*, 4(3), pp.320–38. Available at: http://www.ncbi.nlm.nih.gov/pubmed/25861461 [Accessed June 20,

2016].

Cauwels, A., 2007. Nitric oxide in shock. *Kidney international*, 72(5), pp.557–65. Available at: http://www.ncbi.nlm.nih.gov/pubmed/17538569 [Accessed November 12, 2015].

Cerenius, L. & Söderhäll, K., 2004. The prophenoloxidase-activating system in invertebrates. *Immunological Reviews*, 198, pp.116–126.

Chambers, M.C. et al., 2014. Thorax injury lowers resistance to infection in Drosophila melanogaster. *Infection and immunity*, 82(10), pp.4380–9. Available at: http://www.pubmedcentral.nih.gov/articlerender.fcgi?artid=4187852&tool=pmcentrez&rendertype=abstract [Accessed July 24, 2015].

Chinchore, Y., Gerber, G.F. & Dolph, P.J., 2012. Alternative pathway of cell death in Drosophila mediated by NF-κB transcription factor Relish. *Proceedings of the National Academy of Sciences of the United States of America*, 109(10), pp.E605-12. Available at: http://www.pubmedcentral.nih.gov/articlerender.fcgi?artid=3309745&tool=pmcentrez&rendertype=abstract.

Clark, R.I. et al., 2011. Multiple TGF-β superfamily signals modulate the adult drosophila immune response. *Current Biology*, 21(19), pp.1672–1677.

Condie, J., Mustard, J. & Brower, D., 1991. Generation of anti-Antennapedia monoclonal antibodies and Antennapedia protein expression in imaginal discs. *Dros Info Serv*, 70, pp.52–54.

Conesa, A. et al., 2005. Blast2GO: A universal tool for annotation, visualization and analysis in functional genomics research. *Bioinformatics*, 21(18), pp.3674–3676.

Cordeiro, J. V. & Jacinto, A., 2013. The role of transcription-independent

damage signals in the initiation of epithelial wound healing. *Nature Reviews Molecular Cell Biology*, 14(4), pp.249–262. Available at: http://www.nature.com/doifinder/10.1038/nrm3541 [Accessed June 21, 2016].

Cortez, D. et al., 2001. ATR and ATRIP: partners in checkpoint signaling. *Science (New York, N.Y.)*, 294(5547), pp.1713–6. Available at: http://www.ncbi.nlm.nih.gov/pubmed/11721054 [Accessed July 17, 2015].

Costa, A. et al., 2009. The Imd pathway is involved in antiviral immune responses in Drosophila. *PloS one*, 4(10), p.e7436. Available at: http://journals.plos.org/plosone/article?id=10.1371/journal.pone.0007436#s1 [Accessed April 25, 2016].

Crava, C.M. et al., 2015. Dissimilar Regulation of Antimicrobial Proteins in the Midgut of Spodoptera exigua Larvae Challenged with Bacillus thuringiensis Toxins or Baculovirus. *PloS one*, 10(5), p.e0125991. Available at: http://journals.plos.org/plosone/article?id=10.1371/journal.pone.0125991 [Accessed June 9, 2015].

Crawley, M.J., 2007. The R Book. Available at: http://dl.acm.org/citation.cfm?id=1535318 [Accessed August 26, 2015].

Davis, M.M. & Engström, Y., 2012. Immune response in the barrier epithelia: lessons from the fruit fly Drosophila melanogaster. *Journal of innate immunity*, 4(3), pp.273–83. Available at: http://www.karger.com/Article/FullText/332947 [Accessed August 28, 2015].

Debat, V. et al., 2003. Allometric and nonallometric components of Drosophila wing shape respond differently to developmental

temperature. *Evolution; international journal of organic evolution*, 57(12), pp.2773–2784.

DiAngelo, J.R. et al., 2009. The immune response attenuates growth and nutrient storage in Drosophila by reducing insulin signaling. *Proceedings of the National Academy of Sciences of the United States of America*, 106(49), pp.20853–8. Available at: http://www.pnas.org/content/106/49/20853.full [Accessed August 6, 2015].

Díaz-García, S. & Baonza, A., 2013. Pattern reorganization occurs independently of cell division during Drosophila wing disc regeneration in situ. *Proceedings of the National Academy of Sciences of the United States of America*, 110(32), pp.13032–7. Available at: http://www.pubmedcentral.nih.gov/articlerender.fcgi?artid=3740865&tool=pmcentrez&rendertype=abstract%5Cnhttp://www.ncbi.nlm.nih.gov/pubmed/23878228%5Cnhttp://www.pubmedcentral.nih.gov/articlerender.fcgi?artid=PMC3740865.

Diegelmann, R.F. & Evans, M.C., 2004. Wound healing: an overview of acute, fibrotic and delayed healing. *Frontiers in bioscience : a journal and virtual library*, 9(4), pp.283–289.

Dilão, R. & Sainhas, J., 2004. Modelling butterfly wing eyespot patterns. *Proceedings. Biological sciences / The Royal Society*, 271(1548), pp.1565–9. Available at: http://rspb.royalsocietypublishing.org/content/271/1548/1565 [Accessed March 14, 2016].

Dinwiddie, A. et al., 2014. Dynamics of F-actin prefigure the structure of butterfly wing scales. *Developmental biology*, 392(2), pp.404–18. Available at: http://www.ncbi.nlm.nih.gov/pubmed/24930704

[Accessed May 13, 2015].

Donoghue, M.T. et al., 2011. Evolutionary origins of Brassicaceae specific genes in Arabidopsis thaliana. *BMC Evolutionary Biology*, 11(1), p.47. Available at: http://bmcevolbiol.biomedcentral.com/articles/10.1186/1471-2148-11-47 [Accessed June 12, 2016].

Dubovskiy, I.M. et al., 2013. More than a colour change: insect melanism, disease resistance and fecundity. *Proceedings. Biological sciences / The Royal Society*, 280(1763), p.20130584. Available at: http://rspb.royalsocietypublishing.org/content/280/1763/20130584 [Accessed April 22, 2016].

Eleftherianos, I. & Revenis, C., 2011. Role and importance of phenoloxidase in insect hemostasis. *Journal of innate immunity*, 3(1), pp.28–33. Available at: http://www.karger.com/Article/FullText/321931 [Accessed May 26, 2015].

Evans, I.R. & Wood, W., Understanding in vivo blood cell migration--Drosophila hemocytes lead the way. *Fly*, 5(2), pp.110–4. Available at: http://www.pubmedcentral.nih.gov/articlerender.fcgi?artid=3127059&tool=pmcentrez&rendertype=abstract [Accessed March 10, 2016].

Fan, T. et al., 2011. Patterns and cellular mechanisms of arm regeneration in adult starfish Asterias rollestoni bell. *Journal of Ocean University of China*, 10(3), pp.255–262. Available at: http://link.springer.com/10.1007/s11802-011-1837-y [Accessed June 14, 2016].

Feder, M.E. & Hofmann, G.E., 1999. Heat-shock proteins, molecular chaperones, and the stress response: Evolutionary and ecological

physiology. *Annual Review of Physiology*, 61, pp.243–282.

Ferrandon, D. et al., 1998. A drosomycin-GFP reporter transgene reveals a local immune response in Drosophila that is not dependent on the Toll pathway. *The EMBO journal*, 17(5), pp.1217–27. Available at: http://emboj.embopress.org/content/17/5/1217.abstract [Accessed November 13, 2015].

Flatt, T. et al., 2008. Hormonal Regulation of the Humoral Innate Immune Response in Drosophila melanogaster. *J Exp Biol. J Exp Biol*, 211, pp.2712–2724.

Frank-Kamenetsky, M. et al., 2002. Small-molecule modulators of Hedgehog signaling: identification and characterization of Smoothened agonists and antagonists. *Journal of Biology*, 1(2), p.1. Available at: http://jbiol.biomedcentral.com/articles/10.1186/1475-4924-1-10 [Accessed March 10, 2016].

Freitak, D. et al., 2005. Formation of melanin-based wing patterns is influenced by condition and immune challenge in Pieris brassicae. *Entomologia Experimentalis et Applicata*, 116(3), pp.237–243. Available at: http://www.researchgate.net/publication/227662751_Formation_of_melaninbased_wing_patterns_is_influenced_by_condition_and_immune_challenge_in_Pieris_brassicae [Accessed June 24, 2015].

French, V. & Brakefield, P.M., 1995. Eyespot development on butterfly wings: the focal signal. *Developmental biology*, 168(1), pp.112–123.

French, V. & Brakefield, P.M., 1992. The development of eyespot patterns on butterfly wings: morphogen sources or sinks? *Development*, 116, pp.103–109.

Frisch, I.A., 1930. DEMONSTRATION OF LOCAL IMMUNITY OF THE PERITONEUM BY MEANS OF THE SHWARTZMAN

PHENOMENON. *Archives of Internal Medicine*, 46(3), p.410. Available at: http://archinte.jamanetwork.com/article.aspx?articleid=537072 [Accessed April 24, 2016].

Galko, M.J. & Krasnow, M.A., 2004. Cellular and genetic analysis of wound healing in Drosophila larvae. *PLoS biology*, 2(8), p.E239. Available at: http://www.ncbi.nlm.nih.gov/pubmed/15269788 [Accessed June 14, 2016].

Ganfornina, M.D. & Sánchez, D., 1999. Generation of evolutionary novelty by functional shift. *BioEssays : news and reviews in molecular, cellular and developmental biology*, 21(5), pp.432–9. Available at: http://www.ncbi.nlm.nih.gov/pubmed/10376014 [Accessed June 23, 2015].

George, H.R. & Cristofalo, V.J., 1972. *Growth, Nutrition, and Metabolism of Cells In Culture, Volume 2* illustrate. H. R. George & V. J. Cristofalo, eds., New York: Academic Press, 1972. Available at: https://books.google.com/books?id=kft-yYByfFcC&pgis=1 [Accessed November 20, 2015].

Gibert, P., Moreteau, B. & David, J.R., 2004. Phenotypic plasticity of body pigmentation in Drosophila melanogaster: genetic repeatability of quantitative parameters in two successive generations. *Heredity*, 92(6), pp.499–507.

Gibson, M. & Schubiger, G., 1999. Hedgehog is required for activation of engrailed during regeneration of fragmented Drosophila imaginal discs. *Development*, 126(8), pp.1591–1599. Available at: http://dev.biologists.org/content/126/8/1591.long [Accessed March 10, 2016].

Gidaszewski, N.A., Baylac, M. & Klingenberg, C.P., 2009. Evolution of

sexual dimorphism of wing shape in the Drosophila melanogaster subgroup. *BMC evolutionary biology*, 9(1), p.110. Available at: http://www.biomedcentral.com/1471-2148/9/110 [Accessed August 13, 2015].

Gillooly, J.F. et al., 2002. Effects of size and temperature on developmental time. *Nature*, 417(6884), pp.70–73.

Goldsmith, M.R., Shimada, T. & Abe, H., 2005. The genetics and genomics of the silkworm, Bombyx mori. *Annual review of entomology*, 50, pp.71–100.

De Gregorio, E. et al., 2002. The Toll and Imd pathways are the major regulators of the immune response in Drosophila. *The EMBO journal*, 21(11), pp.2568–79. Available at: http://emboj.embopress.org/content/21/11/2568.abstract [Accessed February 4, 2016].

Grigorian, M., Mandal, L. & Hartenstein, V., 2011. Hematopoiesis at the onset of metamorphosis: terminal differentiation and dissociation of the Drosophila lymph gland. *Development genes and evolution*, 221(3), pp.121–31. Available at: http://www.pubmedcentral.nih.gov/articlerender.fcgi?artid=4278756&tool=pmcentrez&rendertype=abstract [Accessed September 2, 2015].

Gualda, E.J. et al., 2013. OpenSpinMicroscopy: an open-source integrated microscopy platform. *Nature methods*, 10(7), pp.599–600. Available at: http://dx.doi.org/10.1038/nmeth.2508 [Accessed August 13, 2015].

Gurtner, G.C. et al., 2008. Wound repair and regeneration. *Nature*, 453(7193), pp.314–321.

Hambly, C., Harper, E.J. & Speakman, J.R., 2004. The energetic cost of

variations in wing span and wing asymmetry in the zebra finch Taeniopygia guttata. *The Journal of experimental biology*, 207(Pt 22), pp.3977–3984.

Hariharan, I.K., 2015. Organ Size Control: Lessons from Drosophila. *Developmental Cell*, 34(3), pp.255–265. Available at: http://www.cell.com/article/S1534580715004852/fulltext [Accessed August 10, 2015].

Hartl, P., 1993. Mitotic repression of transcription in vitro. *The Journal of Cell Biology*, 120(3), pp.613–624. Available at: http://jcb.rupress.org/content/120/3/613.abstract [Accessed September 4, 2015].

Hassall, C., 2014. Continental variation in wing pigmentation in Calopteryx damselflies is related to the presence of heterospecifics. *PeerJ*, 2, p.e438. Available at: https://peerj.com/articles/438 [Accessed April 22, 2016].

Hazel, W.N., 2002. The environmental and genetic control of seasonal polyphenism in larval color and its adaptive significance in a swallowtail butterfly. *Evolution; international journal of organic evolution*, 56(2), pp.342–348.

Held, L.I., 2013. Rethinking Butterfly Eyespots. *Evolutionary Biology*, 40(1), pp.158–168.

Herboso, L. et al., 2015. Ecdysone promotes growth of imaginal discs through the regulation of Thor in D. melanogaster. *Scientific Reports*, 5, p.12383. Available at: http://www.nature.com/articles/srep12383 [Accessed June 26, 2016].

Hines, H.M. et al., 2012. Transcriptome analysis reveals novel patterning and pigmentation genes underlying Heliconius butterfly wing pattern variation. *BMC genomics*, 13(1), p.288. Available at:

http://www.biomedcentral.com/1471-2164/13/288 [Accessed July 20, 2015].

Hu, W. & Pasare, C., 2013. Location, location, location: tissue-specific regulation of immune responses. *Journal of leukocyte biology*, 94(3), pp.409–21. Available at: http://www.pubmedcentral.nih.gov/articlerender.fcgi?artid=3747123&tool=pmcentrez&rendertype=abstract [Accessed November 10, 2015].

Ishii, K. et al., 2010. Porphyromonas gingivalis peptidoglycans induce excessive activation of the innate immune system in silkworm larvae. *The Journal of biological chemistry*, 285(43), pp.33338–47. Available at: http://www.jbc.org/content/285/43/33338.abstract [Accessed November 12, 2015].

Iwata, M. & Otaki, J.M., 2016. Focusing on butterfly eyespot focus: uncoupling of white spots from eyespot bodies in nymphalid butterflies. *SpringerPlus*, 5(1), p.1287. Available at: http://springerplus.springeropen.com/articles/10.1186/s40064-016-2969-8 [Accessed September 6, 2016].

Jacinto, A., Martinez-Arias, A. & Martin, P., 2001. Mechanisms of epithelial fusion and repair. *Nature cell biology*, 3(5), pp.E117–E123.

Jiang, H. et al., 2011. EGFR/Ras/MAPK signaling mediates adult midgut epithelial homeostasis and regeneration in drosophila. *Cell Stem Cell*, 8(1), pp.84–95.

Jin, X. et al., 2011. Identification and characterization of a serine protease inhibitor with two trypsin inhibitor-like domains from the human hookworm Ancylostoma duodenale. *Parasitology research*, 108(2), pp.287–95. Available at: http://www.ncbi.nlm.nih.gov/pubmed/20852886 [Accessed June 9,

2015].

Joliot, A. et al., 1991. Antennapedia homeobox peptide regulates neural morphogenesis. *Proceedings of the National Academy of Sciences of the United States of America*, 88(5), pp.1864–1868.

Kaneko, Y. et al., 2007. Expression of antimicrobial peptide genes encoding Enbocin and Gloverin isoforms in the silkworm, Bombyx mori. *Bioscience, biotechnology, and biochemistry*, 71(9), pp.2233–2241.

Kanost, M.R., Jiang, H. & Yu, X.Q., 2004. Innate immune responses of a lepidopteran insect, Manduca sexta. *Immunological Reviews*, 198, pp.97–105.

Kavanagh, K. & Reeves, E.P., 2004. Exploiting the potential of insects for in vivo pathogenicity testing of microbial pathogens. *FEMS microbiology reviews*, 28(1), pp.101–12. Available at: http://femsre.oxfordjournals.org/content/28/1/101.abstract [Accessed August 25, 2015].

Keys, D.N. et al., 1999. Recruitment of a hedgehog regulatory circuit in butterfly eyespot evolution. *Science*, 283(January), pp.532–534.

Keys, D.N. et al., 1999. Recruitment of a hedgehog regulatory circuit in butterfly eyespot evolution. *Science (New York, N.Y.)*, 283(5401), pp.532–4. Available at: http://www.ncbi.nlm.nih.gov/pubmed/9915699 [Accessed March 10, 2016].

Khalturin, K. et al., 2009. More than just orphans: are taxonomically-restricted genes important in evolution? *Trends in Genetics*, 25(9), pp.404–413.

Kim, S.-Y. et al., 2013. Multivariate heredity of melanin-based coloration, body mass and immunity. *Heredity*, 111(2), pp.139–46. Available at:

http://www.pubmedcentral.nih.gov/articlerender.fcgi?artid=3716269&tool=pmcentrez&rendertype=abstract [Accessed June 8, 2015].

King, J.G. & Hillyer, J.F., 2013. Spatial and temporal in vivo analysis of circulating and sessile immune cells in mosquitoes: hemocyte mitosis following infection. *BMC biology*, 11(1), p.55. Available at: http://www.biomedcentral.com/1741-7007/11/55.

Klingenberg, C.P., 2011. MorphoJ: An integrated software package for geometric morphometrics. *Molecular Ecology Resources*, 11(2), pp.353–357.

Klingenberg, C.P. & Mcintyre, G.S., 1998. Geometric Morphometrics of Developmental Instability : Analyzing Patterns of Fluctuating Asymmetry with Procrustes Methods. *Evolution*, 52(5), pp.1363–1375.

Koch, P.B. et al., 2000. Butterfly wing pattern mutants: Developmental heterochrony and co-ordinately regulated phenotypes. *Development Genes and Evolution*, 210(11), pp.536–544.

Koch, P.B.B., Brakefield, P.M.M. & Kesbeke, F., 1996. Ecdysteroids control eyespot size and wing color pattern in the polyphenic butterfly Bicyclus anynana (Lepidoptera: Satyridae). *Journal of Insect Physiology*, 42(3), pp.223–230. Available at: http://www.sciencedirect.com/science/article/pii/0022191095001034 [Accessed July 18, 2015].

Kooi, R.E. & Brakefield, P.M., 1999. The critical period for wing pattern induction in the polyphenic tropical butterfly Bicyclus anynana (Satyrinae). *Journal of insect physiology*, 45(3), pp.201–212. Available at: http://www.ncbi.nlm.nih.gov/pubmed/12770367 [Accessed July 16, 2015].

Kosman, D. et al., 2004. Multiplex detection of RNA expression in

Drosophila embryos. *Science (New York, N.Y.)*, 305(5685), p.846.

Krautz, R., Arefin, B. & Theopold, U., 2014. Damage signals in the insect immune response. *Frontiers in plant science*, 5, p.342. Available at: http://www.pubmedcentral.nih.gov/articlerender.fcgi?artid=4093659&tool=pmcentrez&rendertype=abstract [Accessed June 11, 2015].

Lai, S.-C. et al., 2002. Immunolocalization of prophenoloxidase in the process of wound healing in the mosquito Armigeres subalbatus (Diptera: Culicidae). *Journal of medical entomology*, 39(2), pp.266–74. Available at: http://www.ncbi.nlm.nih.gov/pubmed/11931025 [Accessed June 14, 2016].

Landis, G.N. et al., 2004. Similar gene expression patterns characterize aging and oxidative stress in Drosophila melanogaster. *Proceedings of the National Academy of Sciences of the United States of America*, 101(20), pp.7663–8. Available at: http://www.pnas.org/content/101/20/7663.short [Accessed July 13, 2015].

Lanot, R. et al., 2001. Postembryonic Hematopoiesis in Drosophila. *Developmental Biology*, 230(2), pp.243–257. Available at: http://www.sciencedirect.com/science/article/pii/S0012160600901234 [Accessed September 21, 2015].

Lavine, M.D. & Strand, M.R., 2002. Insect Hemocytes and Their Role in Immunity. *Insect Immunology*, 32, pp.25–47.

Lemaitre, B. & Hoffmann, J., 2007. The host defense of Drosophila melanogaster. *Annual review of immunology*, 25, pp.697–743.

Lemaitre, B., Reichhart, J.M. & Hoffmann, J. a, 1997. Drosophila host defense: differential induction of antimicrobial peptide genes after infection by various classes of microorganisms. *Proceedings of the National Academy of Sciences of the United States of America*,

94(26), pp.14614–14619.

Lenth, R. V. & Hervé, M., 2015. lsmeans: Least-Squares Means. R package version 2.17. URL http://CRAN.R-project.org/package=lsmeans. , pp.1–33.

Levesque, M. et al., 2012. Inflammation drives wound hyperpigmentation by recruiting pigment cells to sites of tissue damage. *Disease Models & Mechanisms*, 515, pp.508–515.

Ling, E. & Yu, X.Q., 2005. Prophenoloxidase binds to the surface of hemocytes and is involved in hemocyte melanization in Manduca sexta. *Insect Biochemistry and Molecular Biology*, 35(12), pp.1356–1366.

Livak, K.J. & Schmittgen, T.D., 2001. Analysis of relative gene expression data using real-time quantitative PCR and the 2(-Delta Delta C(T)) Method. *Methods (San Diego, Calif.)*, 25(4), pp.402–408.

Losick, V.P.P., Fox, D.T.T. & Spradling, A.C.C., 2013. Polyploidization and Cell Fusion Contribute to Wound Healing in the Adult Drosophila Epithelium. *Current Biology*, 23(22), pp.2224–2232. Available at: http://www.sciencedirect.com/science/article/pii/S0960982213011457 [Accessed July 6, 2015].

Luckhart, S. & Riehle, M.A., 2007. The insulin signaling cascade from nematodes to mammals: insights into innate immunity of Anopheles mosquitoes to malaria parasite infection. *Developmental and comparative immunology*, 31(7), pp.647–56. Available at: http://www.sciencedirect.com/science/article/pii/S0145305X06002059 [Accessed August 20, 2015].

Lyimo, E.O., Takken, W. & Koella, J.C., 1992. Effect of rearing temperature and larval density on larval survival, age at pupation

and adult size of Anopheles gambiae. *Entomologia Experimentalis et Applicata*, 63(3), pp.265–271. Available at: http://doi.wiley.com/10.1111/j.1570-7458.1992.tb01583.x [Accessed September 13, 2016].

Lyytinen, A., Brakefield, P.M. & Mappes, J., 2003. Significance of butterfly eyespots as an anti-predator device in ground-based and aerial attacks. *Oikos*, 100(2), pp.373–379.

Macdonald, W.P., Martin, A. & Reed, R.D., 2010. Butterfly wings shaped by a molecular cookie cutter: Evolutionary radiation of lepidopteran wing shapes associated with a derived Cut/wingless wing margin boundary system. *Evolution and Development*, 12(3), pp.296–304.

Mace, K. a, Pearson, J.C. & McGinnis, W., 2005. An epidermal barrier wound repair pathway in Drosophila is mediated by grainy head. *Science (New York, N.Y.)*, 308(5720), pp.381–385.

Madhavan, K. & Schneiderman, H.A., 1969. HORMONAL CONTROL OF IMAGINAL DISC REGENERATION IN GALLERIA MELLONELLA (LEPIDOPTERA). *The Biological Bulletin*, 137(2), pp.321–331.

Maere, S., Heymans, K. & Kuiper, M., 2005. BiNGO: a Cytoscape plugin to assess overrepresentation of gene ontology categories in biological networks. *Bioinformatics (Oxford, England)*, 21(16), pp.3448–9. Available at: http://www.ncbi.nlm.nih.gov/pubmed/15972284 [Accessed July 14, 2014].

Mandal, L. et al., 2007. A Hedgehog- and Antennapedia-dependent niche maintains Drosophila haematopoietic precursors. *Nature*, 446(7133), pp.320–4. Available at: http://dx.doi.org/10.1038/nature05585 [Accessed September 2, 2015].

Márkus, R. et al., 2005. Sterile wounding is a minimal and sufficient

trigger for a cellular immune response in Drosophila melanogaster. *Immunology Letters*, 101(1), pp.108–111.

Massimo Pigliucci, 2008. What, if Anything, Is an Evolutionary Novelty? *Philosophy of Science*, 75(5), pp.887–898. Available at: http://www.jstor.org/stable/10.1086/594532.

Mateus, A.R.A. et al., 2014. Adaptive developmental plasticity: Compartmentalized responses to environmental cues and to corresponding internal signals provide phenotypic flexibility. *BMC Biology*, 12, pp.1–15.

Meister, M., 2004. Blood cells of Drosophila: Cell lineages and role in host defence. *Current Opinion in Immunology*, 16(1), pp.10–15.

Merchant, D. et al., 2008. Eicosanoids mediate insect hemocyte migration. *Journal of insect physiology*, 54(1), pp.215–21. Available at: http://www.sciencedirect.com/science/article/pii/S0022191007002119 [Accessed March 10, 2016].

Mirth, C.K. & Shingleton, A.W., 2012. Integrating body and organ size in Drosophila: recent advances and outstanding problems. *Frontiers in endocrinology*, 3, p.49. Available at: http://journal.frontiersin.org/article/10.3389/fendo.2012.00049/abstract [Accessed July 15, 2015].

Moczek, A. & Emlen, D., 2000. Male horn dimorphism in the scarab beetle, Onthophagus taurus: do alternative reproductive tactics favour alternative phenotypes? *Animal behaviour*, 59(2), pp.459–466. Available at: http://www.sciencedirect.com/science/article/pii/S0003347299913428.

Moczek, A.P., 2008. On the origins of novelty in development and

evolution. *BioEssays*, 30(5), pp.432–447.

Moczek, A.P. & Nagy, L.M., 2005. Diverse developmental mechanisms contribute to different levels of diversity in horned beetles. *Evolution and Development*, 7(3), pp.175–185.

Monteiro, A. et al., 2006. Comparative insights into questions of lepidopteran wing pattern homology. *BMC developmental biology*, 6, p.52.

Monteiro, A. et al., 2015. Differential Expression of Ecdysone Receptor Leads to Variation in Phenotypic Plasticity across Serial Homologs. *PLoS genetics*, 11(9), p.e1005529. Available at: http://www.ncbi.nlm.nih.gov/pubmed/26405828 [Accessed June 26, 2016].

Monteiro, A., 2015. Origin, Development, and Evolution of Butterfly Eyespots. *Annual Review of Entomology*, 60(1), pp.253–271. Available at: http://www.annualreviews.org/doi/abs/10.1146/annurev-ento-010814-020942 [Accessed June 11, 2016].

Monteiro, a, Brakefield, P.M. & French, V., 1997. Butterfly eyespots: The genetics and development of the color rings. *Evolution*, 51(4), pp.1207–1216.

Monteiro, a F., Brakefield, P.M. & French, V., 1994. The evolutionary genetics and developmental basis of wing pattern variation in the butterfly Bicyclus anynana. *Evolution*, 48(4), pp.1147–1157.

de Morais Guedes, S. et al., 2005. Proteomics of immune-challenged Drosophila melanogaster larvae hemolymph. *Biochemical and biophysical research communications*, 328(1), pp.106–15. Available at: http://www.sciencedirect.com/science/article/pii/S0006291X0402951

1 [Accessed August 20, 2015].

Mortimer, N.T., Parasitoid wasp virulence: A window into fly immunity. *Fly*, 7(4), pp.242–8. Available at: http://www.pubmedcentral.nih.gov/articlerender.fcgi?artid=3896496&tool=pmcentrez&rendertype=abstract [Accessed July 23, 2015].

Moussian, B. & Uv, A.E., 2005. An ancient control of epithelial barrier formation and wound healing. *BioEssays*, 27(10), pp.987–990.

Müller, G.B., 2007. Evo-devo: extending the evolutionary synthesis. *Nature reviews. Genetics*, 8(12), pp.943–9. Available at: http://www.ncbi.nlm.nih.gov/pubmed/17984972.

Muller, G.B. & Wagner, G.P., 1991. Novelty in Evolution: Restructuring the Concept. *Annual Review of Ecology and Systematics*, 22(1), pp.229–256.

Müller, P. et al., 2013. Morphogen transport. *Development (Cambridge, England)*, 140(8), pp.1621–38. Available at: http://www.pubmedcentral.nih.gov/articlerender.fcgi?artid=3621481&tool=pmcentrez&rendertype=abstract [Accessed March 10, 2016].

Myllymäki, H., Valanne, S. & Rämet, M., 2014. The Drosophila imd signaling pathway. *Journal of immunology (Baltimore, Md. : 1950)*, 192(8), pp.3455–62. Available at: http://www.jimmunol.org/content/192/8/3455.full [Accessed March 1, 2016].

Nam, H.-J. et al., 2012. Genetic evidence of a redox-dependent systemic wound response via Hayan Protease-Phenoloxidase system in Drosophila. *The EMBO Journal*, 31(5), pp.1253–1265. Available at: http://dx.doi.org/10.1038/emboj.2011.476.

Nappi, A.J. & Christensen, B.M., 2005. Melanogenesis and associated cytotoxic reactions: Applications to insect innate immunity. *Insect*

Biochemistry and Molecular Biology, 35(5), pp.443–459.

Nardi, J.B. et al., 2006. Neuroglian-positive plasmatocytes of Manduca sexta and the initiation of hemocyte attachment to foreign surfaces. *Developmental and Comparative Immunology*, 30(5), pp.447–462.

Nardi, J.B., 1994. Rearrangement of epithelial cell types in an insect wing monolayer is accompanied by differential expression of a cell surface protein. *Developmental dynamics : an official publication of the American Association of Anatomists*, 199(4), pp.315–325.

Nardi, J.B., Gao, C. & Kanost, M.R., 2001. The extracellular matrix protein lacunin is expressed by a subset of hemocytes involved in basal lamina morphogenesis. *Journal of Insect Physiology*, 47(9), pp.997–1006.

Neufeld, T.P., 2003. Body building: regulation of shape and size by PI3K/TOR signaling during development. *Mechanisms of Development*, 120(11), pp.1283–1296. Available at: http://www.sciencedirect.com/science/article/pii/S0925477303002041 [Accessed August 19, 2015].

Neves, J. et al., 2015. Of Flies, Mice, and Men: Evolutionarily Conserved Tissue Damage Responses and Aging. *Developmental Cell*, 32(1), pp.9–18. Available at: http://www.ncbi.nlm.nih.gov/pubmed/25584795 [Accessed January 12, 2015].

Neyen, C. et al., 2014. Methods to study Drosophila immunity. *Methods*, 68(1), pp.116–128.

Niemela, P.T. et al., 2013. Personality pace-of-life hypothesis: testing genetic associations among personality and life history. *Behavioral Ecology*, 24(4), pp.935–941. Available at: http://beheco.oxfordjournals.org/content/early/2013/03/14/beheco.ar

t014.abstract [Accessed November 28, 2015].

Niethammer, P. et al., 2009. A tissue-scale gradient of hydrogen peroxide mediates rapid wound detection in zebrafish. *Nature*, 459(7249), pp.996–9. Available at: http://dx.doi.org/10.1038/nature08119 [Accessed March 10, 2015].

Nijhout, H.F., 1985. Cautery-induced colour patterns in Precis coenia (Lepidoptera: Nymphalidae). *Journal of embryology and experimental morphology*, 86(1), pp.191–203. Available at: http://www.ncbi.nlm.nih.gov/pubmed/4031740 [Accessed June 14, 2016].

Nijhout, H.F., 1999. Control Mechanisms of Polyphenic Development in Insects. *BioScience*, 49(3), p.181. Available at: http://bioscience.oxfordjournals.org/cgi/doi/10.2307/1313508 [Accessed June 23, 2016].

Nijhout, H.F., 2001. Elements of Butterfly Wing Patterns. *Journal of Experimental Zoology*, 291(3), pp.213–225.

Nijhout, H.F., 1980. Pattern formation on lepidopteran wings: Determination of an eyespot. *Developmental Biology*, 80(2), pp.267–274.

Nijhout, H.F. et al., 2007. The control of growth and differentiation of the wing imaginal disks of Manduca sexta. *Developmental biology*, 302(2), pp.569–76. Available at: http://www.sciencedirect.com/science/article/pii/S0012160606013169 [Accessed July 15, 2015].

Nijhout, H.F., 1991. *The development and evolution of butterfly wing patterns*,

Nijhout, H.F., Cinderella, M. & Grunert, L.W., 2014. The development of wing shape in Lepidoptera: Mitotic density, not orientation, is the

primary determinant of shape. *Evolution and Development*, 16(2), pp.68–77.

NimbleGen, 2011. NimbleGen Arrays User ' s Guide: Gene Expression Arrays v6.0. , p.54. Available at: http://www.nimblegen.com/downloads/support/05434505001_NG_Expression_UGuide_v6p0.pdf.

Nishikawa, H. et al., 2013. Molecular basis of wing coloration in a Batesian mimic butterfly, Papilio polytes. *Scientific reports*, 3, p.3184. Available at: http://www.pubmedcentral.nih.gov/articlerender.fcgi?artid=3822385&tool=pmcentrez&rendertype=abstract.

Ohno, Y. & Otaki, J.M., 2012. Eyespot colour pattern determination by serial induction in fish: Mechanistic convergence with butterfly eyespots. *Scientific Reports*, 2.

Oostra, V. et al., 2014. On the fate of seasonally plastic traits in a rainforest butterfly under relaxed selection. *Ecology and evolution*, 4(13), pp.2654–67. Available at: http://www.pubmedcentral.nih.gov/articlerender.fcgi?artid=4113290&tool=pmcentrez&rendertype=abstract [Accessed July 16, 2015].

Oostra, V. et al., 2011. Translating environmental gradients into discontinuous reaction norms via hormone signalling in a polyphenic butterfly. *Proceedings. Biological sciences / The Royal Society*, 278(1706), pp.789–797.

Otaki, J.M., 2011. Artificially induced changes of butterfly wing colour patterns: dynamic signal interactions in eyespot development. *Scientific Reports*, 1.

Outomuro, D., Adams, D.C. & Johansson, F., 2012. The Evolution of Wing Shape in Ornamented-Winged Damselflies (Calopterygidae,

Odonata). *Evolutionary Biology*, 40(2), pp.300–309. Available at: http://link.springer.com/10.1007/s11692-012-9214-3 [Accessed May 18, 2016].

Patel, N.H. et al., 1989. Expression of engrailed proteins in arthropods, annelids, and chordates. *Cell*, 58(5), pp.955–68. Available at: http://www.ncbi.nlm.nih.gov/pubmed/2570637 [Accessed July 21, 2015].

Pawitan, Y. et al., 2005. False discovery rate, sensitivity and sample size for microarray studies. *Bioinformatics (Oxford, England)*, 21(13), pp.3017–24. Available at: http://bioinformatics.oxfordjournals.org/content/21/13/3017.full.html [Accessed August 27, 2015].

Pelletier, J.C. et al., 2009. (1-(4-(Naphthalen-2-yl)pyrimidin-2-yl)piperidin-4-yl)methanamine: a wingless beta-catenin agonist that increases bone formation rate. *Journal of medicinal chemistry*, 52(22), pp.6962–5. Available at: http://dx.doi.org/10.1021/jm9014197 [Accessed March 10, 2016].

Pesch, Y.-Y. et al., 2016. Chitinases and Imaginal disc growth factors organize the extracellular matrix formation at barrier tissues in insects. *Scientific reports*, 6, p.18340. Available at: http://www.nature.com/srep/2016/160203/srep18340/full/srep18340.html.

Pfaffl, M.W. & Pfaffl, M.W., 2001. A new mathematical model for relative quantification in real-time RT-PCR. *Nucleic acids research*, 29(9), p.e45. Available at: http://www.ncbi.nlm.nih.gov/pubmed/11328886.

Pieau, C., Dorizzi, M. & Richard-Mercier, N., 1999. Temperature-dependent sex determination and gonadal differentiation in reptiles. *Cell. Mol. Life Sci.*, 55(91), pp.887–900.

Pigliucci, M., 2001. *Phenotypic plasticity: beyond nature and nurture*,

Poinar, G. & Yanoviak, S.P., 2008. Myrmeconema neotropicum n. g., n. sp., a new tetradonematid nematode parasitising South American populations of Cephalotes atratus (Hymenoptera: Formicidae), with the discovery of an apparent parasite-induced host morph. *Systematic Parasitology*, 69(2), pp.145–153.

Previtali, M.A. et al., 2012. Relationship between pace of life and immune responses in wild rodents. *Oikos*, 121(9), pp.1483–1492. Available at: http://doi.wiley.com/10.1111/j.1600-0706.2012.020215.x [Accessed November 28, 2015].

Prudic, K. et al., 2015. Eyespots deflect predator attack increasing fitness and promoting the evolution of phenotypic plasticity. *Proc. R. Soc. B*, 282(20141531).

Prudic, K.L. et al., 2011. Developmental plasticity in sexual roles of butterfly species drives mutual sexual ornamentation. *Science (New York, N.Y.)*, 331(6013), pp.73–75.

Prum, R.O., 2005. Evolution of the morphological innovations of feathers. *Journal of experimental zoology. Part B, Molecular and developmental evolution*, 304(6), pp.570–9. Available at: http://www.ncbi.nlm.nih.gov/pubmed/16208685 [Accessed June 12, 2016].

Quackenbush, J., 2002. Microarray data normalization and transformation. *Nature genetics*, 32 Suppl, pp.496–501. Available at: http://www.nature.com/ng/journal/v32/n4s/pdf/ng1032.pdf [Accessed August 31, 2015].

Quiroz-Castañeda, R.E. et al., 2015. Identification of a new Alcaligenes faecalis strain MOR02 and assessment of its toxicity and pathogenicity to insects. *BioMed research international*, 2015,

p.570243. Available at: http://www.pubmedcentral.nih.gov/articlerender.fcgi?artid=4312618&tool=pmcentrez&rendertype=abstract [Accessed November 12, 2015].

R Development Core Team, 2015. R: A language and environment for statistical computing. R Foundation for Statistical Computing, Vienna, Austria. URL http://www.R-project.org/. *R Foundation for Statistical Computing, Vienna, Austria.*

Rajpurohit, S., PARKASH, R. & RAMNIWAS, S., 2008. Body melanization and its adaptive role in thermoregulation and tolerance against desiccating conditions in drosophilids. *Entomological Research*, 38(1), pp.49–60. Available at: http://doi.wiley.com/10.1111/j.1748-5967.2008.00129.x [Accessed April 23, 2016].

Rao, X.-J. & Yu, X.-Q., 2010. Lipoteichoic acid and lipopolysaccharide can activate antimicrobial peptide expression in the tobacco hornworm Manduca sexta. *Developmental and comparative immunology*, 34(10), pp.1119–1128. Available at: http://dx.doi.org/10.1016/j.dci.2010.06.007.

Ravosa, M.J., 1991. Evolutionary Innovations - Nitecki,Mh. *American Journal of Physical Anthropology*, 85(4), pp.473–474.

Razzell, W. et al., 2013. Calcium flashes orchestrate the wound inflammatory response through duox activation and hydrogen peroxide release. *Current Biology*, 23(5), pp.424–429.

Razzell, W., Wood, W. & Martin, P., 2011. Swatting flies: modelling wound healing and inflammation in Drosophila. *Disease models & mechanisms*, 4(5), pp.569–574.

Reed, R.D. et al., 2011. optix drives the repeated convergent evolution of

butterfly wing pattern mimicry. *Science (New York, N.Y.)*, 333(6046), pp.1137–1141.

Regan, J.C. et al., 2013. Steroid Hormone Signaling Is Essential to Regulate Innate Immune Cells and Fight Bacterial Infection in Drosophila. *PLoS Pathogens*, 9(10).

Reiner, A., Yekutieli, D. & Benjamini, Y., 2003. Identifying differentially expressed genes using false discovery rate controlling procedures. *Bioinformatics*, 19(3), pp.368–375.

Reinke, J.M. & Sorg, H., 2012. Wound repair and regeneration. *European surgical research. Europäische chirurgische Forschung. Recherches chirurgicales européennes*, 49(1), pp.35–43. Available at: http://www.karger.com/Article/FullText/339613 [Accessed August 10, 2015].

Reznick, D., Bryant, M.J. & Bashey, F., 2002. r - AND K -SELECTION REVISITED: THE ROLE OF POPULATION REGULATION IN LIFE-HISTORY EVOLUTION. *Ecology*, 83(6), pp.1509–1520. Available at: http://www.esajournals.org/doi/abs/10.1890/0012-9658(2002)083%5B1509:RAKSRT%5D2.0.CO;2 [Accessed November 28, 2015].

Ririe, K.M., Rasmussen, R.P. & Wittwer, C.T., 1997. Product differentiation by analysis of DNA melting curves during the polymerase chain reaction. *Analytical biochemistry*, 245(2), pp.154–160.

Robertson, K.A. & Monteiro, A., 2005. Female Bicyclus anynana butterflies choose males on the basis of their dorsal UV-reflective eyespot pupils. *Proceedings. Biological sciences / The Royal Society*, 272(1572), pp.1541–1546.

Rosales, C., 2011. Phagocytosis, a cellular immune response in insects.

ISJ, 8, pp.109–131.

Roskam, J.C. & Brakefield, P.M., 1999. Seasonal polyphenism in Bicyclus (Lepidoptera: Satyridae) butterflies: different climates need different cues. *Biological Journal of the Linnean Society*, 66, pp.345–356.

Rowley, A.F. & Ratcliffe, N.A., 1978. A histological study of wound healing and hemocyte function in the wax-mothGalleria mellonella. *Journal of Morphology*, 157(2), pp.181–199. Available at: http://doi.wiley.com/10.1002/jmor.1051570206 [Accessed June 14, 2016].

Royston, P., 1993. A toolkit for testing for non-normality in complete and censored samples. *Journal of the Royal Statistical Society. Series D (The Statistician)*, 42(1), pp.37–43.

Rus, F. et al., 2013. Ecdysone triggered PGRP-LC expression controls Drosophila innate immunity. *The EMBO journal*, 32(11), pp.1626–38. Available at: http://www.pubmedcentral.nih.gov/articlerender.fcgi?artid=3671248&tool=pmcentrez&rendertype=abstract [Accessed July 20, 2015].

Russo, J. et al., 1996. Insect immunity: early events in the encapsulation process of parasitoid (Leptopilina boulardi) eggs in resistant and susceptible strains of Drosophila. *Parasitology*, 112 (Pt 1, pp.135–42. Available at: http://www.ncbi.nlm.nih.gov/pubmed/8587797 [Accessed September 4, 2015].

Saastamoinen, M. & Rantala, M.J., 2013. Influence of developmental conditions on immune function and dispersal-related traits in the Glanville fritillary (Melitaea cinxia) butterfly. *PloS one*, 8(11), p.e81289. Available at: http://journals.plos.org/plosone/article?id=10.1371/journal.pone.008

1289 [Accessed June 24, 2015].

Saenko, S. V et al., 2008. Conserved developmental processes and the formation of evolutionary novelties: examples from butterfly wings. *Philosophical transactions of the Royal Society of London. Series B, Biological sciences*, 363(1496), pp.1549–1555.

Saenko, S. V, Brakefield, P.M. & Beldade, P., 2010. Single locus affects embryonic segment polarity and multiple aspects of an adult evolutionary novelty. *BMC biology*, 8(1), p.111. Available at: http://www.biomedcentral.com/1741-7007/8/111 [Accessed June 22, 2015].

Saenko, S. V, Marialva, M.S. & Beldade, P., 2011. Involvement of the conserved Hox gene Antennapedia in the development and evolution of a novel trait. *EvoDevo*, 2(1), p.9. Available at: http://www.evodevojournal.com/content/2/1/9.

Samakovlis, C. et al., 1990. The immune response in Drosophila: pattern of cecropin expression and biological activity. *The EMBO journal*, 9(9), pp.2969–76. Available at: http://www.pubmedcentral.nih.gov/articlerender.fcgi?artid=552014&tool=pmcentrez&rendertype=abstract [Accessed September 4, 2015].

Sampson, C.J., Amin, U. & Couso, J.-P., 2013. Activation of Drosophila hemocyte motility by the ecdysone hormone. *Biology open*, 2(12), pp.1412–20. Available at: http://bio.biologists.org/content/early/2013/11/11/bio.20136619.abstract [Accessed September 4, 2015].

Sane, S.P. & Dickinson, M.H., 2001. The control of flight force by a flapping wing: lift and drag production. *J. Exp. Biol.*, 204(15), pp.2607–2626. Available at: http://jeb.biologists.org/content/204/15/2607.short [Accessed August

20, 2015].

Schindelin, J. et al., 2012. Fiji: an open-source platform for biological-image analysis. *Nature Methods*, 9(7), pp.676–682.

Schubiger, M., Sustar, A. & Schubiger, G., 2010. Regeneration and transdetermination: the role of wingless and its regulation. *Developmental biology*, 347(2), pp.315–24. Available at: http://www.pubmedcentral.nih.gov/articlerender.fcgi?artid=2976676&tool=pmcentrez&rendertype=abstract [Accessed March 10, 2016].

Schwanwitsch, B.N., 1929. Two schemes of the wing-pattern of butterflies. *Zeitschrift f??r Morphologie und ??kologie der Tiere*, 14(1), pp.36–58.

Seroude, L. et al., 2002. Spatio-temporal analysis of gene expression during aging in Drosophila melanogaster. *Aging cell*, 1(1), pp.47–56.

Shiga, Y. et al., 2002. Evolving role of Antennapedia protein in arthropod limb patterning. *Development (Cambridge, England)*, 129(15), pp.3555–3561.

Shingleton, A.W. et al., 2009. Many ways to be small: different environmental regulators of size generate distinct scaling relationships in Drosophila melanogaster. *Proceedings. Biological sciences / The Royal Society*, 276(1667), pp.2625–33. Available at: http://www.pubmedcentral.nih.gov/articlerender.fcgi?artid=2686648&tool=pmcentrez&rendertype=abstract [Accessed July 19, 2015].

Shingleton, A.W., 2010. The regulation of organ size in Drosophila: Physiology, plasticity, patterning and physical force. *Organogenesis*, 6(2), pp.76–87.

Shirai, L.T. et al., 2012. Evolutionary history of the recruitment of conserved developmental genes in association to the formation and diversification of a novel trait. *BMC evolutionary biology*, 12(1), p.21.

Available at: http://www.biomedcentral.com/1471-2148/12/21 [Accessed August 31, 2015].

Simon, A. & Biot, E., 2010. ANAIS: Analysis of NimbleGen arrays interface. *Bioinformatics*, 26(19), pp.2468–2469.

Singh, S. et al., 2014. Microbial population dynamics in the hemolymph of Manduca sexta infected with Xenorhabdus nematophila and the entomopathogenic nematode Steinernema carpocapsae. *Applied and environmental microbiology*, 80(14), pp.4277–85. Available at: http://www.pubmedcentral.nih.gov/articlerender.fcgi?artid=4068695&tool=pmcentrez&rendertype=abstract [Accessed November 12, 2015].

Smith-Bolton, R.K. et al., 2009. Regenerative growth in Drosophila imaginal discs is regulated by Wingless and Myc. *Developmental cell*, 16(6), pp.797–809. Available at: http://www.pubmedcentral.nih.gov/articlerender.fcgi?artid=2705171&tool=pmcentrez&rendertype=abstract [Accessed July 15, 2015].

Smoot, M.E. et al., 2011. Cytoscape 2.8: New features for data integration and network visualization. *Bioinformatics*, 27(3), pp.431–432.

Spencer, C.A., 2000. Mitotic Transcription Repression In Vivo in the Absence of Nucleosomal Chromatin Condensation. *The Journal of Cell Biology*, 150(1), pp.13–26. Available at: http://jcb.rupress.org/content/150/1/13.short [Accessed September 4, 2015].

Stearns, S., 1989. The evolutionary significance of phenotypic plasticity - phenotypic sources of variation among organisms can be described by developmental switches and reaction norms. *Bioscience*, 39(7), pp.436–445. Available at:

http://www.jstor.org/stable/10.2307/1311135.

Stebbins, G.L., 1970. Adaptive Radiation of Reproductive Characteristics in Angiosperms, I: Pollination Mechanisms. *Annual Review of Ecology and Systematics*, 1(1), pp.307–326.

Stieper, B.C. et al., 2008. Imaginal discs regulate developmental timing in Drosophila melanogaster. *Developmental biology*, 321(1), pp.18–26. Available at: http://www.sciencedirect.com/science/article/pii/S001216060800907X [Accessed July 15, 2015].

Strand, M.R., 2008. The insect cellular immune response. *Insect Science*, 15(1), pp.1–14.

Swaddle, J.P., 1997. Within-individual changes in developmental stability affect flight performance. *Behavioral Ecology*, 8(6), pp.601–604. Available at: http://beheco.oxfordjournals.org/content/8/6/601.short [Accessed August 20, 2015].

Tanaka, H. & Yamakawa, M., 2011. Regulation of the innate immune responses in the silkworm, Bombyx mori. *Invertebrate Survival Journal*, 8, pp.59–69.

Tang, H., 2009. Regulation and function of the melanization reaction in Drosophila. *Fly*.

Tang, H.Y. et al., 2011. FOXO Regulates Organ-Specific Phenotypic Plasticity In Drosophila E. Hafen, ed. *PLoS Genetics*, 7(11), p.e1002373. Available at: http://dx.plos.org/10.1371/journal.pgen.1002373 [Accessed June 26, 2016].

Tanji, T. et al., 2007. Toll and IMD pathways synergistically activate an innate immune response in Drosophila melanogaster. *Molecular and cellular biology*, 27(12), pp.4578–88. Available at:

http://www.pubmedcentral.nih.gov/articlerender.fcgi?artid=1900069&tool=pmcentrez&rendertype=abstract [Accessed May 25, 2015].

Taylor, S. et al., 2010. A practical approach to RT-qPCR-Publishing data that conform to the MIQE guidelines. *Methods*, 50(4), pp.S1–S5. Available at: http://dx.doi.org/10.1016/j.ymeth.2010.01.005.

Teng, X. et al., 2012. Validation of reference genes for quantitative expression analysis by real-time rt-PCR in four lepidopteran insects. *Journal of insect science (Online)*, 12(60), p.60. Available at: http://www.pubmedcentral.nih.gov/articlerender.fcgi?artid=3481461&tool=pmcentrez&rendertype=abstract.

Tian, L. et al., 2010. Genome-wide regulation of innate immunity by juvenile hormone and 20-hydroxyecdysone in the Bombyx fat body. *BMC genomics*, 11(1), p.549. Available at: http://www.biomedcentral.com/1471-2164/11/549 [Accessed July 20, 2015].

Tong, X. et al., 2014. Over-expression of Ultrabithorax alters embryonic body plan and wing patterns in the butterfly Bicyclus anynana. *Developmental Biology*, 394(2), pp.357–366. Available at: http://linkinghub.elsevier.com/retrieve/pii/S0012160614004114 [Accessed March 7, 2017].

True, J.R. & Carroll, S.B., 2002. Gene co-option in physiological and morphological evolution. *Annual review of cell and developmental biology*, 18, pp.53–80.

Trumpp, A. et al., 2001. c-Myc regulates mammalian body size by controlling cell number but not cell size. *Nature*, 414(6865), pp.768–73. Available at: http://dx.doi.org/10.1038/414768a [Accessed August 17, 2015].

Tsakas, S. & Marmaras, V., 2010. Insect immunity and its signalling: an

overview. *ISJ*, 7, pp.228–238.

Valanne, S., Wang, J.-H. & Rämet, M., 2011. The Drosophila Toll signaling pathway. *Journal of immunology (Baltimore, Md. : 1950)*, 186(2), pp.649–56. Available at: http://www.jimmunol.org/content/186/2/649.full [Accessed February 18, 2016].

Valtonen, T.M. et al., 2010. Starvation reveals maintenance cost of humoral immunity. *Evolutionary Biology*, 37(1), pp.49–57.

Vandesompele, J. et al., 2002. Accurate normalization of real-time quantitative RT-PCR data by geometric averaging of multiple internal control genes. *Genome biology*, 3(7), p.RESEARCH0034.

Vilmos, P. & Kurucz, É., 1998. Insect immunity: Evolutionary roots of the mammalian innate immune system. *Immunology Letters*, 62(2), pp.59–66.

van der Vliet, A. & Janssen-Heininger, Y.M.W., 2014. Hydrogen peroxide as a damage signal in tissue injury and inflammation: murderer, mediator, or messenger? *Journal of cellular biochemistry*, 115(3), pp.427–35. Available at: http://www.pubmedcentral.nih.gov/articlerender.fcgi?artid=4363740&tool=pmcentrez&rendertype=abstract [Accessed March 10, 2016].

Wagner, G.P. & Lynch, V.J., 2010. Evolutionary novelties. *Current Biology*, 20(2), pp.R48-52. Available at: http://www.sciencedirect.com/science/article/pii/S0960982209019459 [Accessed May 12, 2015].

Wang, J.-L. et al., 2014. 20-hydroxyecdysone transcriptionally regulates humoral immunity in the fat body of Helicoverpa armigera. *Insect molecular biology*, 23(6), pp.842–56. Available at: http://www.ncbi.nlm.nih.gov/pubmed/25224836 [Accessed July 23,

2015].

Wang, S. et al., 2009. The tyrosine kinase Stitcher activates Grainy head and epidermal wound healing in Drosophila. *Nature cell biology*, 11(7), pp.890–895.

Wang, Y. et al., 2007. Proteolytic activation of pro-spätzle is required for the induced transcription of antimicrobial peptide genes in lepidopteran insects. *Developmental and comparative immunology*, 31(10), pp.1002–12. Available at: http://www.ncbi.nlm.nih.gov/pubmed/17337053 [Accessed June 20, 2016].

Watanabe, I. & Okada, S., 1967. Effects of temperature on growth rate of cultured mammalian cells (L5178Y). *The journal of cell biology*, 32, pp.309–323.

Watt, W.B., 1968. Adaptive significance of pigment polymorphisms in Colias butterflies. I. Variation of melanin pigment in relation to thermoregulation. *Evolution*, 22(3), pp.437–458.

West-Eberhard, M.J., 2003. *Developmental Plasticity and Evolution*, New York: Oxford University Press.

Westerman, E.L. et al., 2014. Mate preference for a phenotypically plastic trait is learned, and may facilitate preference-phenotype matching. *Evolution*, 68(6), pp.1661–1670.

Whitman, D.W. & Agrawal, A.A., 2009. What is Phenotypic Plasticity and Why is it. *Africa*, 581(15), pp.1–63. Available at: http://www.scipub.net/entomology/gifs/Ch_1-Phenotypic-Plasticity-of-Insects.pdf.

Williams, M.J., 2007. Drosophila hemopoiesis and cellular immunity. *Journal of immunology (Baltimore, Md. : 1950)*, 178(8), pp.4711–4716.

Windig, J.J. et al., 1994. Seasonal polyphenism in the wild: survey of wing patterns in five species of Bicyclus butterflies in Malawi. *Ecological Entomology*, 19(3), pp.285–298.

Wittkopp, P.J. & Beldade, P., 2009. Development and evolution of insect pigmentation: genetic mechanisms and the potential consequences of pleiotropy. *Seminars in cell & developmental biology*, 20(1), pp.65–71.

Wood, W. et al., 2002. Wound healing recapitulates morphogenesis in Drosophila embryos. *Nature cell biology*, 4(11), pp.907–912.

Wood, W., Faria, C. & Jacinto, A., 2006. Distinct mechanisms regulate hemocyte chemotaxis during development and wound healing in Drosophila melanogaster. *Journal of Cell Biology*, 173(3), pp.405–416.

Wu, S. et al., 2010. Expression of antimicrobial peptide genes in Bombyx mori gut modulated by oral bacterial infection and development. *Developmental and Comparative Immunology*, 34(11), pp.1191–1198.

Wu, Y. et al., 2009. A blood-borne PDGF/VEGF-like ligand initiates wound-induced epidermal cell migration in Drosophila larvae. *Current biology : CB*, 19(17), pp.1473–7. Available at: http://www.pubmedcentral.nih.gov/articlerender.fcgi?artid=2783944&tool=pmcentrez&rendertype=abstract [Accessed June 11, 2015].

Xu, X.-X. et al., 2012. Manduca sexta gloverin binds microbial components and is active against bacteria and fungi. *Developmental and comparative immunology*, 38(2), pp.275–84. Available at: http://www.ncbi.nlm.nih.gov/pubmed/22858411 [Accessed June 20, 2016].

Xu, X.X. et al., 2012. Manduca sexta gloverin binds microbial

components and is active against bacteria and fungi. *Developmental and Comparative Immunology*, 38(2), pp.275–284.

Yi, H.-Y. et al., 2014. Insect antimicrobial peptides and their applications. *Applied microbiology and biotechnology*, 98(13), pp.5807–22. Available at: http://www.ncbi.nlm.nih.gov/pubmed/24811407 [Accessed June 9, 2015].

Yoo, S.K. et al., 2012. Early redox, Src family kinase, and calcium signaling integrate wound responses and tissue regeneration in zebrafish. *The Journal of cell biology*, 199(2), pp.225–34. Available at: http://www.ncbi.nlm.nih.gov/pubmed/23045550 [Accessed June 21, 2016].

Yu, K. et al., 1996. The Drosophila decapentaplegic and short gastrulation genes function antagonistically during adult wing vein development. *Development*, 122(12), pp.4033–4044. Available at: http://dev.biologists.org/content/122/12/4033.long [Accessed March 10, 2016].

Zelditch, M.L., Swiderski, D.L. & Sheets, H.D., 2012. *Geometric Morphometrics for Biologists: A Primer*, Academic Press. Available at: https://books.google.com/books?hl=en&lr=&id=5DLZ4lALRTEC&pgis=1 [Accessed August 7, 2015].

Zeng, X.-C. et al., 2014. Genome-wide search and comparative genomic analysis of the trypsin inhibitor-like cysteine-rich domain-containing peptides. *Peptides*, 53, pp.106–14. Available at: http://www.sciencedirect.com/science/article/pii/S0196978113002830 [Accessed June 9, 2015].

Zeng, Y.A. & Verheyen, E.M., 2004. Nemo is an inducible antagonist of Wingless signaling during Drosophila wing development.

Development (Cambridge, England), 131(12), pp.2911–20. Available at: http://dev.biologists.org/content/131/12/2911.full [Accessed August 20, 2015].

Zhou, K. et al., 2015. Genome-wide identification of lineage-specific genes within Caenorhabditis elegans. *Genomics*, 106(4), pp.242–248.

[1] Gene accession number in GenBank; [2] Homology of the best blast hit in NCBI blastx against all possible proteins; [3] The fold change in microarrays of wounded vs. non-wounded wings for each individual at 4 and 8h; [4] Primers used in experiments of qPCR and ISH.

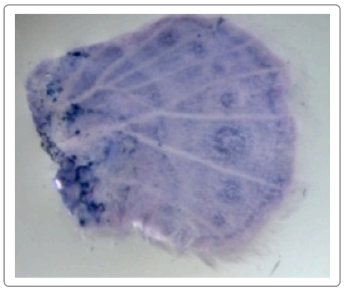

Figure S2.1- DDC expression in late pupal hindwings (~114hours post-pupation).

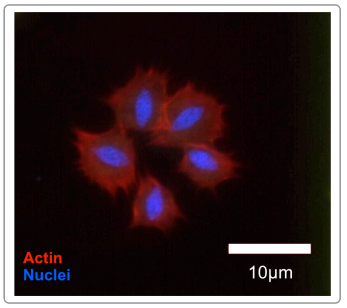

Figure S2.2- Actin rich hemocytes isolated from early pupal hemolymph.

B - Chapter 3

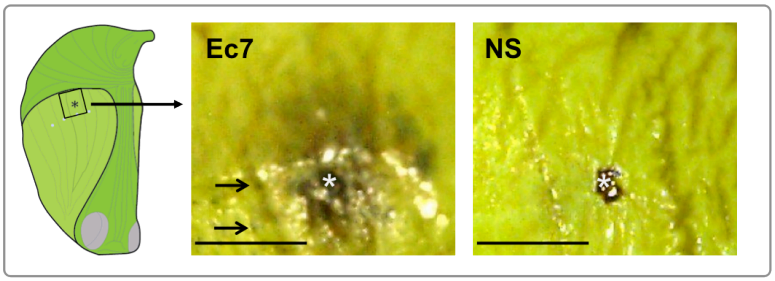

Figure S3.1- 6 hours post-wounding melanotic spots on non-dissected wings. Black arrows indicate examples of melanotic spots near wound side under the cuticle. White asterisk represent the wound site; scale bar 0.5mm.

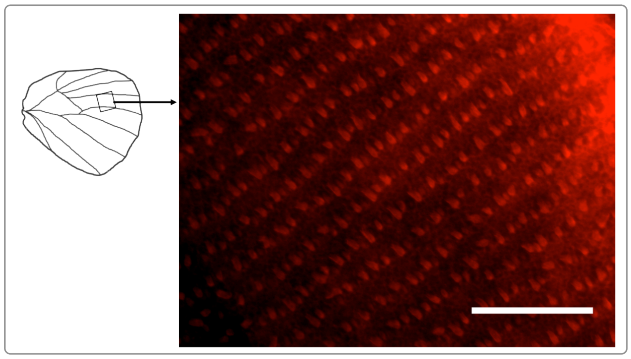

Figure S3.2- Early dorsal scale development. Approximately 40h post-pupation thee scales star to be secreted on *B. anynana* pupal wings. Actin stained with rhodamine-phaloidin; scale bar 50µm

C - Chapter 4

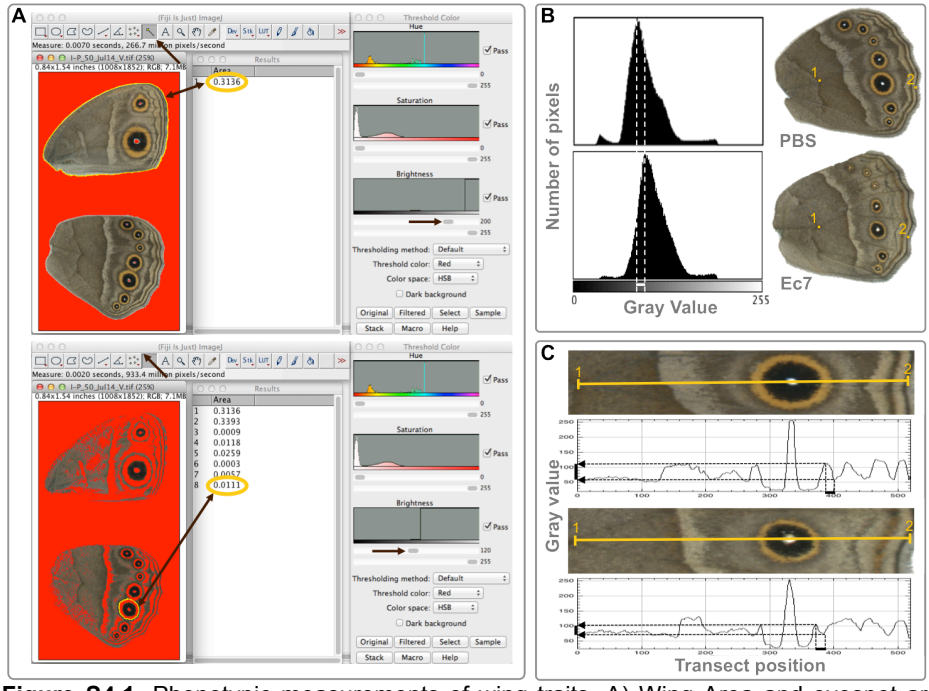

Figure S4.1- Phenotypic measurements of wing traits. A) Wing Area and eyespot area traits. B) Hindwing overall darkness. C) Hindwing color contrast.

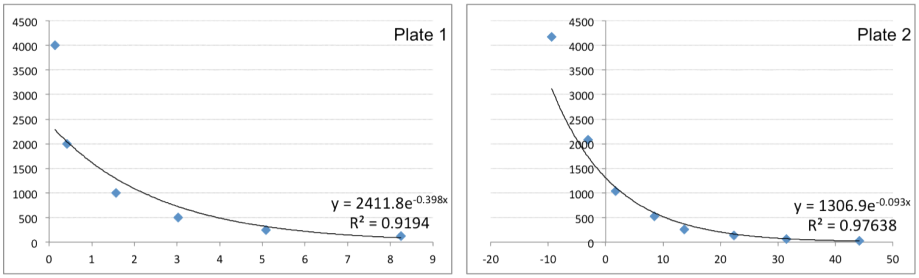

Figure S4.2- Calibration curves for quantification of 20E levels. yy axis is the total quantity of 20E (ρg), and xx axis is the absorbance.

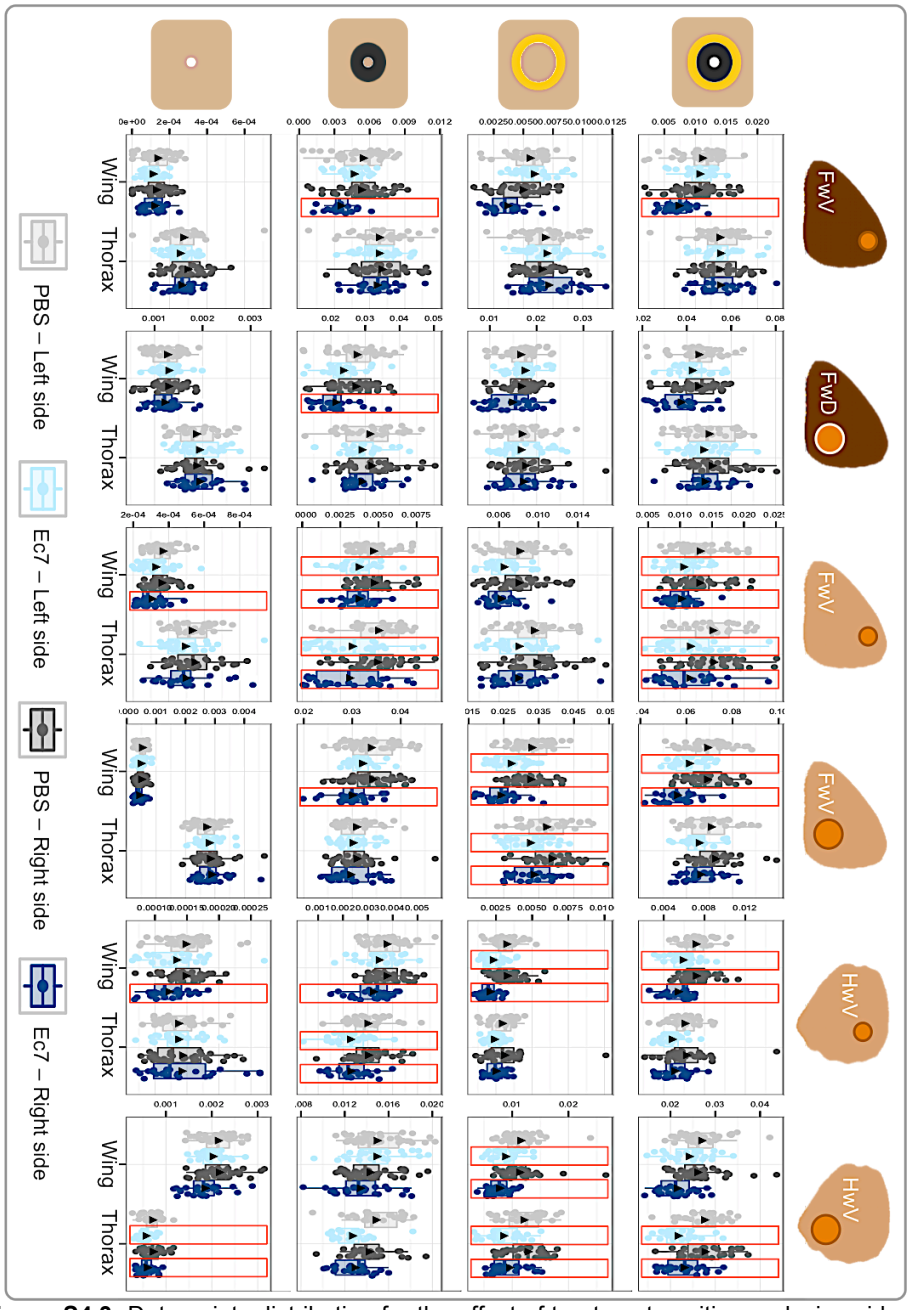

Figure S4.3- Data points distribution for the effect of treatment position and wing side on different eyespot traits. Traits that are significantly smaller than PBS are marked with red rectangles (lsmeans p-value≤0.01)

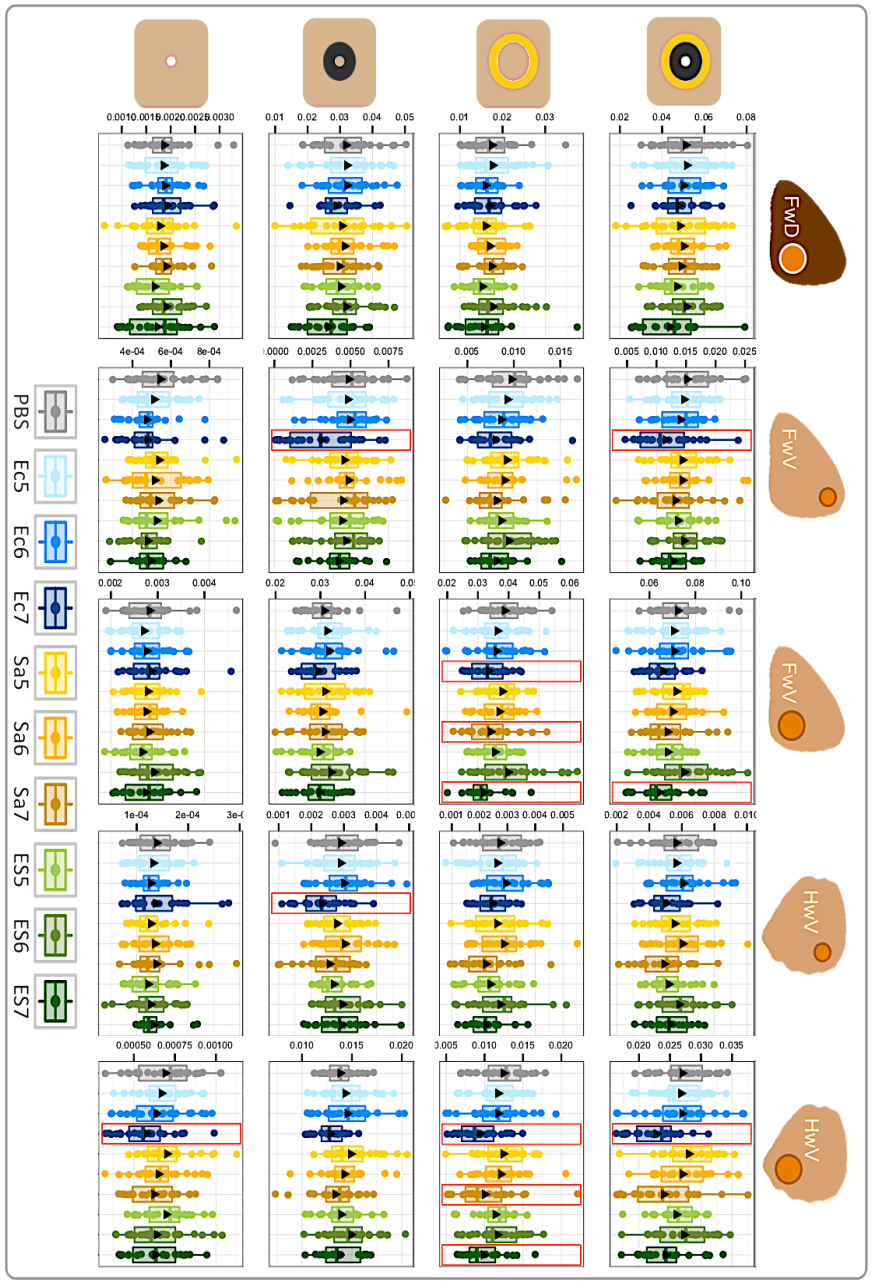

Figure S4.4- Data points distribution for the effect of bacteria type and dosage on different eyespot traits. Traits that are significantly smaller than PBS are marked with red rectangles (lsmeans p-value≤0.01).

ITQB-UNL | Av. da República, 2780-157 Oeiras, Portugal
Tel (+351) 214 469 100 | Fax (+351) 214 411 277

www.itqb.unl.pt